DIII–D RESEARCH OPERATIONS ANNUAL REPORT

OCTOBER 1, 1998 THROUGH SEPTEMBER 30, 1999

DIII–D
NATIONAL FUSION FACILITY
SAN DIEGO

PPPL LLNL
ORNL SNL
UCSD UCLA
ANL MIT
LANL INEL
Columbia University PNL
University of Maryland
University of Wisconsin
Cal Tech
University of Texas
Johns Hopkins University
Hampton University
University of Washington
Lehigh University
UCI
RPI
Palomar College
UCB
Georgia Tech
GA
University of Alaska

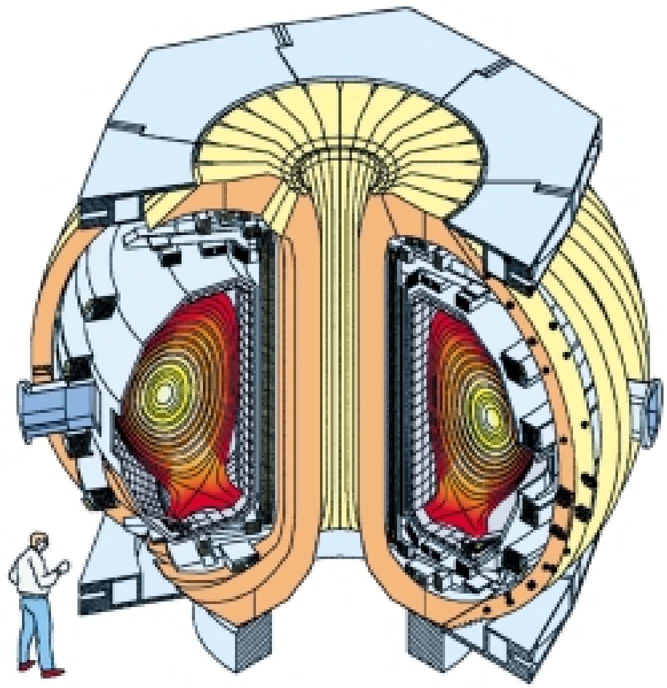

EUROPEAN COMMUNITY
- Joint European Torus
- IPP (Germany)
- Cadarache (France)
- Culham (England)
- Lausanne (Switzerland)
- KFA (Germany)
- FOM (Holland)
- Frascati (Italy)

RUSSIA
- Kurchatov
- Troitsk
- Ioffe
- Keldysh
- Moscow State

JAPAN
- JAERI
- JT–60U
- JFT-2M
- NIFS
- LHD
- Tsukuba U.

OTHER INTERNATIONAL
- KAIST (Korea)
- ASIPP (China)
- CCFM (Canada)
- SWIP (China)
- U. Alberta (Canada)
- U. Toronto (Canada)
- Chalmers U. (Sweden)
- Helsinki U. (Finland)
- U. Wales (Wales)
- KBSI (Korea)
- SINICA (China)
- Southwest Inst. (China)

INDUSTRY
- CPI
- Gycom
- CompX
- Orincon
- Creare
- Thermacore
- IR&T
- Surmet
- HiTech Metallurgical
- TSI Research
- FAR Tech

DIII–D
NATIONAL FUSION FACILITY
SAN DIEGO

GENERAL ATOMICS

Available to DOE and DOE contractors from the
Office of Scientific and Technical Information
P.O. Box 62
Oak Ridge, TN 37831
Prices available from (615) 576-8401,
FTS 626-8401.

Available to the public from the
National Technical Information Service
U.S. Department of Commerce
5285 Port Royal Rd.
Springfield, VA 22161

GA–A23299
UC–420

DIII–D RESEARCH OPERATIONS ANNUAL REPORT TO THE U.S. DEPARTMENT OF ENERGY

OCTOBER 1, 1998 THROUGH SEPTEMBER 30, 1999

by
PROJECT STAFF

Work prepared under
Department of Energy Contract Nos.
DE-AC03-99ER54463, W-7405-ENG-48,
DE-AC02-76CH03073 and DE-AC05-96OR22464

GENERAL ATOMICS PROJECTS 3466, 3467,
3470, 3473, 30033, 30034, 03990
DATE PUBLISHED: JULY 2000

TABLE OF CONTENTS

LIST OF FIGURES

LIST OF TABLES

1. DIII–D NATIONAL FY99 PROGRAM OVERVIEW

1.1. MISSION OF THE DIII–D NATIONAL FUSION PROGRAM

The overall mission statement of the DIII–D Program is "To establish the scientific basis for the optimization of the tokamak approach to fusion energy production." This mission is elaborated by three research goal statements.

1. The DIII–D Program's primary focus is the Advanced Tokamak (AT) Thrust that seeks to find the ultimate potential of the tokamak as a magnetic confinement system.

2. Where it has unique capabilities, the DIII–D Program will undertake the resolution of key issues for advancing various magnetic fusion concepts.

3. The DIII–D Program will advance the science of magnetic confinement on a broad front, utilizing its extensive facility and national team research capability.

Determining the ultimate potential of the tokamak as a confinement system is a complex scientific endeavor. The integration of AT elements into achievable single discharges requires programmatic compromise and tradeoffs evolved over a multiyear period.

1.1.1. Research Progress

The principal focus of DIII–D research is the advanced tokamak program aimed at improvement of the tokamak concept towards higher performance and steady-state operation through internal profile modification and control, plasma shape, and magnetohydrodynamic stabilization. The dependence of the core performance on the boundary conditions, and the operational regimes envisioned, put stringent requirements on the divertor and edge plasma, leading to inclusion of divertor optimization and control in our tokamak optimization program. The main line advanced tokamak is the pursuit of the high bootstrap fraction AT scenario, described as the negative central shear (NCS) scenario because it derived from the exciting discoveries of magnetic shear in tokamaks in the last few years. This regime has the best set of characteristics to take forward to a steady-state fusion reactor. The hollow current profile is compatible with the high confinement arising from a transport barrier since the off-axis bootstrap current produced by the transport barrier will produce most of the required off-axis current peak. The rest of the noninductive current can be either on-axis for central q control or off-axis to supplement and align the bootstrap current peak with the required total current profile. The NCS q profile and the broad pressure profile resulting from a transport barrier and q_{min} being at large radius are compatible with high normalized beta. Wall stabilization is also needed owing to the closer proximity of the current peak to the plasma edge. This scenario can be made with either the L–mode or H–mode edge. Which is best for stability and confinement is an active subject of ongoing research.

Progress on this scenario in 1999 is shown in Fig. 1.1–1. Without any active current profile control, discharges with β_N H_{89} ~ 9 for 2 s (16 energy confinement times) exceeding our expectations for 1999 preparatory work. The duration of these discharges was limited by the uncontrolled inward diffusion of the current profile which resulted in the growth of a resistive wall mode. Hence in 2000, we will apply microwave electron cyclotron current drive power in 2000 to counteract the resistive diffusion of the current. Success in that endeavor will set the basis for longer pulse sustainment of these discharges in 2001. This research progresses to DIII–D being the laboratory for the study of the moderate pulse AT called for in the FESAC goals.

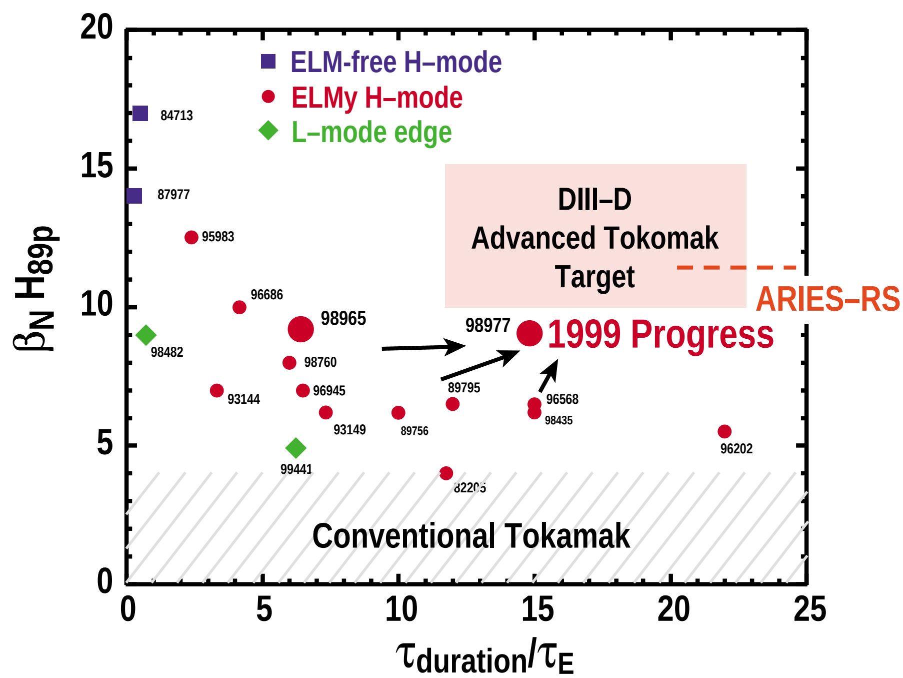

Fig. 1.1–1. Recent advanced tokamak progress. The two large circles are 1999 results.

Research in 1999 has affected the choice of research thrusts in 2000. Since the limiting mode is the resistive wall mode, the research thrust on the resistive wall mode will continue in 2000. Our AT scenario in 1999 went smoothly into an edge localized mode (ELM) H–mode without encountering the terminations of high performance from edge instabilities prominent in most previous efforts on DIII–D. We have developed a detailed understanding of the edge instabilities involving second stable ballooning access afforded by the edge bootstrap current. In 1999, our research thrust on edge instabilities made progress on developing methods to actively intervene in the edge stability situation. Likewise, our AT scenario in 1999 was also not limited by neoclassical tearing modes.

Our research thrust on internal transport barriers (ITB) is aimed at longer term optimization of AT scenarios. Theory work has identified exceptional tokamak performance with nearly 100% bootstrap current in a very hollow profile with a peak near the outer edge of the plasma produced by a broad pressure profile with a transport barrier near the plasma edge. Therefore it is desirable to move the transport barrier location to a large radius. Very exciting exploratory work on ITBs was done in 1999 using counter injection to alter the radial electric field profile to affect the E×B turbulence shearing rate to move the foot of the transport barrier from the inner 40% of the plasma radius using co-injection to 60% using counter-injection. Favorable results were also obtained using neon to lower turbulence growth rates. Exploratory results on using inside-launch pellet injection to form transport barriers were also obtained. This pellet work is important since relatively more bootstrap current can be obtained from a density gradient than from a temperature gradient within an overall stability constraint on the pressure gradient.

1.1.2. Improved Facility Capabilities

The DIII–D facility capabilities were improved in FY99. The key capability being implemented were high power, long pulse gyrotrons. The new gyrotrons have 1 MW output power and are equipped with diamond windows for 10-s operation. Experiments in the year 2000 will be conducted with four gyrotrons. Two gyrotrons have the new diamond windows. One is an old developmental prototype and the other is the first production tube of the new diode gun design. The other two gyrotrons will be older units limited to 2 s pulses. This complement of EC sources will enable us to attempt the high bootstrap fraction experiments.

For density control, the upper divertor private flux baffle and inner leg pump which were installed at the end of 1999 are expected to give density control for high triangularity plasmas using the upper pumps or for low triangularity plasmas using the lower pump. Because of the importance of triangularity, the upper divertor density control capability is an essential element of the year 2000 campaign. The new upper divertor will also allow resumption of the studies of optimizing the core/divertor plasma performance balance by better retaining neutrals and impurities in the divertor using copious flows in the scrapeoff layer.

The Oak Ridge National Laboratory pellet fueling capability was extended to inside launch in 1999. This capability proved valuable in triggering ITBs in the density channel.

Wall stabilization research made a good beginning in 1999 with development of feedback control using a six-coil system and by accelerating installation of three Princeton Plasma Physics Laboratory power supplies originally planned for 2000.

A Thomson scatter system was added to measure the central electron temperature and density profile in support of the research program and improvements to the Lawrence Livermore National Laboratory motional Stark effect diagnostic were implemented.

2. FUSION SCIENCE

2.1. SUMMARY OF THE 1999 DIII–D EXPERIMENT CAMPAIGN

In FY99 the DIII–D National Team produced advances in science of magnetic confinement on a broad front by utilizing a superb diagnostic set, an increasingly flexible and capable plasma control systems, and a comprehensive set of analysis codes and theory support that enable learning in depth from the experiments done. DIII–D Advanced Tokamak (AT) research in FY99 was carried out with extensive international collaboration to perform coordinated experiments with facilities of differing scale or capabilities to develop mutual databases and theoretical understanding.

In order to focus on critical issues, DIII–D experimental research in 1999 was structured to gain a path to the eventual AT integrated plasma scenarios targeted on a five-year timescale. This approach made it natural to create cross-disciplinary teams to pursue integrated plasma scenarios. The research organization is a matrix type of approach in which one dimension of the matrix is a set of Thrusts aimed at a key objective of the research and is allocated a significant block of run time in which to realize its objectives. The research thrusts and their leaders change year-to-year to keep up with the evolution of the experimental program. The 1999 roadmap of thrusts is given in Fig. 2.1–1. The second dimension of the experimental matrix is comprised of the four enduring topical areas of fusion energy science: stability, confinement and transport, divertor/edge physics, and heating and current drive. A summary of the run time statistics for the 1999 DIII–D Research Plan is given in Table 2.1–1.

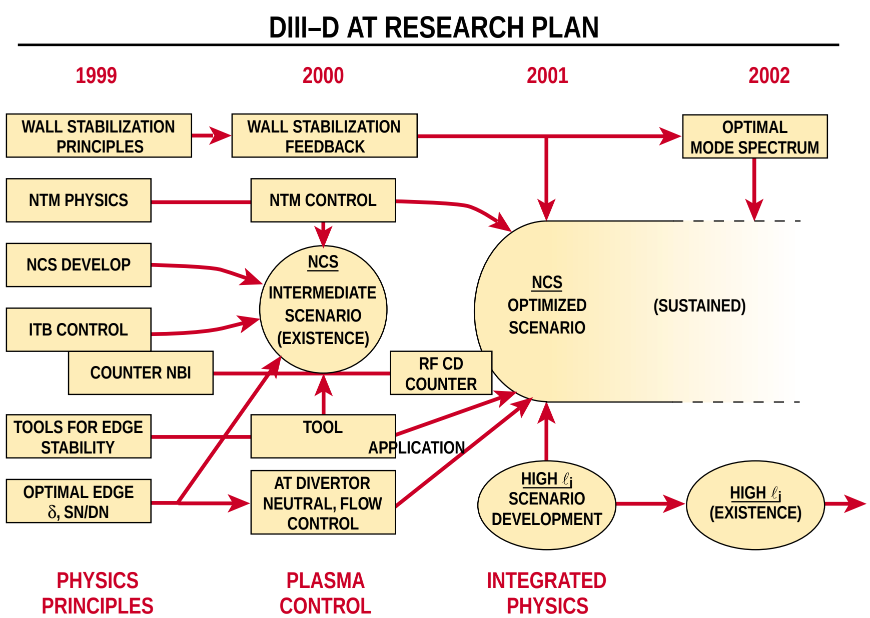

Fig. 2.1–1. The 1999 DIII–D AT Program scientific road map.

TABLE 2.1–1
RUN TIME STATISTICS FOR THE 1999 DIII–D RESEARCH PLAN

Research Thrusts and Topical Science	Days Allocated	Days Scheduled	Days Completed
• Regulate the edge bootstrap current and/or the edge pressure gradient to extend the duration of AT modes (M. Wade, ORNL; Deputy B. Rice, LLNL)	8	8	6
• Preparation of an NCS AT plasma demonstration (Leader T. Luce, GA; Deputy P. Politzer, GA)	7	9	7
• Validate neoclassical tearing model and begin stabilization with ECCD (Leader R. La Haye, GA)	6	5	3
• Validate the model of wall stabilization and begin feedback stabilization experiments (Leader G. Navratil, Columbia U.)	6	9	9
• Develop the basis for choosing single- versus double-null and the optimum triangularity (M. Fenstermacher, LLNL; Deputies T. Osborne and T. Petrie, GA)	6	12	9
• Expand the spatial extent and time duration of internal transport barriers (Leader C. Greenfield, GA)	8	13	13
• Confinement and transport physics (Leader K. Burrell, GA)	7	5	4.5
• Stability physics (Leader E. Strait, GA)	3	3	2
• Divertor edge physics (Leader S. Allen, LLNL)	4	6	5
• Heating and current drive physics (Leader R. Prater, GA)	3	3	3
• Contingency for hardware problems	15	—	15.5
TOTAL	73	73	73

2.2. TOPICAL SCIENCE RESEARCH

2.2.1. Confinement and Transport Physics

Significant experimental results were obtained in confinement and transport physics in 1999. Perhaps the most impressive set of results were obtained in the experiment that investigated use of impurity injection to improve the core plasma confinement (RI–mode). As shown in Fig. 2.2–1 impurity injection resulted in a substantial improvement in global confinement and neutron production and a reduction in turbulence level. The local electron and ion thermal diffusivities decreased with the change in ion transport being the greater. The reduction in transport was clearly correlated with reduced density fluctuations as measured by beam emission spectroscopy and by far infrared scattering. Comparisons between the E×B shearing rate and the gyrokinetically determined turbulence growth rate showed that the E×B shearing rate was below the growth rate before impurity injection but exceeded it after injection. In other words, impurity injection reduced the turbulence growth rate so that the E×B shear feedback loop could result in reduced transport. Evidence was obtained of a change in fluctuations which correlated with the confinement improvement, suggesting that impurity effects on short wavelength fluctuations may be connected with the reduction in electron thermal transport. In addition to providing a wealth of fundamental physics, this experiment has given us a new tool for triggering core transport reduction.

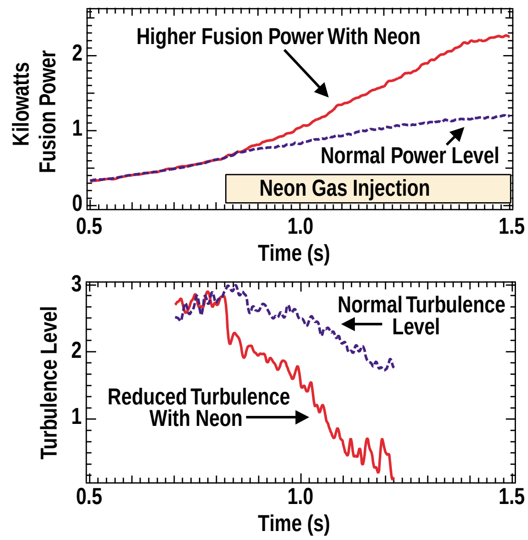

Fig. 2.2–1. Injecting a neon additive results in higher fusion power because of reduced turbulence levels.

In the H–mode physics area, we combined several experiments into one set of shots in order to maximize the amount of information that we could obtain. Two results from this set of experiments stand out. First, we used the beam emission spectroscopy system to obtain two-dimensional turbulence data at the plasma edge across the L to H transition. Processing this data to produce a movie allows one to see the turbulent eddies convect past the field of view. A snapshot of the University of Wisconsin data is shown in Fig. 2.2–2. Second, we thoroughly documented the pellet-triggered H–modes which we had identified on DIII–D in 1998. Both high and low field side launch pellets can trigger the H–mode with the power threshold reduction being greater for the high field side launch. The best result was a 30% reduction in power threshold.

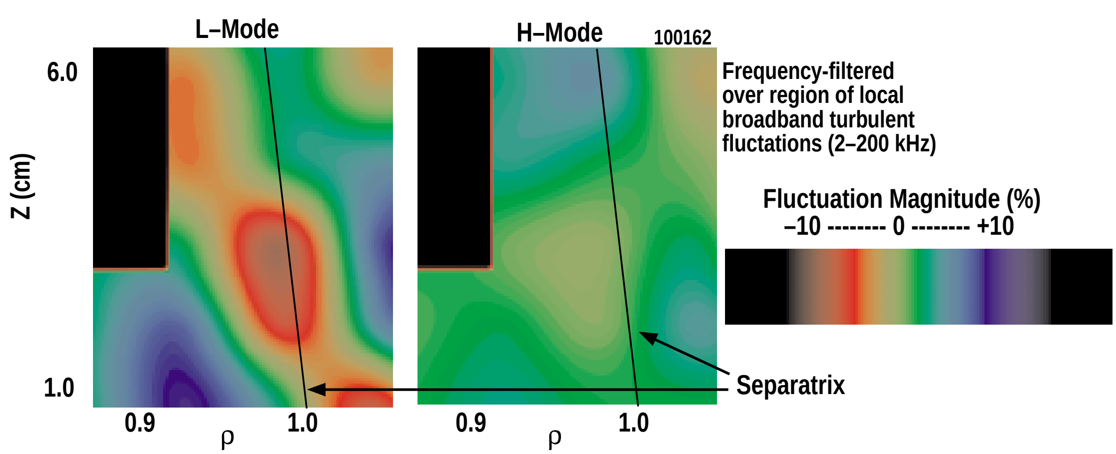

Fig. 2.2–2. Initial two-dimensional edge turbulence images obtained with beam emission spectroscopy at L–H transition. The imaged region is 5 cm radially (ρ) by 7 cm poloidally (q) near outer midplane with 1 cm resolution. The data was splined/interpolated for visualization.

The Fundamental Turbulence Studies group performed an experiment whose primary goal was to provide a comprehensive test of whether ion temperature gradient (ITG) turbulence is the dominant microinstability and source of anomalous transport in DIII–D as predicted by theory. The experiment was performed by studying the changes in turbulence during a density scan in Ohmic plasmas from the neo-Alcator regime and into the saturated Ohmic confinement regime. Far infrared scattering measurements observed an enhanced low frequency feature in the scattered spectra at high density, consistent with the theoretical prediction that the ITG mode is more unstable there. Theory also predicts that the electron temperature gradient mode is important at all densities; reflectometry measurements indicate the presence of two modes. More detailed comparisons with the predictions of gyrokinetic codes is in progress.

Nondimensional Transport studies concentrated on the effect of rotation on confinement using counter neutral beam injection (NBI). A previous, co-injected ρ_* scan in edge localized mode (ELMing) H–mode plasmas was duplicated with all the dimensional parameters except the Mach number and Z_{eff}. The ρ_* scaling of global confinement was Bohm-like for counter injected discharges while the one for co-injected discharges was gyro-Bohm-like. Theory-based transport modeling is now needed to see if this change in the transport scaling can be explained either by the different Mach number and, hence, different E×B shearing rate or by the differing Z_{eff}.

In the area of Core Transport Barrier Physics and Control, we investigated whether ion cyclotron range of frequencies (ICRF) could be used to control the plasma toroidal rotation. Theoretical predictions indicate that spatial transport of resonantly heated ions could produce torque on the plasma which might alter the toroidal rotation. Previous DIII–D experiments had also shown that electron heating from ICRF fast wave and ECH increased radial transport of angular momentum, also altering toroidal rotation. The goal of the experiment was to see which of these effects is dominant in our plasmas. By utilizing counter-NBI plasmas, we set up a condition where the postulated ICRF torque would increase the magnitude of the rotation while the electron heating effect would decrease it. The results were consistent with the increased transport being the dominant effect.

In addition to the planned experiments, we made a discovery of a mode of operation with no ELMs and no sawtooth oscillations which had controlled, constant density and impurity levels shown in Fig. 2.2–3. These discharges were created using counter NBI into plasmas where the density was lowered using cryopumping. The operational key was a line-averaged density below $\lesssim 3 \times 10^{19}$ m^{-3} and a neutral beam power above about 7.5 MW. The constant density and impurity levels are connected with the presence of low level magnetohydrodynamic (MHD) oscillations in the plasma edge which apparently increases the particle transport enough that divertor cryopumping is still effective in spite of the absence of ELMs. These oscillations have little effect on the H–mode edge pressure profiles; the profile width is the same whether or not these modes are present. A key issue for divertor design for a fusion power plant is the pulsed heat load to the divertor plates caused by ELMs. The ELM-free operation seen in these discharges solves this problem by getting rid of the ELMs without paying the usual price of uncontrolled density rise in an ELM-free phase. If we can understand why this occurs and apply this in larger scale plasmas, we will have solved a significant fusion technology problem.

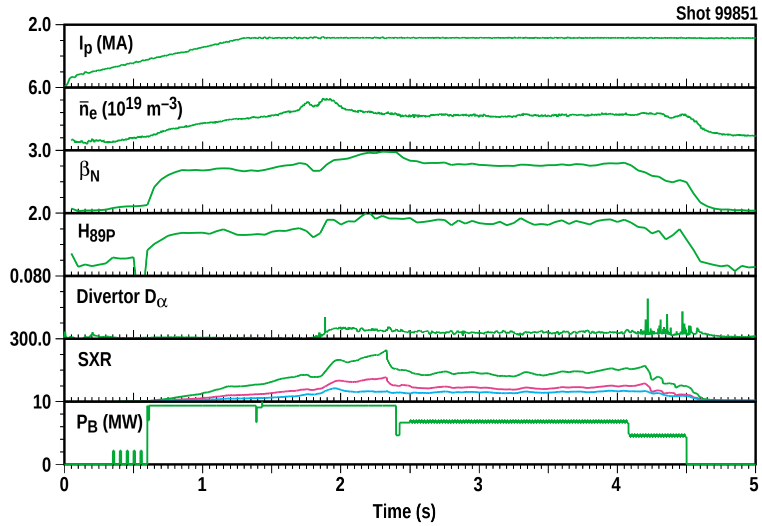

Fig. 2.2–3. A steady-state, ELM-free sawtooth-free DIII–D discharge with density control.

Plasma turbulence is responsible for particle and heat transport in magnetic fusion experiments. However, the exact nature of the turbulence is not yet completely understood. This is due to the complex nature of turbulence and to the experimental challenges involved in making measurements in a 50 million degree temperature plasma. Progress was made in understanding by considering the similarities of plasma turbulence to a sand pile that is being created by pouring sand onto it. The sand pile exhibits avalanches ranging in size from a single sand grain up to large parts of the sand pile. Data from the DIII–D plasma is also consistent with such theory models as shown in Fig. 2.2–4 below. Large transport events occur much less frequently than small transport events, consistent with predictions for the frequency of occurrence of large and small avalanches. Previously researchers knew that heat and particles were transported by both large and small scale processes (avalanches). This new research shows how their frequency changes with avalanche size. The ideas contained in the avalanche model called self-organized criticality by physicists are powerful. Improved understanding and control of plasma turbulence will increase general understanding of turbulence in widespread applications in other fields of science as well as should lead to the improvement and optimization of magnetic fusion concepts.

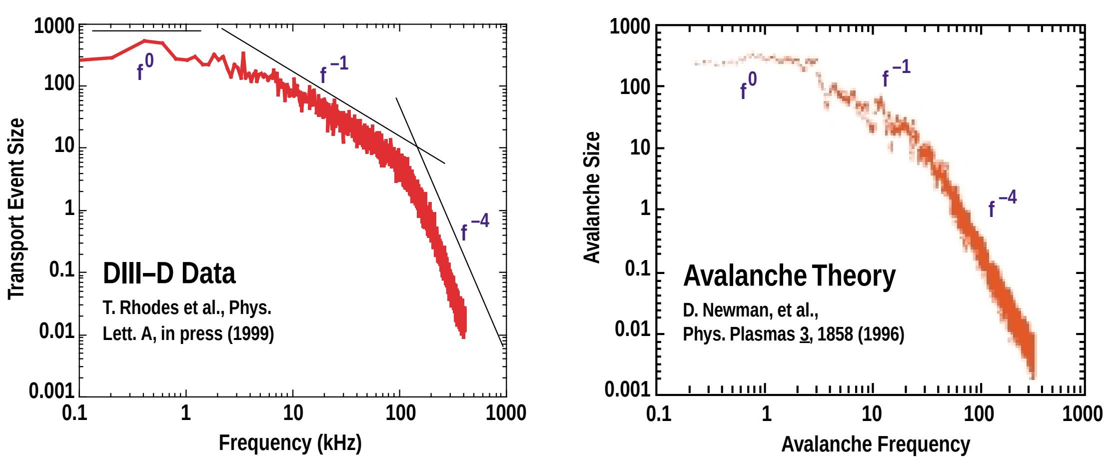

Fig. 2.2–4. Example of data from the DIII–D fusion plasma compares well with avalanche model predictions.

2.2.2. Stability and Disruption Physics

The goals of the DIII–D Stability and Disruption Physics research are to address critical issues for advanced tokamak plasmas, and to pursue broader issues of MHD stability physics. The greatest part of stability research was carried out as two thrusts: neoclassical tearing modes (NTMs) and resistive wall modes (RWMs). This year's topical science efforts focused on sawtooth physics and disruption mitigation, as well as the Research Thrust topics of NTMs, resistive wall stabilization, and edge plasma stability.

Experiments and modeling of edge plasma stability indicate that ELMs are triggered by moderate-wavelength instabilities, driven in the H–mode edge pedestal by the steep pressure gradient and its associated bootstrap current. Modeling and experiments support a picture in which second regime access at the edge enables steep pressure gradients to form because short wave length ballooning modes are stable. Eventually, intermediate mode numbers modes are destabilized. A comparison of the edge pressure gradient with the calculated n = 5 instability threshold is shown in Fig. 2.2–5. Several approaches to control of edge instabilities and improved performance were pursued. Discharge shaping was used to lower the stability limit for short-wavelength ballooning modes at the edge, thereby limiting the pressure gradient to the first regime ballooning mode limit and reducing ELM amplitudes. Edge stability was also explored through manipulation of the edge pressure gradient with injection of pellets and krypton gas. In a new regime using pumping of the divertor private flux region, very high densities (up to 1.4 times the Greenwald limit) were obtained while maintaining high confinement. High-performance discharges with an L–mode edge were explored, including a high-performance discharge with an L–mode edge having 100% noninductive current. This discharge has the highest product of normalized beta and confinement factor of any discharge with an L–mode edge.

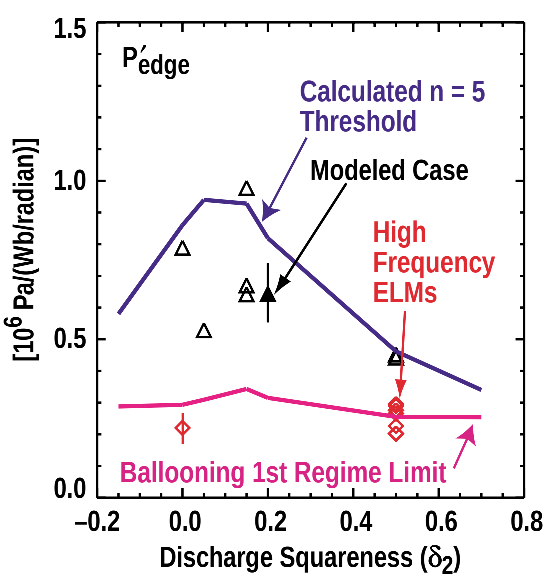

Fig. 2.2–5. The measured edge pressure gradient P'_{edge} scales with discharge shape like the predicted threshold for n = 5 ideal, king/ballooning modes.

Our program continued to explore and validate basic MHD stability physics, making use of DIII–D's extensive set of diagnostics for precise, detailed measurements of the pressure and current density profiles and the internal structure of MHD modes. A sawtooth physics experiment had the goal of validating models of sawtooth reconnection by comparing two discharge shapes with different stability properties. An elliptical cross-section discharge was developed which was Mercier unstable even with central q greater than 1. As expected, partial reconnection events were observed with little change in central q. Development was begun for the companion case, a bean shape with Mercier stability even at central q less than 1, in which Kadomtsev-type full reconnection is expected. Database analysis of other discharges using 60 MHz ion cyclotron heating shows that when the sawtooth period is lengthened, the central electron temperature often saturates. The saturation is correlated with the onset of high-frequency MHD activity, suggesting that fast-ion diffusion caused by TAE or energetic particle modes is responsible for the saturation.

Disruption studies this year focused on data analysis and modeling. Physics understanding of mitigation techniques was further developed, highlighted by recent success in modeling mitigation experiments using a massive He gas puff. The first clear determination that the resistivity of post-thermal quench disruption plasmas is classical was obtained in analysis of these discharges, using measured profiles of electron temperature and Z-effective. Further modeling of the massive He injection experiments shown in Fig. 2.2–6 using the KPRAD code has shown that nearly all of the magnetic energy is converted into radiation. Both killer pellet and massive puff disruption mitigation techniques were shown to rely on anomalous rapid inward transport of impurity to center of plasma, an important issue for future investigation. Analysis of JT–60U and Alcator C–Mod disruption halo current data was completed as part of the multimachine halo current model comparison effort. Results confirm that the principal difference among the devices is the efficiency of current transfer from core to halo during disruption resulting from a combination of higher vertical instability growth rate and higher post-thermal quench plasma temperatures.

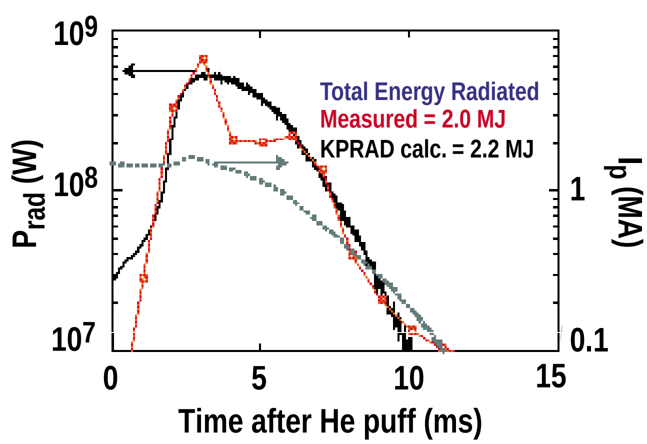

Fig. 2.2–6. Models of disruption mitigation predict important features of radiative balance of massive He gas puff when instantaneous radial transport is assumed.

In another series of experiments of 31 consecutive discharges, shown in Fig. 2.2–7, demonstrated that disruption-free operation is possible.

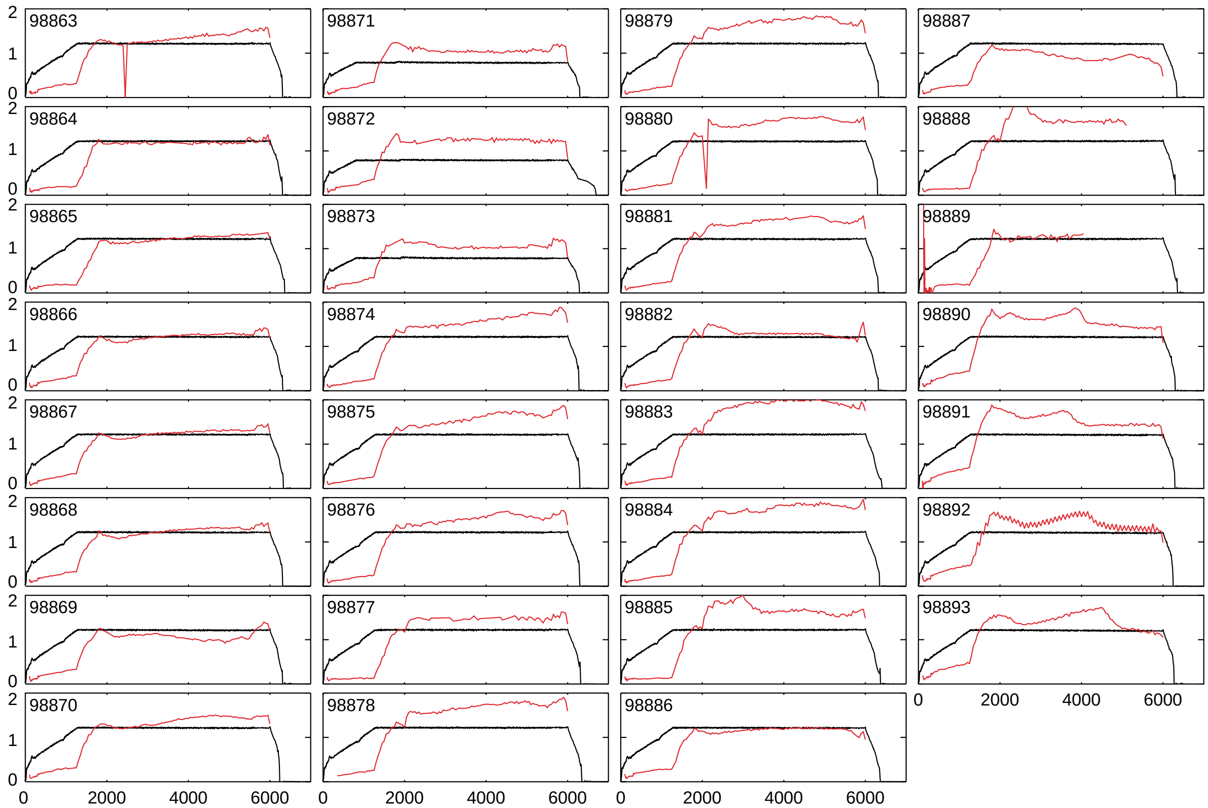

Fig. 2.2–7. Disruption-free operation is possible away from stability limits for 31 consecutive discharges for a total 160 s duration. The experiments encompassed a range of parameters: I_p = 0.8–1.2 MA, q_{95} = 3.1–6.0, P_{NB} = 3.0–7.5 MW, and β_N = 1.0–2.0.

Several diagnostics and plasma control algorithms were upgraded for this year's experiments. New high-resolution edge motional Stark effect (MSE) measurements were put into use, revealing a very deep, narrow radial electric field well at the plasma edge during ELM-free VH–mode discharges. Several new algorithms were developed for the plasma control system, including RWM feedback control for the C–coil, modified neutral beam control for avoiding the RWM, and density feedback using the upper cryopump in double-null (DN) and upper single-null (SN) discharges. Feedback control of impurity gas injection to achieve a high fraction of radiated power without a radiative collapse was developed and used in radiating mantle experiments. "Isoflux" shape control using real-time equilibrium fitting (EFIT) reconstructions came into routine use.

2.2.3. Boundary and Divertor Physics

The main function of the boundary plasma is to control particle and power flux at the interface between the core plasma and the material walls. The long range goal of the DIII–D divertor and scrapeoff layer (SOL) science program is to: (1) use state-of-the art 2–D diagnostics to identify the relevant physical processes; (2) model these processes with computational models (*e.g.*, UEDGE), and (3) sufficiently understand the relevant physical processes in the edge plasma so that computational models can predict operation for new operating modes on existing machines and for new machine and concepts.

We have identified and studied the radiative divertor or “detached” mode of operation which reduces the divertor heat and particle flux by deuterium puffing. Intrinsic carbon radiation is a key ingredient in this mode. We are extending the operating regime (*i.e.*, operation at lower core n_e) for near-term AT operation by concentrating radiation in the divertor with injected impurities such as argon. The two tools to achieve this goal are so-called “puff and pump” techniques (deuterium injection and pumping to provide a force on impurities towards the divertor) and divertor baffling (to better control neutrals). The baffling and pumping are also important ingredients in the control of density and impurities for the core plasma. We also investigated the role of triangularity, single- and double-null on both divertor and AT conditions. Substantial progress has been made in the measurement (DiMES probe) and modeling (REDEP) of erosion and redeposition in the DIII–D divertor during detached operation. These studies are also important in understanding the best means to control carbon radiation in an all-carbon machine like DIII–D.

The 1999 experiments in the edge and divertor area were executed both in the Divertor Topical Science area and the Thrust 5 focused on the effects of plasma shape in unbalanced DN plasmas. A series of experiments focused on plasma flows and carbon sources and transport. We obtained new flow data with both the Mach probes and the spectroscopic diagnostic in detached plasmas. Measurements with divertor biasing in ohmic plasmas showed that the divertor potential could be changed with biasing. DiMES measurements (DiMES is an impurity probe) showed no appreciable net erosion in detached plasmas. Data also indicated that the net carbon source in DIII–D has been decreasing over the past seven years (presumably due to wall condition of the graphite), but the core carbon concentration has not changed appreciably. Carbon sources and transport will also be an important topic in the FY00 campaign. Experiments at high core electron density (greater than the Greenwald density) were performed; degradation of confinement was not observed. We are now theorizing that divertor pumping may play an important role in this operation and will be the focus of a future experiment.

It has been hypothesized that an important mechanism in exhaust control is plasma flow caused by plasma-generated electric fields. Recent advances in computational models have confirmed this physics flow effect. We have now obtained experimental measurements of such flows with two different diagnostic instruments: (1) a probe that sweeps through the plasma to measure flows and electric fields, and (2) a high resolution spectrometer to measure light emitted by impurities in the flowing plasma. The computational modeling reproduces the major features of the new data, giving increased confidence in the validity of the simulations, see Fig. 2.2–8.

DIII–D researchers have also been able to increase the particle flow in the divertor by applying electric fields with a power supply. Ultimately, they aim to have sufficient control of plasma flow so that the heat and particles can be controlled over a wide operational range.

Computer simulations suggested that the shape of the divertor controls the exhaust and may reduce impurities in the central plasma. Using this understanding, a new shaped divertor was designed and is now being installed for experiments beginning in February 2000. These experiments will further test models that can be applied to a wide range of magnetic fusion concepts.

DIII–D experiments in FY99 showed that inside launched pellets penetrated three times deeper even though they were injected five times slower (see Fig. 2.2–9). These encouraging results suggest that the stronger magnetic field on the inside of the plasma ring propels the fuel deeper toward the plasma center. This new capability provides a new tool to optimize and further develop understanding of high temperature plasmas and to develop better ways to fuel larger fusion plasmas including power plants. One example is that pellets can be used to form internal transport barriers (ITBs) as shown in Fig. 2.2.–10.

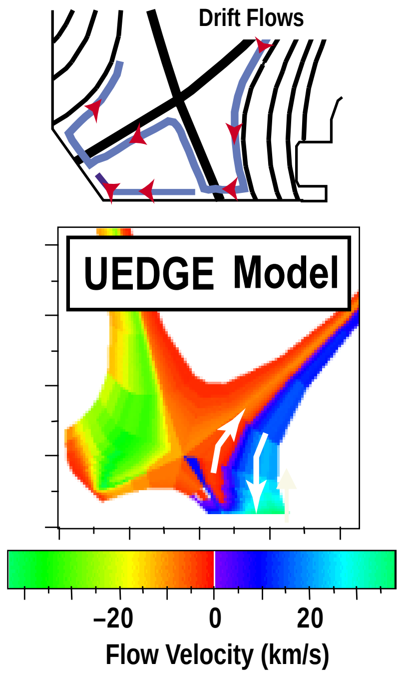

Fig. 2.2–8. Flow measurements from the DIII–D experiment (above) have now been compared with the LLNL computer model (below) that includes flow to advance the understanding of the flow of fusion plasma exhaust.

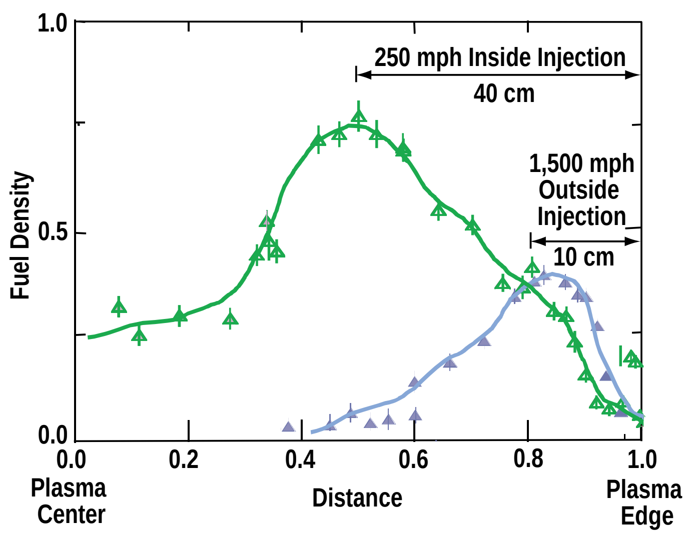

Fig. 2.2–9. Ice pellets injected at 250 mph from the inside penetrate 40 cm into the hot plasma. Pellets injected from the outside penetrate only 10 cm even though their speed is 1500 mph.

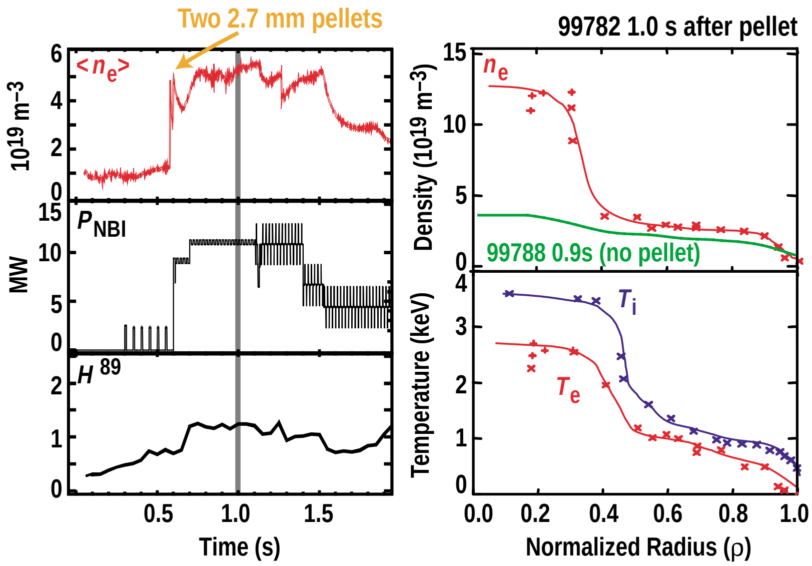

Fig. 2.2–10. Pellets injected from the high field side during the current ramp can form an internal transport barrier where the density and temperature rise abruptly.

2.2.4. Heating and Current Drive Physics

Progress was made in the area of heating and current drive on electron cyclotron current drive (ECCD), fast wave current drive (FWCD), and neutral beam current drive (NBCD). ECH proved to be very effective at raising the electron temperature to 5 keV early in the formation of the discharge, see Fig. 2.2–11. This proved to be very useful for the startup of advanced tokamak discharges. Control of the electron temperature provides a means to freeze in different ohmic current profiles such as in discharges with the plasma current peaked off-axis.

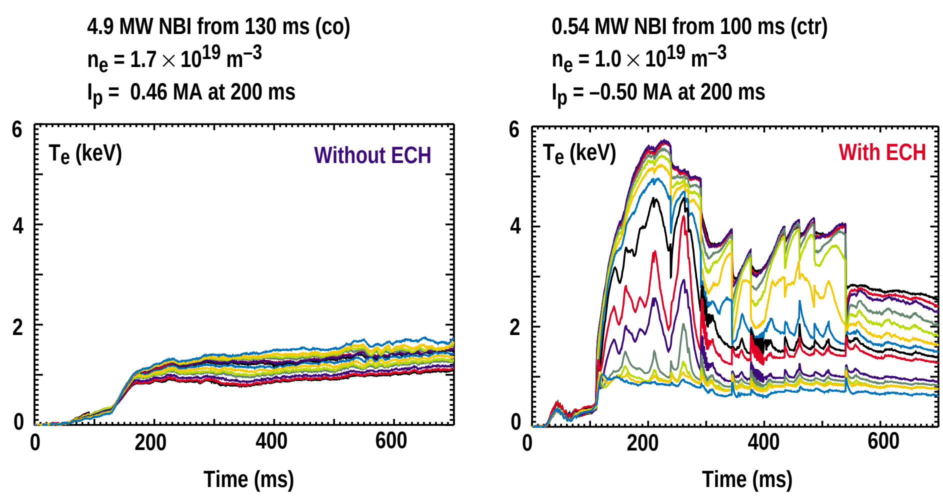

Fig. 2.2–11. ECH is very effective at raising electron temperature during startup of AT discharges.

ECCD research efforts concentrated on two topics: experimental verification of the properties of counter-ECCD, and a re-analysis of previous experiments on ECCD. On the first topic, ECCD was applied to discharges with the plasma current direction reversed from the usual case, so that EC waves propagating in the usual direction drive current counter to the plasma current instead of parallel to it as in previous experiments. Although the EC power was low, a clear measurement of counter-ECCD was made. The ECCD measured had an efficiency and profile quite similar to those of co-ECCD. This is important because it verifies calculations with a Fokker-Planck code showing that the Ohmic electric field is not playing a strong role in the current drive.

The counter-ECCD measurements showed the same behavior as last year's co-ECCD experiments, that the location of the peak of the current drive was well aligned with the calculations, but that the width of measured profile and the integrated driven current exceeded that of the calculations. One hypothesis to explain the discrepancy is that the analysis technique used to determine the ECCD might have built-in limitations on the strength of the gradient of the current density, and the narrowness of the current drive profile might be essentially limited by reconstruction of the equilibria. To test this, calculations were performed of what effects should be observed in the plasma, particularly in the poloidal field measurements from the MSE diagnostic if the driven current profile were as expected from theory. These simulations indicated that the poloidal field measurements (the most sensitive measure we have of the current profile) were consistent in location and profile with a driven current as predicted by theory.

The agreement of experiment and the simulations is shown in Fig. 2.2–12. The figure shows the toroidal current density derived from the differences in poloidal magnetic field between adjacent channels of the MSE system as a function of the minor radius. The spatial discreteness of the MSE measurements gives rise to the histogram-like nature of the curves. The right side shows the changes in current density, as reflected in the simulated MSE signals, which would be expected from the calculated current drive, shown as the curve labelled "ECCD." The left side shows the same changes measured in the experiments. The important thing to note is that the location and the width of the strong response near normalized radius of 0.33 is the same for the experiment and simulation.

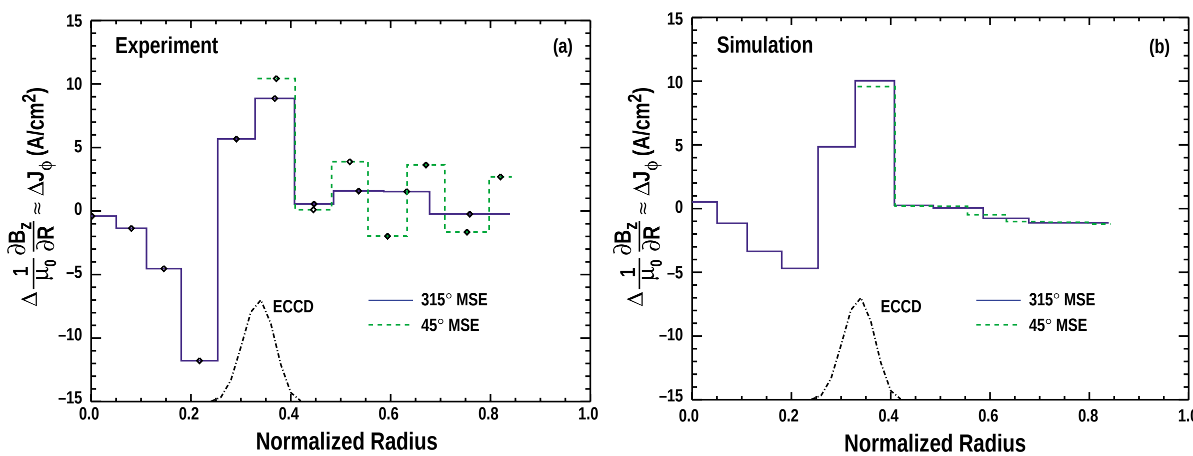

Fig. 2.2–12. Profiles of driven ECCD derived from MSE measurements for experiment and a simulation.

Quantitative interpretation of the integrated current is more difficult to obtain from this approach to the data, but estimates show that in all cases examined so far the integrated current is closer to but larger than the theory values. In particular, one case from last year had an integrated current calculated to be close to zero due to a cancellation of the Fisch-Boozer current by the Ohkawa current. Applying the simulation technique to this case still shows a positive driven current. The fact that the current profile is closer to the narrow calculated profile is very good news for prospective experiments which rely on narrow, well-controlled driven currents, such as experiments to test stabilization of NTMs by localized ECCD. More work is needed now to improve the quantitative analysis provided by the time-dependent equilibrium process through changes in the EFIT program to allow greater structure.

The first tests anywhere of the dependence of the FWCD efficiency on the parallel index of refraction, $n_{||}$, were performed. Because waves with smaller $n_{||}$ interact with electrons with greater velocity in the parallel direction, the current drive efficiency is expected to be higher because these energetic electrons are less collisional and slow down more slowly through collisions with ions. The experiments were done by operating the high power transmitters at 117 MHz near their highest frequency, compared with previous experiments at 60 to 83 MHz. Comparing 60 and 117 MHz cases, the $n_{||} = ck_{||}/\omega$ changes by a factor 0.66, after allowing for the different antennas used in the two cases. (Here c is the speed of light, $k_{||}$ is the inverse parallel wavelength imposed by the structure of the antenna, and ω is the applied frequency.) Theory says that the current drive efficiency should change by a factor $n_{||}^{-2}$ or about 2.3. The experimental results from the two cases shown in Fig. 2.2–13 show that the measured efficiency changes by a factor 1.9, in approximate agreement with theory.

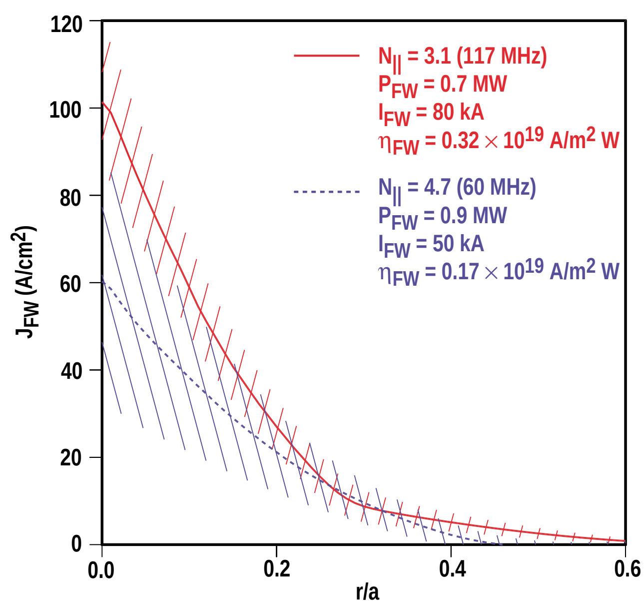

Fig. 2.2–13. Profile of driven FWCD for 60 MHz and 117 MHz cases.

Experiments were also done on NBCD. These experiments were motivated by the previous measurements of NBCD that indicated that the driven current profile was wider than calculated under most conditions. By measuring NBCD in a counter-current discharge and comparing with a matched co-NBCD discharge, systematic errors in the determination of the profile of driven current could be reduced. Bootstrap current effects, for example, can be subtracted out empirically. The difficulty proved to be the impurities which have significantly higher density under counter-injection than under co-injection. Despite this complication, the result of the experiment is that the driven current profile is in better agreement with the calculations from the TRANSP code than from the simple neutral beam model which is in ONETWO. To improve this capability in ONETWO, the TRANSP beam deposition model is being incorporated into ONETWO.

2.3. RESEARCH THRUSTS

2.3.1. Wall Stabilization Principles Thrust

Stabilization by a conducting wall is predicted to strongly enhance the ideal kink mode beta limit in AT plasmas with a broad pressure profile and broad, negative central shear current density profile. However, the presence of a resistive wall is expected to destabilize a slowly growing RWM. The overall goal of this thrust is to validate the model of wall stabilization and begin feedback stabilization experiments aimed at sustained operation at beta significantly above the no-wall limit.

The improved detection capability of a new DIII–D saddle loop array led to observation of RWMs in several new regimes and showed that even small amplitude (1 to 2 Gauss) saturated modes can be a limiting factor for high-performance H–mode discharges. Since even small-amplitude RWMs can cause a significant slowing of plasma rotation, diminishing rotational stabilization of the RWM.

It was found that the n=1 RWM limits the performance of low-l_i AT plasmas to $\beta_N \le 4\,l_i$ and that plasma rotation was unable to completely suppress the RWM for $\beta_N \ge 4\,l_i$. Plasma toroidal rotation was strongly reduced whenever the detectable RWM is present ($\delta B_r \ge 1$ Gauss). Tests of the q_{min} dependence of rotation threshold were inconclusive since we were unable to vary q_{min} above and below 2 at RWM onset time. RWM "bursting" was observed in DND plasmas near $\beta_N^{no-wall}$ limit.

Initial tests of active feedback control were carried out using the existing C–coil, driven by three new power amplifiers provided by PPPL. These experiments yielded promising results, showing cancellation of the radial magnetic flux leaking through the resistive wall and extending the lifetime of a high beta plasma near the ideal kink stability limit by about 100 ms. Three feedback algorithms were tested: "Smart Shell"; "Fake Rotating Shell"; and "Mode Control."

Experiments were carried out to extend lifetime of plasma above the no-wall limit. An example is shown in Fig. 2.3–1. The high β duration was extended with addition of "derivative gain" in feedback loop (both for "Smart Shell" and "Mode Control" algorithms). Such improvement in high β plasma duration are consistent with VALEN code predictions.

2.3.2. Neoclassical Tearing Mode Thrust

Neoclassically driven tearing modes are metastable modes, destabilized by the helical perturbed bootstrap current arising from a "seed island." The plasma without the NTM is "metastable" in that it awaits sufficient helical perturbation so that the helically perturbed bootstrap current can reinforce the initial seed and cause the mode to grow. As a consequence, the tearing mode island flattens the pressure in the island resulting in a degradation of beta at fixed power and eddy currents induced in the vessel wall can slow rotation leading to further confinement degradation and locking. DIII–D experiments in 1999 extended the range of data for scaling of the instability threshold. A multimachine database including DIII–D, Joint European Torus (JET), and ASDEX–Upgrade data suggests that stability may improve at large magnetic Reynolds number, due to reduced seed island amplitudes. Experiments also showed that current profile modification can raise the threshold in beta significantly higher by eliminating sawteeth as a source of seed islands. A low-beta experiment helped confirm the theoretical foundation for NTM theory by testing classical tearing mode stability, using measured pressure and current density profiles.

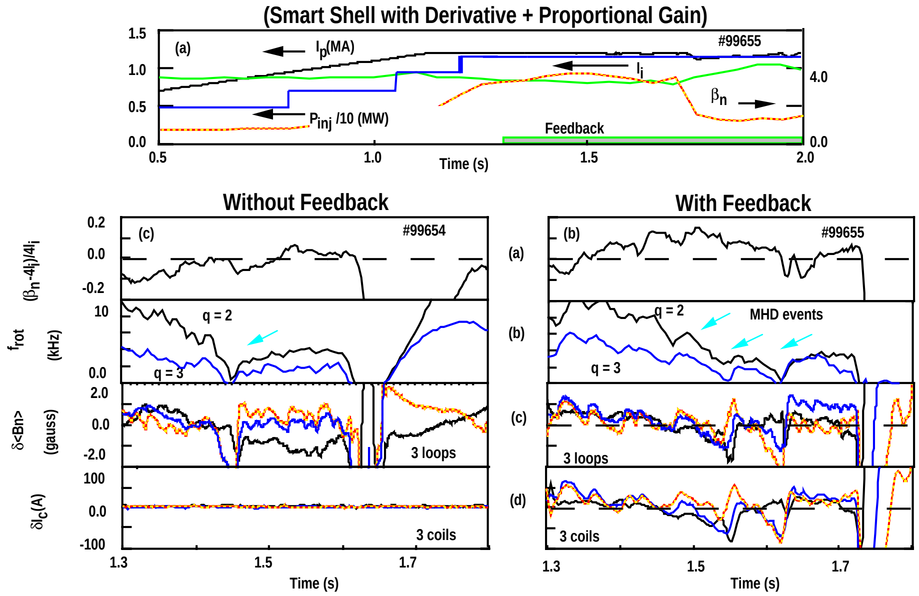

Fig. 2.3–1. Feedback stabilized RWM and extended plasma duration.

For the classical tearing mode, an ohmic discharge with only a 10% duty cycle diagnostic neutral beam was run at very low poloidal beta (β_p) so as to make the bootstrap effect negligible in order to study the classical stability with our excellent suite of diagnostics for code comparison. Tearing mode was induced as q_{lim} was slowly ramped down and code analysis of stability of the MHD equilibria was determined from EFIT. The PESTIII code with a conducting wall at 1.3 of the plasma surface provided the best prediction of stability.

For AT plasmas with q_{min} typically >1.5, the onset of NTMs depends on both β_p and the q-profile. Data was added to our previous work to fill in the values of q_{min} which are sensitive to NTMs, either 3/2, 2/1 or 5/2, and which q_{min} values have "gaps." An unexpected observation was made in discharges with l_i low enough and β_N high enough for slowly growing n = 1 RWM to occur. The RWMs were observed to excite m/n = 2/1 NTMs, whose growth lowered β_N sufficiently that the RWM went away. Thus the RWM acts as the seed for the NTM. This is shown in Fig. 2.3–2.

Finally experiments were done on the scaling of the NTM onset for the 3/2 mode in sawteething, ELMing H–mode discharges and added to the dimensionless database with ASDEX Upgrade and JET. The medium-size tokamaks ASDEX Upgrade and DIII–D have a common scaling as seen in Fig. 2.3–3, while the large size tokamak JET has a different collisionality ν scaling. All three devices show a nearly linear scaling of critical β_N with ρ_{i*} consistent with the original polarization threshold model, but the different ν scaling indicates a more complex behavior than a simple separable scaling law. For test of the polarization/threshold theory and of the role of differential rotation between flux surfaces on the seed coupling, a few discharges were run with the charge exchange recombination measurement of rotation obtained on a very fast time resolution of 0.5 ms. Preliminary analysis of this data shows: (1) differential rotation between the q = 1 and q = 3/2 surfaces becomes small just before the sawtooth crash, thus allowing stronger coupling; and (2) the 3/2 NTM induced at the sawtooth crash rotates in the ion drift direction in the quasi-neutrality $E_r = 0$ frame, this direction and magnitude determining the strength of the polarization/inertial threshold or lack thereof.

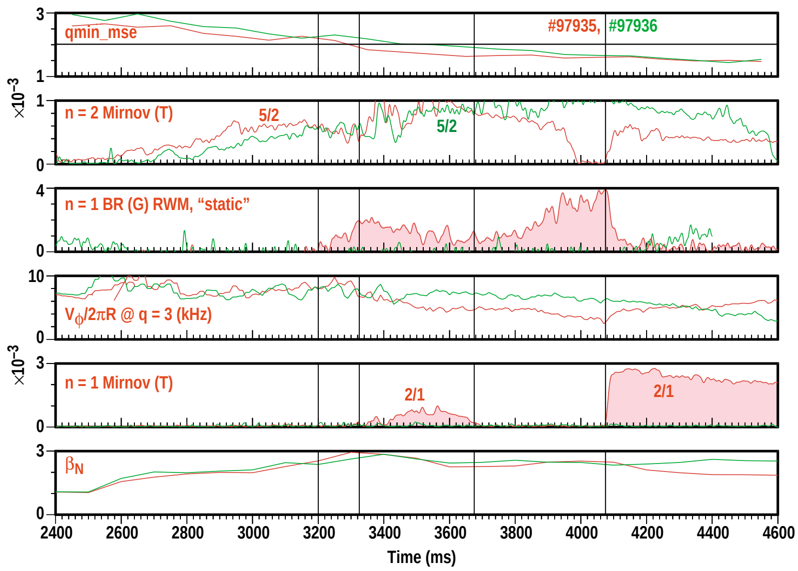

Fig. 2.3–2. n = 1 RWM induces n = 1, m = 2 NTM in AT with $\beta_N \sim 4 \times l_i$.

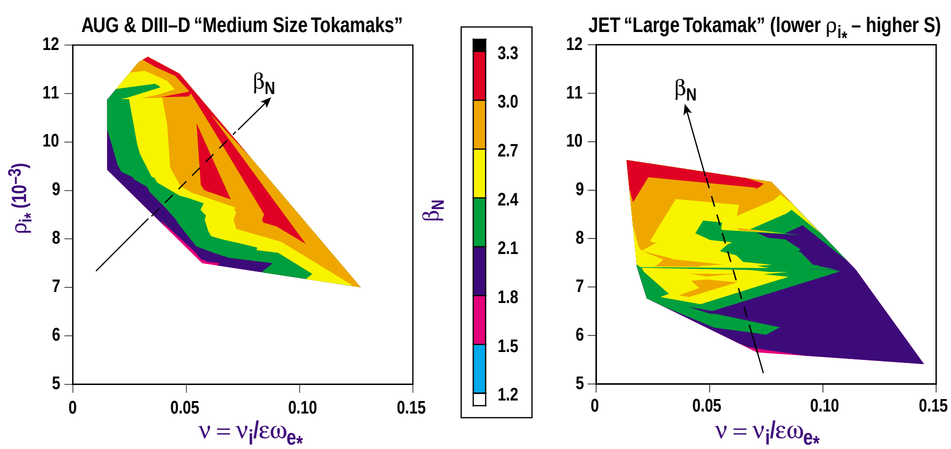

Fig. 2.3–3. Contour plots of critical β_N for sawtooth induced 3/2 NTM.

It is anticipated that with additional microwave gyrotrons will allow the study of off-axis radially localized current drive suppression of NTMs in 2000.

2.3.3. Advanced Tokamak Scenario Thrust

The high bootstrap current approach is the primary AT scenario being pursued by DIII–D in its long-term development of the AT potential. The key to realizing this scenario in steady state is the maintenance of a hollow current profile using ECCD to prevent resistive diffusion of the off-axis current peak. Over the next three years, the EC power on DIII–D will be increased steadily from the present system to an eight-gyrotron system. More importantly, the five newest gyrotrons will be equipped with diamond windows to enable longer (10 s) pulses. Set against this background of a steady buildup in the necessary hardware, this thrust is aimed at a first demonstration in 2001 of a noninductive high-performance AT scenario. Once such a scenario has been demonstrated, optimization of normalized and absolute performance will be carried out. Both physics understanding and direct implementation on larger devices will be key to developing confidence for a true fusion power system.

Progress toward the AT demonstration discharge was significant in 1999. Guided by previous scenario modeling, exploratory experiments to determine the limiting β at parameters suitable for the demonstration (B = 1.6 T, I = 1.2 MA) were initiated. Surprisingly, these discharges made a smooth transition into an ELMing H–mode while maintaining β near the maximum value. The longest duration discharge (β_N H_{89} ~ 9 for 2 s) of this type is shown in Fig. 2.3–4. This discharge exhibits the three typical features seen in most of these high performance discharges. First, the initial rapid increase in β during the ELM-free period is terminated before the first ELM and without the catastrophic loss of performance typical of previous high performance discharges. This saturation is attributed to bursting high frequency instabilities seen on external magnetic coils which appear to be Alfvénic and driven by the NBI fast ion population. Second, the small excursions in β_N (and large ones in H_{89}) are correlated with the growth of very low frequency (<100 Hz) n = 1 magnetic perturbations identified as RWM. These set the limit on β in the quasi-steady phase. Finally, due to resistive diffusion, the current evolves to where a RWM (in this case combined with a tearing mode) grows and irreversibly ends the high performance phase. This points to the focus of next year's campaign which is current profile control and sustainment with ECCD.

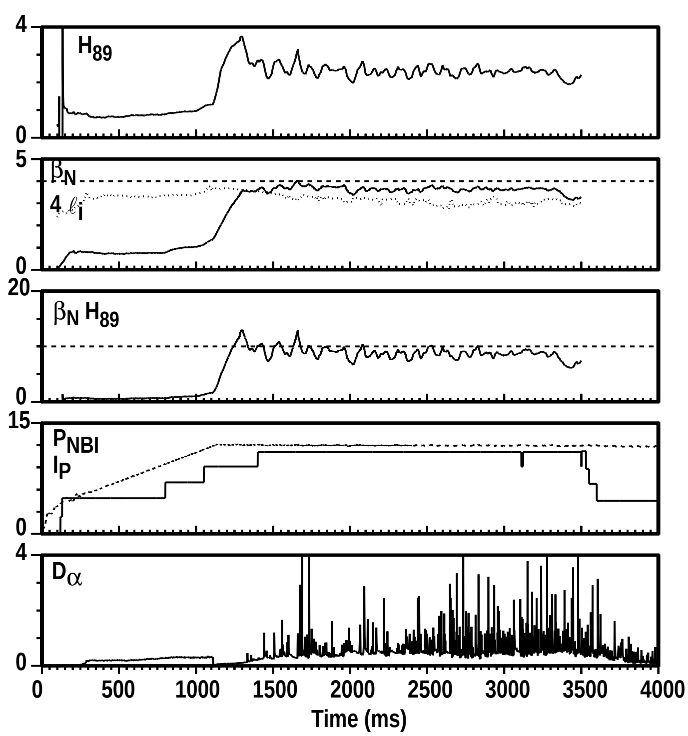

Fig. 2.3–4. β_N H_{89} ~ 9 sustained for ~16 τ_E.

Analysis of the internal loop voltage in this type of discharge indicates that about 75% of the plasma current is supplied noninductively, of which calculations indicate 50% may be attributed to bootstrap current. The analysis shows (consistent with the original scenario modeling) that the edge current is consistent with being entirely bootstrap current, the central current is overdriven by the neutral beams, and the remaining Ohmic current is at the half radius. This implies that replacement of some of the neutral beam power with off-axis ECCD should lead to a fully noninductive current sustainment.

2.3.4. Internal Transport Barrier Thrust

The spatial extent of the internal transport barrier must be extended in order to increase the energy content and the fusion output from within the barrier region. This must be done with the barrier pressure gradient below MHD stability limits.

Experiments conducted in 1999 concentrated on studies of the ITB with counter-injected neutral beams. The experiments were successful in demonstrating that barriers can be formed with counter-NBI, and are broader than their co-injected counterparts. This is not surprising, since with co-injection, the diamagnetic and toroidal rotation terms of the E×B shearing rate oppose in such a way that broadening or increasing the pressure gradient will decrease the shearing rate (Fig. 2.3–5), thereby allowing drift ballooning modes such as the ITG mode to become more unstable. With counter-NBI, the two terms are aligned so that increasing or broadening the pressure profile can actually be stabilizing to such microinstabilities. Although progress was made in exploiting this feature of counter-NBI, it is believed that further optimization with counter-injection may allow further ITB broadening.

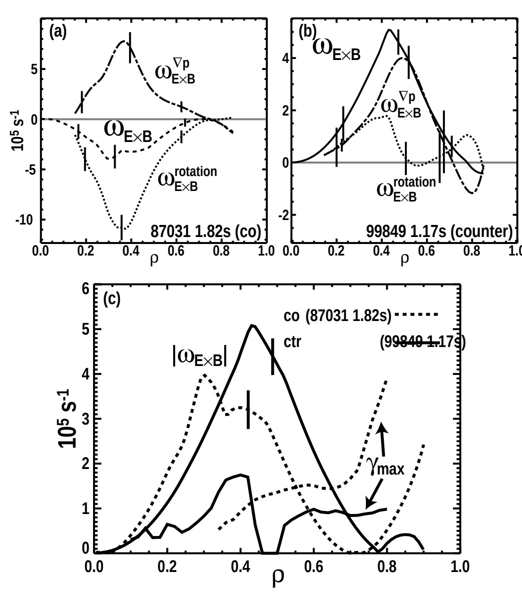

Fig. 2.3–5. The main ion pressure gradient and rotation terms of the E×B shearing rate are opposed with co-, and aligned with counter-injection so that increasing or broadening the pressure profile is stabilizing to drift-ballooning modes with counter-injection.

Another important discovery of counter-injection is that counter-NBCD was effective in arresting the evolution of the current profile during the ITB phases of the discharge. With finer control of the neutral beam power, we believe there is a possibility of simultaneously exploiting both the favorable effect on the shearing rate and the counter-NBCD to expand and sustain a core barrier.

First attempts at producing a transport barrier using high-field-side pellet-injection were also successful, see Fig. 2.2–10. In these experiments, extremely steep barriers were produced in the electron density profile, with $T_i/T_e \sim 1.25$ achieved and maintained for hundreds of milliseconds with counter-injection.

Finally, an experiment was carried out to determine the relationship between the transport barrier location and the location of the minimum safety factor ρ_{qmin}. Incorporating a fast current ramp and high power neutral beam (co) injection very early in the discharge did this. Although discharges were produced with very large $\rho_{qmin} \leq 0.9$, the transport barrier was not formed at this large radius. It is felt that the aforementioned cancellation of terms of the shearing rate may be responsible for limiting the barrier location in such co-injected discharges.

2.3.5. Edge Stability Thrust

The edge stability thrust is aimed at improving steady-state AT performance by eliminating instabilities that originate in the plasma edge. ELMs are destabilized by the large pressure gradient and associated current density that results from the edge-localized transport barrier in H–mode. In 1999, this thrust was aimed at understanding the physics of stability in the H–mode edge region in order to find ways to stabilize these modes or to reduce their impact on the discharge performance.

Several approaches to modification of edge region instabilities were explored. First, access to the ballooning mode second stability regime in the edge region was suppressed by choice of a low squareness discharge shape. This had been shown previously to result in low-amplitude ELMs that made only small perturbations in the discharge core. In this type of discharge, we planned to optimize a high quality ITB with good confinement. In these experiments, an ITB was produced, but the results were dominated by locked modes apparently unrelated to ELMs. Further analysis of these experiments is required to understand the results and determine whether improved results can be obtained with this technique.

In two other approaches, we sought to retain the advantage in H-factor that results from the higher edge pressure pedestal produced when there is edge region ballooning mode second stable regime access, but to prevent or limit the consequences of the edge instabilities. First, the growth of the edge pressure gradient (and therefore the resulting bootstrap current) was modified by impurity mantle radiation in order to keep the pressure gradient from reaching the unstable limit. These experiments were successful in preventing the occurrence of ELMs as shown in Fig. 2.3–6. The impurity radiation reduced the peak edge pressure gradient by 10% to 20%, holding it below the instability threshold. However, the discharges suffered from a radiative collapse resulting from buildup of the injected impurity. We anticipate that the problem of impurity buildup can be solved through pumping with the new upper divertor configuration that will be available starting in the year 2000.

In other experiments, the triggering of ELMs by injection of deuterium pellets was studied. These experiments produced interesting data on the instability threshold as a function of pressure gradient and edge pedestal width. Finally, discharges useful for understanding edge instabilities were produced. These discharges had relatively high performance during the initial portion of the ELMing phase. Analysis is required to understand why good performance was maintained during ELMs in these discharges in contrast to what is normally observed.

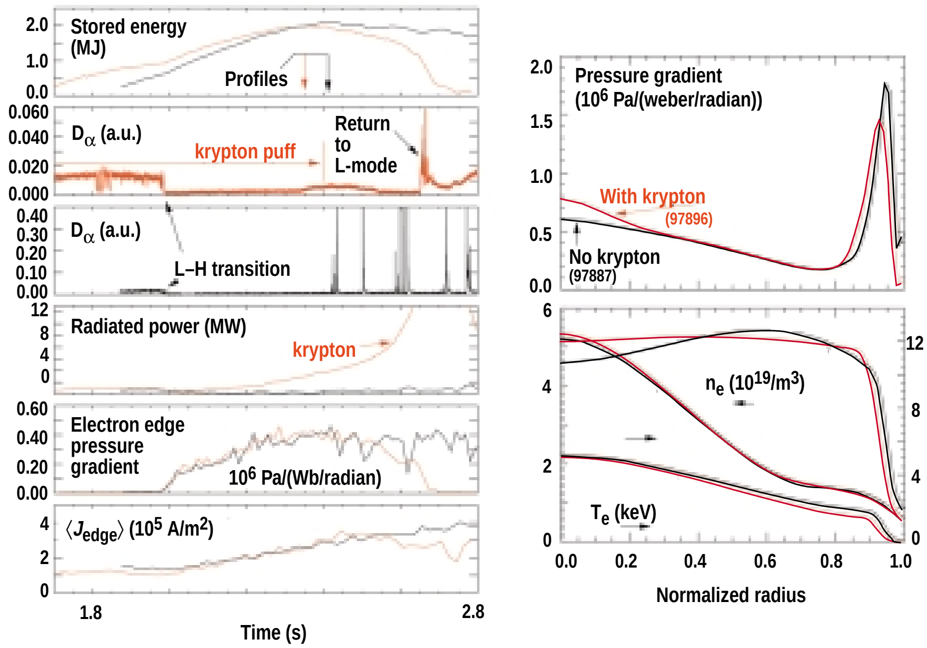

Fig. 2.3–6. With sufficient radiated power, P'_{edge} is reduced and ELMs are not triggered.

2.3.6. Optimal Shape Thrust

This thrust built a deeper understanding of the physics of the coupled regions just inside the separatrix (the H–mode pedestal region) and the scrapeoff layer and divertor regions just outside the separatrix. In the FY99 experimental campaign, we acquired a set of systematic data scans of the edge pedestal, divertor, and other plasma performance measures versus the triangularity, the distance between the separatrices, and the volume of the divertor.

Other experiments systematically varied the up/down magnetic balance of highly triangular, unpumped H–mode plasmas. Changes in divertor heat loading and particle flux, energy confinement, and density operating range in H–mode were observed when the magnetic configuration was varied. To quantify "magnetic balance," we define a parameter dr_{SEP}, which is the radial distance between the upper divertor separatrix and the lower divertor separatrix as determined at the outboard midplane. For attached plasmas, the variation in heat flux sharing between divertors is large for small shifts from one divertor to the other divertor within ±0.5 cm of magnetic balance (Fig. 2.3–7). This sensitivity is consistent with the measured scrapeoff length of the parallel divertor heat flux which can be approximated with a simple model using only the midplane scrapeoff lengths of electron density and temperature, suggesting that divertor processes (*e.g.*, recycling) are not dominating the physics. At magnetic balance (dr_{SEP} = 0), we find that the peak heat flux toward the divertor in the grad-B direction is twice that of the other divertor. The peak heat flux in the outer divertor may exceed that of the inner divertor by tenfold in a balanced double null. The variation of the peak particle flux between divertors is less sensitive to changes in magnetic balance, suggesting that divertor processes are much more important here than in the heat flux case. We believe that these divertor “asymmetries” are driven by E×B poloidal drifts. In detached plasmas, however, we find the heat flux split between divertors to be much less sensitive to the magnetic balance (Fig. 2.3–7).

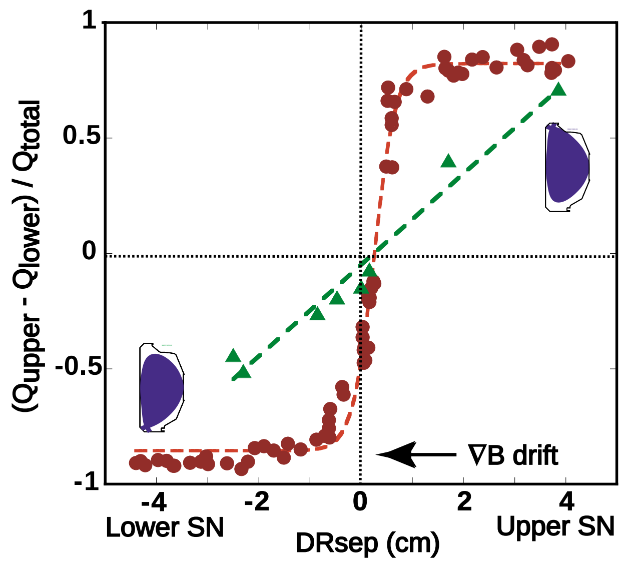

Fig. 2.3–7. Normalized peak heat flux balance as a function of magnetic balance parameter dr_{SEP}. Data from attached plasmas (circles) show a sharp transition from lower to upper heat flux dominance as dr_{SEP} is varied by ±0.5 cm. In partially detached operation (triangles) the transition is much broader indicating the importance of local recycling effects in the divertor.

Another type of experiment performed addressed the desire to achieve the performance advantages of high triangularity operation with the core plasma volume maximized and the divertor volume minimized. In low triangularity single-null divertor configurations, only the primary X–point is present inside the vacuum vessel. As triangularity is increased the location of the secondary X–point, which maps at the midplane to a flux surface radially outboard of the primary, moves from outside the vacuum vessel to inside and divertor physics (recycling, target heat flux, *etc.*) becomes important in this secondary divertor. Since the secondary divertor takes up volume that could be used for the burning core plasma, the focus of this experiment was to determine the minimum secondary divertor volume consistent with good core, pedestal, and divertor performance. These experiments indicated that performance may be affected when core plasma screening of neutrals in the secondary divertor is reduced. The heat flux in the secondary divertor increased when the secondary divertor target began to act as a heat flux limiter as the power scale length mapped to the divertor target.

In this thrust, a new high-density operating regime with high confienment was discovered by combining gas fueling and divertor pumping. These experiments achieved densities 40% above the conventional (Greenwald) limit with energy confinement 90% above L–mode scaling. Previous conventional gas puff fueling of unpumped H–mode plasmas lead to loss of energy confinement at high plasma density. Divertor pumping maintains the temperature in the X–point region while the H–mode pedestal temperature decreases and the edge pedestal density increases with gas puffing. Maintaining high X–point temperature seems to avoid a regime in which confinement is reduced.

The high density good confinement discharges on DIII–D show spontaneous repeaking of the density profile edge pedestal pressure. The usual decrease in energy confinement with gas puffing is associated with a reduction in edge pedestal pressure density as a result of the decrease in edge pressure gradient at low temperature. The pressure gradient decrease is consistent with what would be expected for a transition from ideal to resistive tearing modes. The effect of the reduction in pressure pedestal is through stiffness of the temperature profile which is apparent in the high density regime on DIII–D. The energy confinement is also reduced in discharges with stiff temperature profiles when the density profile broadens at fixed pedestal pressure. The density profile peaking occurs under conditions that reduce the central temperature suggesting the neoclassical Ware pinch.

2.4. NEW COMPUTATIONAL INFRASTRUCTURE FOR DATA ANALYSIS

Enhancements to the computational infrastructure at the DIII–D National Fusion Facility in FY99 focused on both hardware and software improvements to increase the data analysis throughput rate and data retrieval rate. The underlying philosophy behind these development efforts is uniformity, both in terms of the look and feel of graphical user interfaces (GUIs), in terms of access methods to analyzed datasets, and access to existing computer power.

The conversion from OpenVMS to Unix-based MDSplus was successfully completed in FY99. A new Unix-based computer system with 100 GB of storage was purchased to handle this conversion. The data stored in MDSPlus continues to increase with presently 5000 archived shots representing 40 GB of analyzed data. The benefits of Unix MDSplus are faster serving of data and easier integration into the DIII–D Unix analysis environment. This analyzed data repository combined with the 3 TB raw data mass storage system and the fast network connections gives any member of the DIII–D National Team rapid 24-hour, 7 days a week access to all DIII–D data regardless of location. This rapid accessibility is a dramatic improvement over past capabilities.

The DIII–D tokamak operation was greatly enhanced by the adoption of the Electronic Logbook from C–Mod along with their interface program. Entries into the logbook can be made by any staff member and are divided into broad headings covering the experiment, diagnostics, and engineering. The logbook provides the ability to see comments from others in real time and the ability to rapidly query past entries. The electronic logbook allows the DIII–D National Team to monitor, from anywhere, the shot-to-shot progress of the experiment. Adopting the C–Mod system provided the scientific staff new capabilities faster then creating this system. Software engineers at C–Mod, DIII–D, and NSTX continue software sharing in other areas.

Work on data viewing and analysis tools has focused on an efficient and uniform GUI design with object-oriented programming for maximum code flexibility and access to both DIII–D PTDATA and MDSplus data. The uniform GUI design decreases the nonproductive time a new researcher must spend learning a new system. Also, existing users do not need to remember a new interface every time they switch analysis tools. GUI viewing tools are being written in Interactive Data Language (IDL), a commercial product for scientific data manipulation and visualization. To facilitate this tool design a new object-oriented IDL-based graphics library, GAPlotObj, was created and has become a fundamental component of the new DIII–D viewing tools, providing a uniform GUI for graphical data manipulation. The GAPlotObj graphics library allows for multiple 2–D and/or 3–D graphics with cursors for data readout, zooming, panning, slicing, and data selection for manipulation. Two main viewing and analysis tools, EFITTools and ReviewPlus, have been created that use the GAPlotObj graphics library. EFITTools combines the ability to perform an interactive EFIT, a kinetic EFIT, a time-dependent EFIT, and the visualization of any EFIT calculation under one GUI umbrella. The ReviewPlus tool is a general-purpose data visualization program that provides interactive 2–D and 3–D graphs of data stored in either PTDATA or MDSplus.

Computer power for data analysis is provided by a central Unix Server and a load balanced cluster of eight Unix workstations. The interactive load balancing capability was successfully implemented this year and has more than tripled the Unix computer power available to the researcher without having to purchase any new workstations. Interactive load balancing is accomplished with the commercial software LSF Suite 3.2 from Platform Computing. This software operates in a heterogeneous computational environment thereby combining all of the newer Unix-based computers into one central processing unit (CPU) cluster. The benefits of such a cluster are: (1) all computers are easily and transparently available to all researchers, (2) CPU upgrades are as simple as removing one workstation and adding another, and (3) a new on-site collaborator can easily add their own computer to the CPU cluster. Such an implementation has been possible because of the fast 100 BaseT network connecting workstations, the central file server that is available from all workstations, and the unified data access methodology. Computer power has also been expanded by the porting of the MDSplus client to the MacOS thereby allowing the DIII–D staff to use their fast Macintosh G3 and G4 systems to perform data analysis. Typically, users are running IDL on the Macintosh and taking advantage of EFITTools and ReviewPlus or their own IDL programs.

Enhancements to off-site data analysis have been numerous in FY99. To alleviate the ever increasing load placed on our CPU resources by off-site collaborators, our analysis environment encourages usage of off-site computers. Such analysis is simplified by the availability of raw and analyzed DIII–D data via the MDSplus client/server interface. Additionally, the new IDL-based viewing and manipulation tools are being distributed to remote collaborators either in the form of compiled binary executables or from a source code management system (CVS). Creating tools in IDL has the added benefit of being able to move among different operating systems with minor modifications. These tools have presently been installed at C–Mod, NSTX, SSPX, and JET, as well as DIII–D.

Another aspect of remote data analysis is the ability to hold meetings to discuss on-going analysis. We have enhanced our capability to support remote meetings. Our current capability includes two conference rooms near the staff offices that have been equipped to share a Polycom ShowStation IP. This device acts as a viewgraph machine for the researcher in the conference room and a Web server for those not in the conference room. The off-site collaborator can see the viewgraphs via a Web browser or, if their remote conference room is equipped with another ShowStation, the viewgraphs can be projected on their screen by their ShowStation. Complementing the ShowStation is a Polycom Viewstation that handles both ISDN and IP-based videoconferencing. Multipoint video conferences are handled by an ESNET bridge. This equipment allows remote participants to easily hear presentations and audience comments during meetings without burdening the local users with the need to manually distribute and adjust microphones. Audio and video conferencing are synergistic with the previously mentioned ShowStation IP for viewing materials in that they present high quality audio along with video views of the meeting. The combination of A/V conferencing with the interactive presentation nature of the ShowStation IP provides a powerful remote collaboration capability.

2.5. NEW DIAGNOSTICS

Several new diagnostics were commissioned in FY99, the central Thomson scattering system being the most notable. Another group of diagnostics were designed and the installation on DIII–D started in FY99. Further, a study to determine the appropriate measurement technique for detailed edge current measurements was commissioned and completed.

Due to port access restrictions, it is very difficult to send a probing laser beam through the center of the DIII–D plasma. Because of this, the DIII–D Thomson scattering system has until this year produced electron temperature and density profiles only in the outer 70% of the radius of a typical plasma. While this limitation has always been of concern, the prominence of core transport barriers in recent years in high temperature magnetically confined plasmas brought this short coming to a critical level. We therefore designed and built a horizontal laser beam line (the older core system has a vertical beam line). The collection optics for the new beam line are shared with the older vertical beam line. This geometry allows cost effective central measurements. The system was completed in the first quarter of FY99 with first plasma data taken in December of 1998. The new system has six spatial channels, the entire Thomson scattering diagnostic has 44 channels.

In FY99, a number of new diagnostics were commissioned with operation of the systems to start in January 2000. These included diagnostics required to characterize the upper divertor modifications that will be completed in the first quarter of FY00. We completed the design and began the fabrication and installation of an array of fixed Langmuir probes, five magnetic probes, fast pressure gauges in the divertor plenum and private flux region, and a visible TV system for the new upper divertor. In addition to the upper divertor diagnostics, the external saddle loop array was expanded from six loops around the midplane to 30 loops. Twelve loops were added above the midplane and twelve below. These loops will be used in year 2000 to study the poloidal structure of RWMs with the eventual goal of using them to control feed back coils to be built above and below the midplane.

It was determined in FY98 that the MSE diagnostic was unable to adequately measure the edge current profile in high performance discharges (discharges near stability limits) due to electric field effects on the measurement. Modeling studies indicate that the edge current profile plays a critical role in stability of many discharges of interest to the DIII–D program. An evaluation was undertaken and completed in FY99 to determine the best measurement technique with the intention of starting an engineering design in FY00. The conclusion of the study was that a Li beam polarization diagnostic would be the most effective in terms of resolution, time response, and cost. We expect to start work on the diagnostic in January 2000.

3. FACILITY OPERATIONS

3.1. OVERVIEW

FY99 was a very productive and successful year for the Operations Group. During the year, the 100,000th shot was recorded with every indication that the facility can continue to support a strong and productive program well into the next millennium. Activities followed a pattern that is becoming well established as effective for meeting the needs of the program; Operations during the months of January through July and upgrades, refurbishment, and major maintenance tasks during the remainder of the year. In the first three months of the fiscal year, major in-vessel installations and calibrations were completed. The tokamak was returned to operations in January, and 74 days of operations for the research program were carried out. Following the completion of the research program, the vacuum vessel was again vented and installation of the upper inner divertor cryogenic pump and baffle was begun along with a number of other upgrades, refurbishment, calibration, and maintenance.

Highlights of the FY99 activities include: the initiation of resistive-wall-mode (RWM) feedback experiments which were accelerated into the 1999 campaign, initial operation of the first of the new 1 MW class 110 GHz gyrotrons with a diamond window allowing long pulse operation, and the addition of a new Hierarchical Storage Management (HSM) system for the storage of DIII–D data with rapid access. A new addition to the DIII–D facility was begun and essentially completed during the year to provide space for the new electron cyclotron heating (ECH) equipment and other program needs. The DIII–D program continues to support an active education program focused on introducing students to science, fusion energy, and career opportunities in research. The DIII–D program continues to pay careful attention to safety and radiation exposure. Over the past several years, the accident rate for the DIII–D program has been noticeably below that of comparable laboratories and industry.

Work on a number of major new systems was completed at the beginning of the first quarter of FY99. Major changes included a new central Thomson scattering system (complementing the existing core and divertor systems), inside launch pellet injection, and the addition of boron nitride Faraday shields to two fast wave antennas. The vessel was closed and five weeks of calibrations and startup activities were completed on schedule for the beginning of the research program in early January. Much of this success is owing to comprehensive planning efforts.

The FY99 Research Program was carried out during the months of January through July. The planned 74 days of experimental operations were carried out with an availability of 75% which is consistent with our 10-year historical level. A new neutral beam continued to perform with an extremely high level of availability. The addition of a beam substitution algorithm which automatically replaces a failed beamline with an unused beamline resulted in “saving” a number of discharges that would have otherwise been lost. During the year, a number of important experimental capabilities were made available. The capability to do RWM mode experiments using the set of six existing picture frame magnetic field correction coils and three new wide band current regulators was initiated. This activity was accelerated by six months into this year to take advantage of a window of opportunity in the program. New inside launch pellet injection capabilities were commissioned. The new multiple-input multiple-output version of the plasma controller was implemented. Refinement of the operation of the vessel heating system along with the addition of a small boost heater in the air circulation circuit resulted in considerably improved efficiency of the vessel bake cycle, and improved heating of the outer wall ports and attached systems.

Following the end of the operating year in July, the vessel was opened for another period of major installation. The major tasks included the installation of the upper inner divertor cryogenic pump and associated baffle, installation of the poloidally and toroidally steerable ECH launcher provided by Princeton Plasma Physics Laboratory, and a number of diagnostic modifications, most notably on Thomson scattering, charge exchange recombination, and motional Stark effect. This vent was completed on schedule at the end of the calendar year.

Considerable progress was made in the radio frequency programs. A 1 MW class 110 GHz diamond window gyrotron from CPI was brought into operation. This gyrotron along with two 2-s gyrotrons, one from CPI and one from Gycom, brought to three the number of 1 MW units available to DIII–D. Testing of all three tubes was completed, but unfortunately age-related failures of the two CPI tubes resulted in power never being simultaneously applied to tokamak plasmas. The final output stages of the two ABB 2 MW ion cyclotron range of frequencies transmitters were rebuilt by the manufacturer to increase their power capability, but unfortunately they are still troubled by spurious resonances which require time-consuming painstaking adjustments to prepare for operation at any given frequency.

Continued and enthusiastic attention was paid to safety and radiation management. The activities of a proactive safety committee continued wherein all safety-related matters are addressed. Continued attention to safety has resulted in a relatively low number of accidents. A summary was put together for Department of Energy (DOE) safety specialists showing how the DIII–D safety program coupled with the company safety program comprises an Integrated Safety Management (ISM) Program working to protect General Atomics (GA) staff and collaborators. Under the radiation management program, challenging as low as reasonably achievable (ALARA) goals were set and largely met. The in-vessel work beginning in late FY99 required particular planning to reduce the levels of radiation from activation of the tokamak vessel and other components experienced by employees working inside the vessel.

3.2. TOKAMAK OPERATIONS

FY99 was a very successful year for tokamak operations. The vent that was started in August 1998 was completed on schedule, operations ran smoothly during the year, and many new systems were brought on-line following the vent and during the year that were used productively during the experimental campaign. A summary of the yearly highlights is shown in Fig. 3.2–1.

At the beginning of FY99, the vessel was open for installation of a number of new systems. The primary vent tasks included the addition of a new central Thomson scattering system, installation of new, boron nitride coated Faraday shields for two of the fast wave antennas, and installation of inside launch pellet injection hardware. The vent was completed on schedule in mid-October and all the new systems performed well during the year's operation. The physics program was conducted from early January until July after which the vessel was vented again in August for the major installation of the upper inner cryopump.

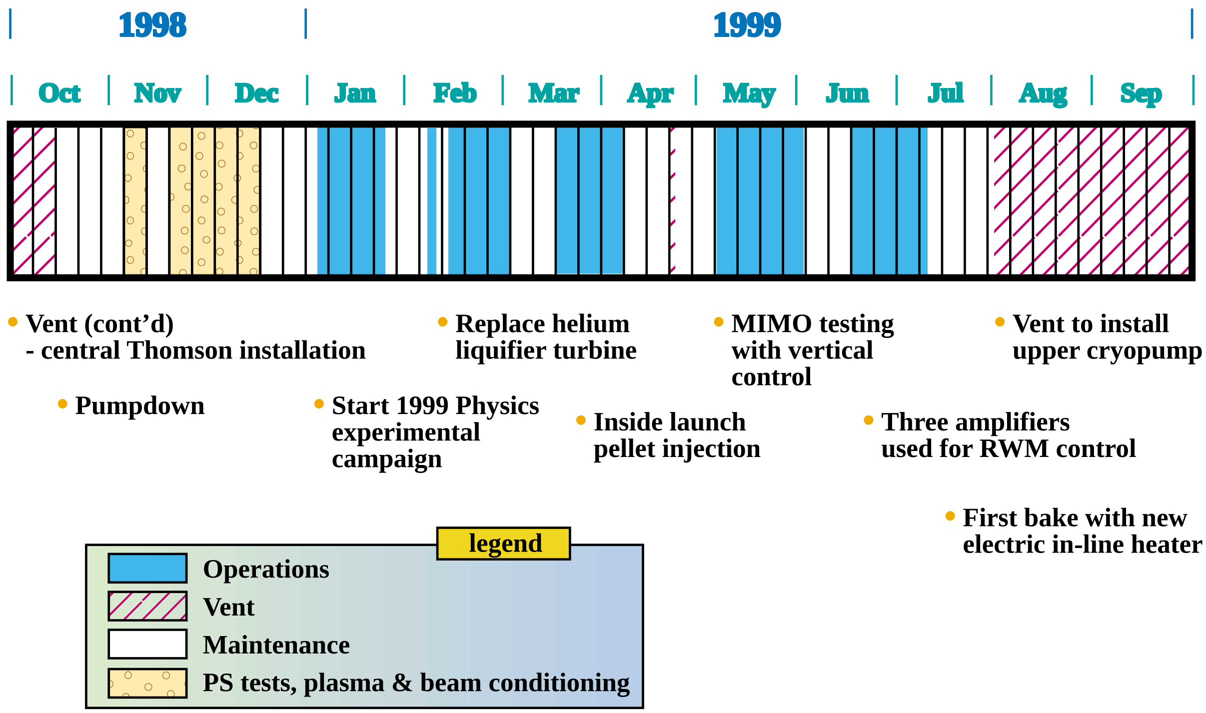

Fig. 3.2–1. DIII–D FY99 operational highlights.

During FY99, the facility was used for a total of 264 days with physics experiments conducted on 74 days. The tokamak was operated for an additional 39 days for a combination of diagnostic calibration, systems checkout and commissioning, and plasma cleaning following the vent. An additional 21 days were used for vessel conditioning including high temperature baking and boronization. A full breakdown of the year is shown in Fig. 3.2–2.

Machine availability for the year was 75%, consistent with our historical level (Fig. 3.2–3). Significant down time was caused by a helium liquifier turbine failure and intermittent failures of the toroidal field power supply caused by aging IC sockets and edge connectors. A total of 1986 shots were fired during experimental operations.

Many of the improvements that were made to the tokamak and associated hardware in FY99 improved operational efficiency and reliability. A system of boltless patch panel pins was developed that permits major changes to the magnetic configuration to be performed in minutes rather than hours and this has significantly increased our operational flexibility. A major programming effort has led to the development of the Fault Identification and Communication System code (FICS) to automatically identify and warn the machine operators of system failures or of degrading system performance before they cause lost time. Following a major study of our vessel heating system, an electric heater was added to the air system to supplement the vessel inductive bake system. The new system can now heat the vessel to 350°C in under 7 h compared to 14 h in previous years. This permits more effective vessel conditioning with significantly reduced manpower requirements.

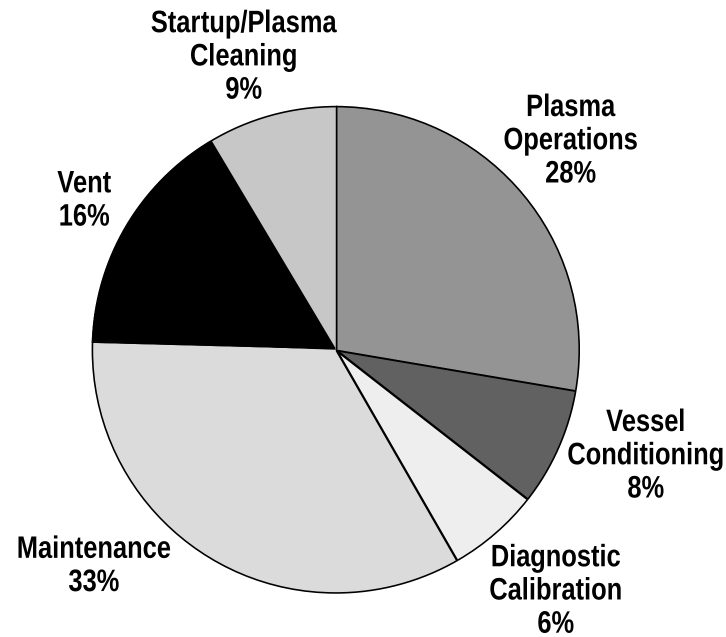

Fig. 3.2–2. Facility utilization for FY99.

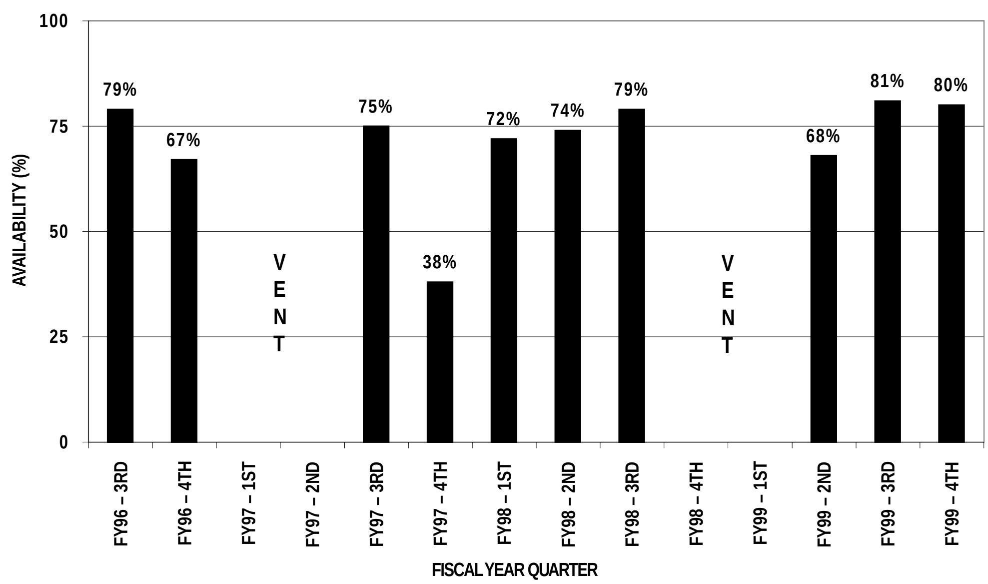

Fig. 3.2–3. Tokamak availability FY96 through present.

A number of safety issues were addressed during the year. Failure Modes Effects Analysis techniques were applied to the diborane system to analyze critical equipment failure modes. Both single and double failure mode effects were analyzed. Three items were identified that will allow us to restore safe conditions in the event of a power outage or failure of the dedicated boronization vacuum pump. A second safety issue that was addressed was the development of a new system that automatically checks the computer entry log and prevents the resumption of machine operation if someone is still logged in the machine area. This automatic system replaces the previous system that relied solely on administrative checking.

Two major highlights in the operation of the tokamak included the testing of the multiple-input multiple output (MIMO) control algorithm and the addition of new amplifiers for control of the resistive wall mode (RWM). Following extensive off-line testing, the first machine tests of the MIMO system were performed in April and May. The new MIMO controller provided vertical stability and excellent steady state accuracy and dynamic response of both the X–point and plasma shape. In addition, as part of the system development, a complete closed loop simulator was developed and this should permit off-line control system development and optimization. The first set of experiments to test closed loop feedback control of the RWM were also conducted in the third quarter. This was enabled by the addition of a single switching power amplifier in May and the installation of two additional amplifiers in June, more than six months ahead of the scheduled date for the full system installation.

3.3. HEATING SYSTEMS

3.3.1. Neutral Beam Operations

Sixty-eight days of plasma heating experiments were supported by neutral beams in FY99. During November and December of 1998, several additional weeks of beam system operation were required to condition ion sources, perform beam power calibrations, and support DIII–D vessel cleaning and diagnostic calibrations after a four-month shutdown. In the fourth quarter, to support special needs of two experiments, beam systems were operated in hydrogen for one day and in helium-3 (first time in DIII–D) for two days.

Several improvements to the beam system were implemented in FY99. These included an upgrade of the beam modulation cycle capability, installation of the beam total on-time protection circuit, setting of beam pulse length by the physicists, and automatic beam availability calculations and recording. These upgrades and improvements have enhanced reliability and availability of the beam system in supporting DIII–D plasma physics experiments.

The availability of the neutral beam system by month is shown below in Fig. 3.3.1–1. The “available” category is based on the beam system requirement requested by the physics experiments. The difference between the “available” and “injecting” categories represents beam systems which were available but were not used for injection during physics experiments. The various causes for downtime are shown below in Fig. 3.3.1–2.

3.3.2. ICRF Operations

ABB/Thomcast conducted a major retrofit of their two ICRF transmitters because of deficiencies which resulted in three tube failures. After analysis by GA, ABB, and Thomson Tube it was concluded that the original final amplifier tubes were unable to meet the required power specifications without premature failure. Thomcast offered to conduct the four-month retrofit work on a warranty basis.

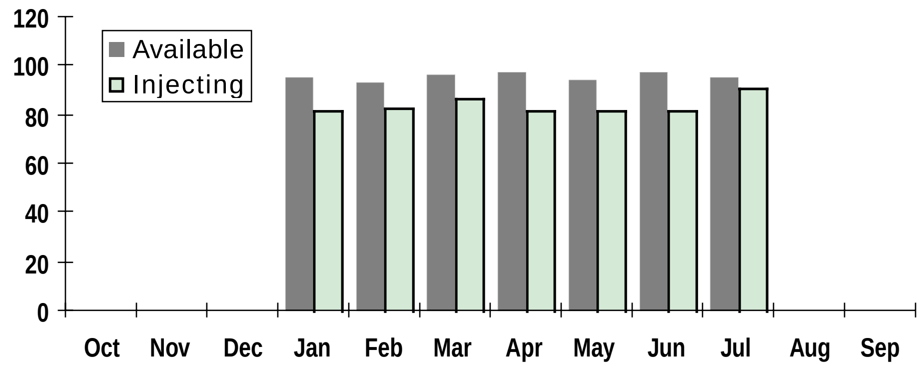

Fig. 3.3.1–1. Neutral beam availability by month.

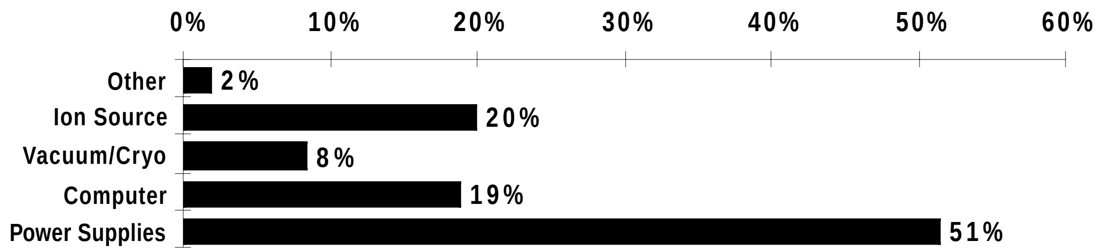

Fig. 3.3.1–2. Causes of downtime by category (percent of total down time).

After completion of the work, initial attempts to run the first system resulted in oscillation in the driver. The driver cavity was modified to lower the resonance somewhat in frequency and to lower the Q. This enabled 1.9 MW operation at 83.24 MHz for 20-s pulses into dummy load. Early in this process, the physics community requested that all three transmitters (FMIT, ABB#1, and ABB#2) be capable of operating at ~60 MHz. This meant that the Thomcast engineer had to spend considerable time retuning both ABB transmitters to operate at this frequency. The systems have demonstrated greater than 1.8 MW at this new frequency into dummy load.

New outer dc breaks, of PPPL design, were installed on the 0 and 180 deg systems. During initial moderate power validation of the breaks, it was determined that an additional outer shield was needed to lower leakage for operation at 60 MHz. All three ICRF systems were used to support physics operations at various frequencies. After the DIII–D shutdown in August, the final amplifier tube from the FMIT transmitter was removed and sent to Massachusetts Institute of Technology (MIT). MIT had experienced a failure in one of their tubes and had no spares on hand. GA will receive a replacement tube direct from Eimac as soon as it becomes available.

3.3.3. ECRF Operations

The year was highlighted by the installation and initial operation of the prototype of a new generation of 110 GHz gyrotrons in the 1 MW class equipped with synthetic diamond output windows and generating Gaussian rf beams directly. This CPI gyrotron, dubbed Toto, is a rebuilt version of a development gyrotron and was designed to qualify the window and beam forming technology required to generate over 1 MW for pulses up to 10 s in length and to produce a well-focused

Gaussian beam suitable for injection into waveguide. Tests verified that the beam quality was excellent and the performance of the diamond window was as expected.

The addition of Toto brought the DIII–D gyrotron complement to a total of three units; the Gycom gyrotron, Katya, producing 800 kW for 2.0 s, a second CPI development gyrotron, Dorothy, which had been tested to 1.09 MW for 0.6 s pulses and 0.75 MW for 1.3 s pulses, and Toto. Before the full power of this set could be brought to bear in experiments, both Toto and Dorothy suffered unrelated failures. Toto vented during operations due to failure of a braze in the collector area and Dorothy suffered a filament failure. Both gyrotrons were sent to CPI, where they were successfully repaired, and then they were returned to DIII–D. Toto is operating well and being conditioned for return to service and Dorothy is being held in reserve as a spare. In FY99, limited experiments, described elsewhere in this report, were performed using Katya and the two CPI gyrotrons before their failures.

Specialized hardware unique to the evacuated waveguide in the DIII–D system was developed and tested. A polarimeter capable of measuring the elliptical polarization of the high power rf beam at any miter bend in the evacuated transmission line was used to check the performance of the polarizers and other transmission line components under actual service conditions. A second development was a mode conversion analyzer used to verify the accuracy of the alignment of the rf beam at the waveguide input. This device showed that the operational technique used to align the beam yielded excellent accuracy and minimal mode conversion. A prototype 1 MW cw dummy load developed by Calabazas Creek Research was tested at limited power with good results and a compact mode conversion dummy load developed at GA was also tested successfully. A scanning launcher assembly designed and built by PPPL and capable of varying both the poloidal and toroidal injection angles installed in DIII–D in early FY00. This launcher will make possible a new group of experiments aimed at maximizing electron cyclotron current drive (ECCD) efficiency, controlling the current density profile, mitigating magnetohydrodynamic activity and studying transport in the electron channel.

The DIII–D ECH system is being upgraded both in the number of gyrotrons and the available single unit power. Two Gycom gyrotrons with performance that should match Katya were acquired from the Canadian Tokamak de Varennes project and procurements have been placed for three 1 MW 10 s gyrotrons from CPI with the first arriving in early FY00. At least four of the gyrotrons will be available for experiments in FY00.

3.4. COMPUTER SYSTEMS

During FY99, there were 3,488 tokamak shots containing 577 Gigabytes of raw data. The largest shot was 305 Megabytes, a size increase of 14% over the previous year. Also the DIII–D shot number reached 100,000 with no software problems with the change to a 6-digit shot number. Work this year focused on software/hardware enhancements to data acquisition, Thomson Scattering, and Plasma Control; improving network bandwidth; full deployment of the HSM system and changes to data flow topology; and preparing for the year 2000 transition.

Work progressed on the new Compaq Alpha data acquisition computer to replace the old Modcomp data acquisition computer to permit faster data acquisition and access. However the CAMAC software driver for the new system (being developed by Kinetic Systems) ran into many problems. A working version of the driver was not received until the end of FY99. Fortunately, the old computer performed very reliably. To improve performance, data access was done through another computer, thus substantially reducing the load on the system.

The simplified PTDATA-based Thomson Scattering data analysis code was completed. The new software consists of a raw data processing (acquisition) program, temperature and density profile generation programs, an analysis graphical user interface, and writing of profile results to the MDSplus data system. A new control computer was installed and several analysis programs were implemented.

FY99 DIII–D operations startup provided an opportunity for testing and verifying many changes made to the plasma control system (PCS). The isoflux elongated limiter algorithm was finished. The basic neutral beam substitution capability was added to the PCS which allows substituting spare neutral beams if the primary beamline ceases operation before the end of its designated on time. New code was added for performing RWM feedback control, a new matrix editor user interface, and fixes to the parameter data routines. Towards the end of FY99, efforts shifted to planning for a major upgrade of the PCS. Several possible real-time solutions were investigated. Support was also given to NSTX at PPPL to help with a customized version of the PCS for NSTX use.

Three major networking improvements have provided substantially improved performance and reliability which enhanced DIII–D operations. First, the Fusion Cisco router was upgraded to a newer and much more powerful model. Secondly, the Fusion office buildings were wired with Category 5 cable so that Fast Ethernet could be supported, and Fast Ethernet capable computers in the office buildings and computer center were connected. Thirdly, Fast Ethernet was expanded within the DIII–D facility.

We responded to a number of security directives. The frequency of unauthorized network probes from the outside has escalated substantially throughout the year. A hacker broke into a new Sun computer that had only recently been brought up and had a newly discovered security weakness. Appropriate agencies were notified and the system was removed from the network until a secure system was installed. Further security enhancements are being implemented.

All DIII–D raw data has now been migrated into the HSM system for storage and retrieval. All three levels, magnetic disk, optical disk, and DLT tape are being used, and data is now automatically restored from optical or tape media without operator intervention. With changes in data flow topology, data now moves automatically from its origin node (on a diagnostic) to the HSM system, and thus never leaves disk or becomes unavailable. Data is now automatically archived with one copy kept on site and a second copy stored offsite for security. Several improvements were made to the raw data access routine, to improve the speed that users can access data.

All UNIX and VMS computer systems were made Year 2000 compliant.

The DIII–D year-end review meeting was broadcast over the internet using a Polycom Streamstation, also used was a Polycom Viewstation for video conferencing, and a Showstation for displaying viewgraphs to a web browser. Based on this experience, a home-grown system is being implemented in FY00.

Other work this year included: retirement of the old general purpose VAX-VMS computers which have been replaced by new Alpha-VMS systems; rewriting code for the residual gas analyzer; changes to the primary timing code to get neutral beam substitution information; porting of a wide variety of codes to a LINUX test system; evaluating the feasibility of upgrading the bolometer data acquisition computer to a LINUX-PC; deploying the enterprise-wide Netbackup system to most computer systems; moving e–mail handling to a new server; installing and configuring a new server to be used for MDSplus processed data by physics; and adding more tape drives to handle increased backup requirements and HSM data management.

3.5. DIAGNOSTICS OPERATIONS AND MAINTENANCE

Diagnostic efforts in FY99 focussed on three broad areas. The first was physics plasma operations support, the second was diagnostic calibrations, and the last was refurbishment of existing systems.

During the first quarter of FY99, the diagnostic set was calibrated. The calibrations included three weeks of double shifts inside of the vessel and a week of dedicated machine operations for calibrations requiring other parts of the tokamak such as power supplies, neutral beam injection, or gas injection. Operation of the diagnostic set during the research campaign occupied much of the diagnostic resources during January to June.

Two major and several minor diagnostic refurbishments were undertaken in FY99. Several significant tasks were initiated in an effort to improve the alignment of the Thomson scattering diagnostic by means of a mechanical alignment target in the divertor and new beam steering mirrors and external alignment points for all three systems. Also several tasks to improve the stray light in the divertor Thomson scattering diagnostic were started by means of new in-vessel baffles and beam dump.

In the continued effort to replace the aging detectors in the edge CER system, new CCD cameras were ordered and two cameras were received and integrated into the system. A total of eight cameras are on order and will be used to replace all of the old edge detectors.

The toroidal x-ray system was reinstalled during the research campaign in April with new beryllium windows with an improved design. Data from the improved system was available for the last two months of operations.

3.6. SUPPORT SERVICES

3.6.1. Occupational Safety

The fusion safety program provides for the safe operation of the DIII–D facility and for a safe working environment for employees and visitors. The outstanding DIII–D safety record for the last several years is illustrated in Fig. 3.6–1. Special programs address high voltage and high current, high vacuum systems, ionizing radiation, microwave radiation, cryogenics and the use of power equipment and machine tools. DIII–D is provided support by GA’s Licensing, Safety, and Nuclear Compliance (LSNC) organization and GA’s Human Resources Safety organization in areas such as health physics, industrial hygiene, environmental permitting, hazard communication, hazardous waste, and industrial safety.

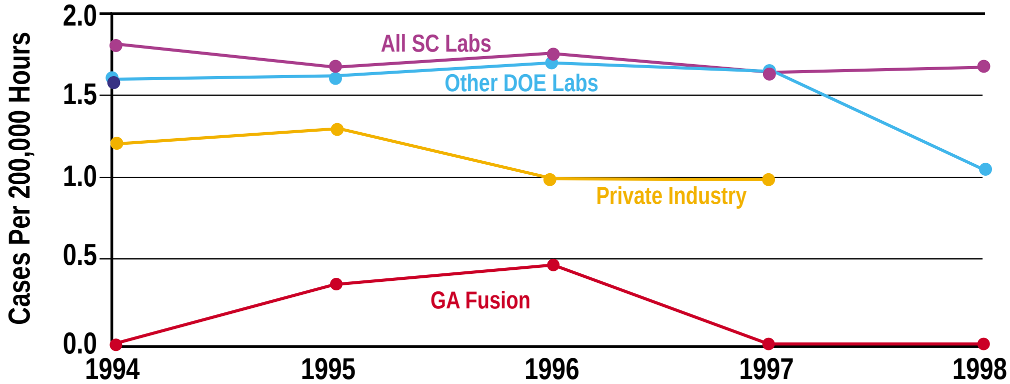

Fig. 3.6–1. Accident case rates for industry and DOE laboratories.

The Fusion Safety Committee focuses on addressing both immediate and longer range safety needs and goals. The Safety Committee meets twice a month and solicits specialized help from five fusion safety subcommittees during reviews of lasers, electrical systems, vacuum systems, the use of cryogens or chemicals. In addition, two individuals are dedicated full-time to on-site “preventive” safety involvement. Their activities include writing and reviewing procedures, developing and conducting special training classes, conducting inspections and follow-up, and providing continuous oversight to assure compliance with established safety policies, procedures, and regulations.

The DIII–D Emergency Response Team (consisting of individuals involved directly with maintenance and operation of the DIII–D equipment) were trained in cardiopulmonary resuscitation (CPR), first aid, use of self-contained breathing apparatus (SCBA) and the use of fire extinguishers, evacuation and crowd control, and facility familiarization. This team can respond within seconds to provide immediate assistance until outside emergency assistance arrive.

All new employees and collaborators must go through a thorough and comprehensive safety indoctrination by the Senior Fusion Safety Officer and the Pit Coordinator. They are informed of the specific potential hazards that are present daily at DIII–D and the special safety precautions and rules that apply, with specific emphasis on the areas where they will be working. Subcontractors also receive a similar indoctrination. This year a total of 31 individuals received this indoctrination.

Training is all-important to the safety of both personnel and equipment. Due to the complexity of the DIII–D site and its potential hazards, numerous safety training classes are conducted. Subjects of the classes included: confined space entry, CPR, back injury prevention, radiological safety, laser safety, electrical and high voltage safety, hazard communication and hazardous waste disposal, fall prevention and protection, crane and forklift operation, lockout/tagout, office ergonomics, machine shop tool usage and basic industrial safety requirements.

Safety inspections are conducted throughout the year to promote an active hazard prevention program. The inspections are conducted by a combination of Fusion, GA Licensing Safety and Nuclear Compliance personnel and outside consultants.

Four internal safety inspections of the DIII–D site were conducted by representatives from GA Safety, Fusion Safety, Fusion Management, and Fusion Facilities Engineering with a total of 83 findings noted. At the close of FY99, there were six items remaining to be completed on the findings list. A special one-time new addition acceptance inspection was conducted while the contractors were still available to correct the items.

The San Diego Fire Department's Combustible, Explosive and Dangerous Materials (CEDMAT) team inspected the DIII–D facility.

DOE-OAK conducted a safety review of the DIII–D site in June with focus on our ISM program which included the guiding principals and core functions. They concluded that the combined GA and fusion safety program did indeed result in an ISM program. They identified nine items that needed attention or correction. At close of FY99, all identified items were corrected.

The Fusion Safety Committee met 24 times this fiscal year to discuss various safety issues. The committee reviewed and approved 17 Hazardous Work Authorizations (HWA) after appropriate recommendations and changes by the Safety Committee and select safety subcommittees, and reviewed two incidents that involved no injury and four accidents that required minor off-site medical treatment and one lost time accident. The committee also approved several updates to the DIII–D safety manuals.

3.6.2. Radiation Management

Radiation management tasks include monitoring the site boundary radiation, monitoring the dose exposures of individuals, ensuring compliance with legal limits, DOE guidelines and DIII–D procedures, monitoring material for activation, maintaining and operating the radiation monitoring detectors (neutron and gamma), and maintaining a database of dose exposures for both the site boundary and for personnel.

The total neutron radiation at the site boundary for FY99 was 6.8 millirem, the total gamma radiation was 3.1 millirem, giving a total site dose for the year of 9.9 millirem (Figs. 3.6–2 and 3.6–3). This is below the SAN DOE annual guideline limit of 40 millirem and the California annual limit of 100 millirem. In turn, these limits are less than a third of the natural radiation level.

The total dose exposure of personnel was kept below the DIII–D procedural limits of 30 millirem/day, 100 millirem/week, and 400 millirem/quarter (1600 millirem/year). The highest personnel dose for the year measured by the radiation monitoring film badges was 270 millirem of gamma radiation. A total of 14 individuals had measurable film badge doses with a total person-rem for the year of 1.19. The highest dose accumulated and measured by the personnel digital dosimeters by an individual from pit runs and vessel entries (but not operations) for FY99 was 447 millirem. A total of 131 individuals received doses with 67% of the doses being below 25 millirem. All doses were logged in the database of personnel radiation doses.

The vessel was vented twice in FY99 for a total of 79 days. Radiation monitoring was performed: alpha, beta airborne samples; alpha, beta, and tritium wipe samples; dose rate and activity levels. The initial dose rate in the vessel was typically 4 to 6 millirem per hour.

Four DIII–D radiation training classes were given as part of the radiation training for new personnel and for refresher training. A total of 116 people received training.

The annual renewal of the DIII–D work authorization was completed. Updates and changes were made to the access control, radiation, and emergency response procedures. Also modified were the ALARA plan and the radiation control program summary documents. A new procedure describing the ALARA experimental planning and the ALARA daily operation was added to the radiation procedures.

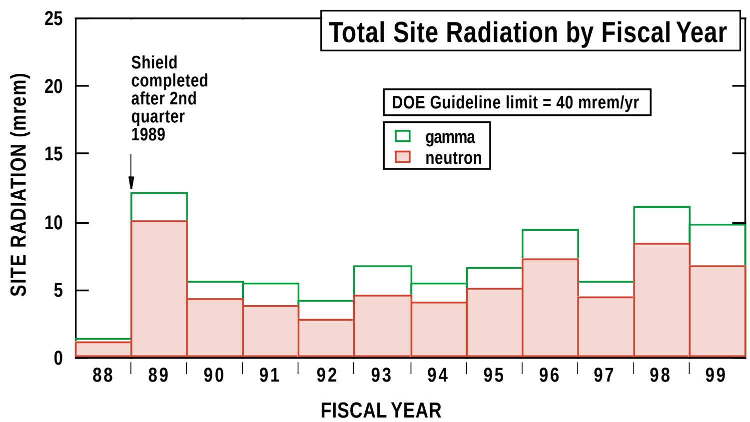

Fig. 3.6–2. History of site dose due to DIII–D operations by fiscal year.

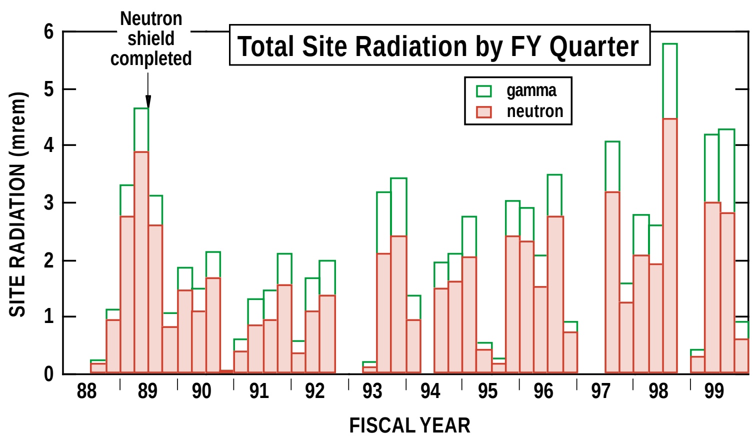

Fig. 3.6–3. History of site dose due to DIII–D operations by fiscal year quarter.

With the expectation that operations during the year might reach 5 millirem per quarter, it was decided to plan for using the full 10 millirem per quarter limit. This involved a minor increase in the areas personnel are excluded from during shots and changing the personnel limits to the full work authorization levels of 30 millirem/day, 100 millirem/week, 400 millirem/quarter (previously in use were 25/day, 100/week, 300/quarter).

A plan was developed to manage the anticipated facility dose and machine activation for an experiment which expected to produce a record daily site radiation dose of 1.1 millirem. The procedure for pit access and surveys were reviewed, modified, and made part of the radiation procedures. In particular, the pit will be closed for general work if the radiation levels reach 100 millirem/h at any location in the pit. However, the experiment did not attain these levels.

The DIII–D ALARA committee met and reviewed both the site radiation production and personnel doses for the previous year. The CY98 ALARA goal for a maximum individual dose from vent work of 180 millirem was exceeded (237 millirem actual) due to additional vent tasks, while a second ALARA goal of 250 millirem for all of CY98 was met (242 millirem actual).

A web page (http://d3dnff.gat.com/radiation) with DIII–D radiation related items was completed. It includes documentation, procedures, memos, and training presentations.

Waste disposal during the year consisted of a 55-gallon drum of mixed waste (oil contaminated with tritium) along with a 55-gallon drum of tritium contaminated dry house trash that was sent to the GA waste yard. Due to the elimination of the GA waste yard, a new procedure was developed by GA LSNC to allow shipment of tritium contaminated oil directly from DIII–D to a disposal vendor. Using the new method, two shipments of tritium contaminated oil (45 gallons) were made directly from DIII–D. The total contamination estimate of the disposed waste for the year was less than 1.5 millicurie of tritium.

Some of the site boundary film badges again showed neutron doses of 20 to 30 millirem. A meeting was held to evaluate this incident and review the past history of the non-zero doses recorded by the site boundary film badges. A set of action items resulting from the meeting were completed and summary memos were written. The conclusion is that these non-zero neutron doses on the badges do not represent doses due to DIII–D operations.

A minor radiological incident occurred in which a set of flanges were improperly released. There was no exposure of personnel and no ultimate release of contaminated material. The flanges were released based on the radiation levels but a tritium contamination survey was not performed. An incident report was written, the radiation procedures were modified, and a class was held to inform and retrain workers.

3.6.3. Quality Assurance

Fusion Quality Assurance (QA) engineers, inspectors, and support personnel maintained a high level of activity during FY99. Significant projects supported were the inspection and alignment of the radiative divertor tooling, the inspection and assembly of radiative divertor components, and the inspection of the ECH 110 GHz power upgrade components.

The Fusion QA Department performed the following specific jobs:

1. Reviewed and approved DIII–D design drawings, specifications, procedures, and procurement requisitions. Participated in design reviews and chaired the Material Review Board.
2. Performed receiving inspections, source inspections, and measurements of purchased and fabricated material, parts, subassemblies and assemblies. Witnessed load (proof) testing of lifting fixtures for gyrotrons, cryostats, neutral beam plasma sources, and ECH launchers.
3. Revised and released for use two DIII–D Work Procedures (WP). WP:01, Initiation, Review, and Approval of DIII–D Task Proposals, was revised to include a section that addresses Potential Safety Hazards/Concerns. WP:03, Design Reviews, had a paragraph added that requires that the draft of HWA be submitted to Fusion Safety for review prior to the preliminary design review. This will help insure that the design will contain the functional elements needed to operate safely.
4. Completed the semiannual building concrete footing and building column settlement surveys; no unexpected subsidence was detected. An inspection of the cracks in the concrete walls adjacent to the machine was also performed with no noticeable changes noted. Also completed the semiannual beamline settlement task.

5. Routinely assisted the project with precise optical alignments of equipment and diagnostic experiments to ensure optimum performance of the devices.
6. Occasionally assisted project personnel including collaborators in obtaining as-built measurements in and around the machine. In addition, we periodically performed reverse engineering of modified or experimental parts.
7. Fusion QA initiated trend reports on supplier performance in an effort to increase awareness of good and poor performance.

3.6.4. Continuous Improvement

The Continuous Improvement process is a means by which every member of the Fusion Group continually examines all of the processes, procedures, methods and activities by which work is accomplished, and implements or suggests improvements. The process involves submitting a suggestion on a Continuous Improvement Opportunity form to a member of the Continuous Improvement Committee (CIC).

The CIC reports to the Fusion Group Senior Vice President. The CIC is chartered to provide an overview of and administer the Continuous Improvement Program. Each Fusion Director appoints at least one representative to serve on the CIC. The CIC receives, investigates, and makes recommendations associated with all suggestions. Six Continuous Improvement Opportunity forms were received and acted upon in 1999. Most suggestions for improvement are handled by normal line management organization.

3.6.5. Planning and Control

The Planning group supported operation and maintenance of the DIII–D facility. The group provided long-term program planning, as well as day-to-day scheduling (cost control, preparation of Field Work Proposals, and Cost and Fee Proposals), processing of purchase requests, expediting and reporting of status. These support activities are essential to constraining the program within prescribed budgets and schedules. Our planning activities (budget, schedule, resource) enabled us to maximize the utilization of available resources for accomplishment of program goals and were important in planning and replanning of scope, budget, and schedule with fluctuating funding levels.

Major planning activities during 1999 included work on the ECH 6 MW and radiative divertor upgrades, a major vent focussing on hardware for these upgrades, diagnostic development, and modifications, TdeV ECH system installation and the construction of a new ECH related addition to the DIII–D building.

3.6.6. Visitor and Public Information

Tours of the DIII–D facilities are open to organizations and institutions interested in fusion development (colleges, schools, government agencies, manufacturers, and miscellaneous organizations). These tours are conducted on a noninterference basis and are arranged through the DIII–D tour coordinator whose responsibilities include security, arranging tour guides, and scheduling tours. During 1999 1,712 people toured DIII–D. Included in this count were 36 DIII–D educational tours (College and K–12) which consisted of 1,151 teachers and students.

DIII–D personnel have also taken an active role in supporting science education within the community. Educator workshops covering topics in plasma science, the electromagnetic spectrum, fusion, and radiation were presented at national, state, and local conferences. School visits by staff members and exhibition of plasma and fusion science related activities at off-site student science expositions has increased. The fusion education web sites, http://fusioned.gat.com and http://fusion.gat.com/PlasmaOutreach continue to be interactive sources for students, teachers, and the general public to obtain information about fusion science or to contact the education group.

4. PROGRAM DEVELOPMENT

4.1. 110 GHz ECH 6 MW UPGRADE PROJECT

4.1.1. Introduction

In support of the Advanced Tokamak research program on DIII–D, methods are being developed to control the current and pressure profiles of plasma discharges, with particular interest in driving off-axis current. The first step was to install 3 MW of electron cyclotron heating (ECH) power at 110 GHz in 1998. Step two is to increase the installed power to 6 MW. This additional power capability will also be enhanced by the ability of extending the pulse length from the present 2 s to 10 s for the new ECH gyrotrons.

4.1.2. Gyrotron and Transmission System

The Upgrade Project is based on the use of three CPI 1 MW class gyrotrons with CVD diamond output windows and diode guns. The departure from the typical CPI triode gun was based on operational experience of existing CPI and Gycom tubes. It was felt that the ease of operation of a diode gun gyrotron far outweighs any loss in modulation flexibility. The transmission line system is comprised of miter bends, polarizer miter bends, power monitor miter bends, straight sections, dummy loads, mirror interface units, and the associated structural supports and vacuum components. The transmission line chosen is GA's standard 31.75 mm corrugated waveguide. This transmission line design has been used successfully for several years on existing high power systems on DIII–D. The use of a diamond gyrotron output window enables the direct injection of a Gaussian mode (HE_{11}) into the waveguide. This, along with our small diameter waveguide, has eliminated the need for any costly phase correction mirrors in the system. Figure 4.1–1 shows the layout of the DIII–D ECH system.

As part of the DIII–D/PPPL collaboration effort, PPPL engineered tanks for the three new gyrotrons. Electronic file transfer techniques and video design reviews enabled this portion of the project to be completed successfully in a timely manner. The three installed tanks are shown in Fig. 4.1–2.

4.1.3. Gyrotron Control and Instrumentation

The gyrotron control system uses software distributed among networked computers interfaced to a programmable logic controller (PLC), the timing and pulse system, power supplies, vacuum and waveguide controls, and instrumentation. During DIII–D operation, the system enables control and monitoring of each of the operational gyrotrons. The use of a PLC simplifies the hardware and software design. It reduces interlock and control circuitry while improving reliability and flexibility. The pulse control system is designed around arbitrary function generators, allowing for various

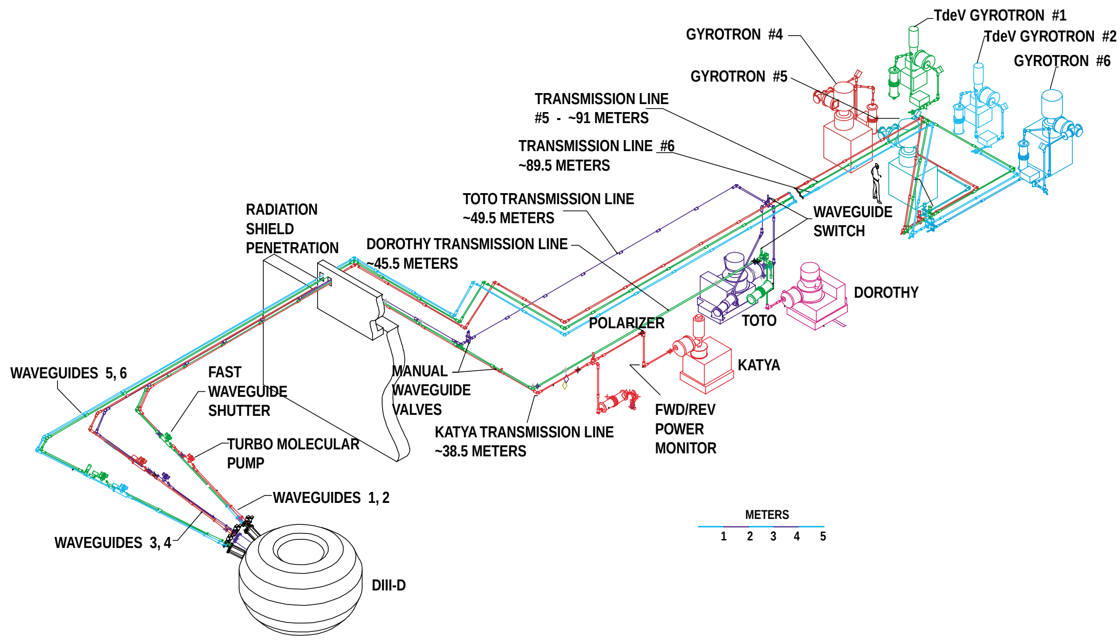

Fig. 4.1–1. The DIII–D ECH system layout.

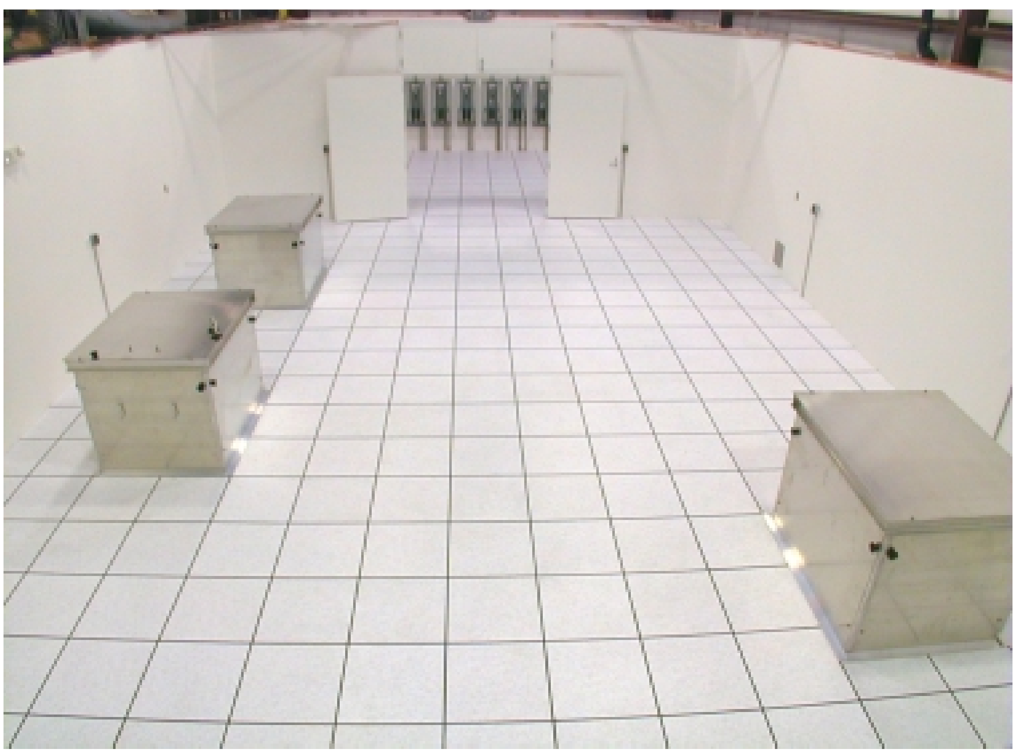

Fig. 4.1–2. PPPL gyrotron tanks installed in the new gyrotron room.

modulation schemes to be implemented, including real-time modulation control. With the recent boost in performance of personal computers, we have departed from the use of workstation computer platforms. We are now able to distribute various computers throughout subsystems and at the same time reduce the overall cost. The distributed computer technique has also enabled us to have a more robust control system while also realizing an increase in speed.

4.1.4. Physical Infrastructure Overview

In order to accommodate the addition of three new gyrotron systems and associated high-voltage power supplies, water cooling, and controls, it was necessary to add additional floor space to the existing DIII–D facility. This was accommodated with the addition of approximately 3000 ft^2 of floor space in addition to the same amount of space for nonrelated activities. Every effort was made early in the design and building layout phase to factor in future growth along with serviceability. The addition of gyrotron systems required not only space for the gyrotrons themselves, but also adequate room for the instrumentation and data acquisition equipment, high-voltage modulator regulators, and the main gyrotron control room.

4.2. RADIATIVE DIVERTOR UPGRADE PROJECT

The Radiative Divertor Upgrade Project will be completed in January 2000 with the installation of the upper inner divertor baffle and pump. This divertor, in conjunction with the upper outer divertor and the divertor located in the lower outer quadrant of the DIII–D vessel (Fig. 4.2–1), allows for the study of heat flux reduction in the immediate regions and particle and impurity control for high triangular discharges. The baffle structures common to all three of the divertors, permit the distribution of the heat flux via radiation, thereby reducing the energetic particle impingement on the divertor structures. The structures also limit the transport of the neutral gases and impurities into the core of the plasma based on their geometries and orientation to the plasmas. The structures, primarily made of Inconel 625, are protected from the plasma by graphite tiles. The inertially cooled tiles are attached to the Inconel water-cooled baffle structures and vessel walls via a stud-clamping arrangement.

Inside each of the baffle structures are cryopumps which collect particles and prevent them from recirculating back into the plasma core. The particles are exhausted from the cryopump tube surfaces as the pumps warm between the plasma shots. Having two pumps on the top of the vessel will allow pumping inboard and outboard of the private flux region. With this unique capability of pumping and injection of gases, various diagnostics will be utilized to understand the impurity transport and plasma flows. Five new diagnostics were installed or refurbished to study the plasma and pump performance.

Over the past year, the water-cooled baffle structures, the cryopump, ex-vessel cryopump transfer line, and over 300 new tiles were manufactured for the project. The water-cooled baffle structures or cooling rings consist of a welded sandwich plate structure. The cryopump consists of five concentric tubes or shells through which liquid helium or nitrogen flow through or over. The cooling rings and cryopump were manufactured by an outside machine shop and were assembled in-house on the shop floor. This allowed for the verification of the assembly and installation procedures prior to installing the hardware in the DIII–D vacuum vessel and determined any interferences/misalignments with the individual components. Also, the external cryopump transfer line was assembled on the shop floor from off-the-shelf components.

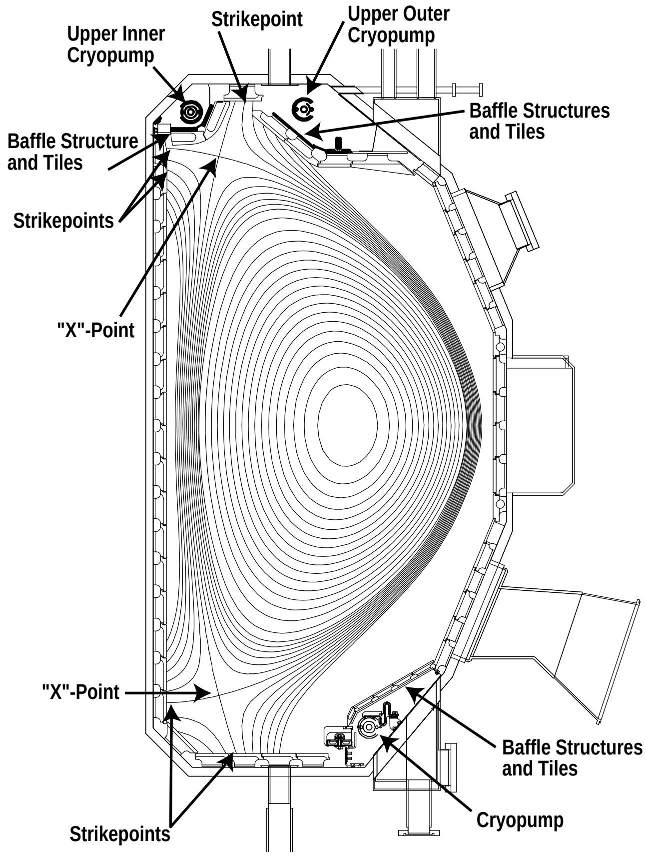

Fig. 4.2–1. General configuration of the radiative divertor and the advanced divertor with double-null plasma field lines in DIII–D.

With well defined procedures and newly developed tools, the physical installation of the cryopump and cooling rings proceeded quickly and efficiently during the last quarter of FY99 and first quarter of FY00. The protective graphite tiles (Fig. 4.2–2) for the cooling rings and vessel walls were installed with greater accuracy than in past years in an effort to minimize the exposed edges of the individual tiles to the plasma which is believed to be a source of carbon contamination in the plasma. If the tile edges could not be aligned to the required tolerances, the tile front surfaces were ground/filed in place to provide a smooth continuous surface between the tiles.

After installation of the cryopump, cooling rings, and tiles, liquid helium and nitrogen were flowed through the cryopump and water was flowed through the cooling rings to verify the systems were completely leak tight and that all the control computer systems, sensors and valves were operating properly. The project was completed on cost and schedule in December 1999.

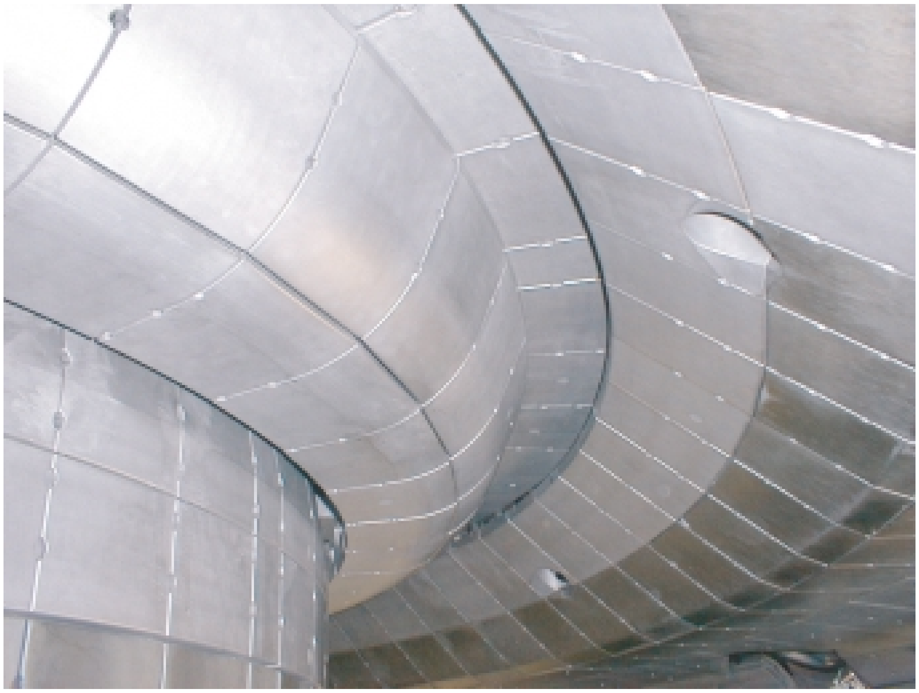

Fig. 4.2–2. Upper outer and inner radiative divertors.

5. COLLABORATIVE PROGRAMS

5.1. DIII–D COLLABORATIVE PROGRAM OVERVIEW

The DIII–D National Program has collaborations from 60 institutions listed on Fig. 5.1–1. They range in size from large multi-topic collaborations with Lawrence Livermore National Laboratory (LLNL), Oak Ridge National Laboratory (ORNL), and Princeton Plasma Physics Laboratory (PPPL) to single investigator collaborations. There were 292 individual DIII–D users in FY99. This user count includes only physicists and engineers who publish technical papers and who were on the DIII–D site for more than 5 days. Many more make shorter visits or use DIII–D data. The directly funded DIII–D physics team in FY99 consisted of 87 FTE with approximately one-third GA employees, one-third from universities, and one-third from national laboratories, see Fig. 5.1–2. In addition, there were nine FTE of collaborations associated with DIII–D operations, largely in the area of diagnostic instrumentation and radio frequency (rf) systems. Sixteen students and nine post doctoral fellows participated in DIII–D research in FY99.

NATIONAL LABS	UNIVERSITIES	INTERNATIONAL LABS
ANL	Alaska	ASIPP (China)
INEL	Alberta	Cadarsche (France)
LANL	Cal Tech	CCFM (Canada)
LLNL	Chalmers U.	Culham (England)
ORNL	Columbia U.	FOM (Netherlands)
PNL	Georgia Tech	Frascati (Italy)
PPPL	Hampton U.	Ioffe (Russia)
SNLA	Helsinki U.	IPP (Germany)
SNLL	Johns Hopkins U.	JAERI (Japan)
	Lehigh	JET (EC)
INDUSTRY COLLABS	MIT	KAIST (Korea)
Comp X	Moscow State U.	KBSI (Korea)
CPI (Varian)	Palomar College	Keldysh Inst. (Russia)
GA	PRI	KFA (Germany)
Gycom	U. Maryland	Kurchatov (Russia)
Orincon	U. Texas	Lausanne (Switzerland)
Creare	U. Toronto	NIFS (Japan)
Themacore	U. Wales	Postech (Korea)
IR&T	U. Washington	Troitsk (Russia)
Surmet	U. Wisconsin	SINICA (China)
TSI	UC Berkeley	SWIP (China)
FAR Tech	UC Irvine	Southwestern Inst. (China)
	UCLA	Tsukuba U. (Japan)
	UCSD	

Fig. 5.1–1. DIII–D National Program collaborators.

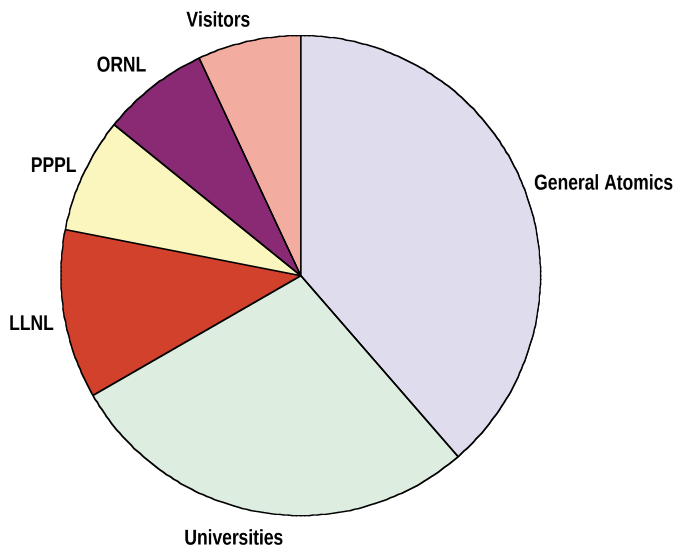

Fig. 5.1–2. The 1999 DIII–D National Physics Team consisted of 87 FTE.

5.2. LAWRENCE LIVERMORE NATIONAL LABORATORY

The LLNL collaboration continues to contribute to the overall Advanced Tokamak goal in both current profile measurement and control and in divertor boundary physics. For the last several years, we have been continually upgrading the MSE system used to measure the radial profile of the plasma current and the radial component of the electric field. In FY99, we installed 10 MSE channels viewing the plasma edge and increased the total number of channels to 36 and the spatial resolution from 25 to 3.5 mm. The main purpose for the higher spatial resolution was to resolve the edge radial electric field well and the edge bootstrap current associated with H–mode operation. Because of the large size of the E_r well and the relatively small poloidal field perturbation due to bootstrap current, the edge MSE measurements are more sensitive to E_r than edge current.

During the year, the LLNL group participated in several experiments to expand the radius of q_{min} and to obtain transport barriers and improved performance in ELMing H–mode discharges. We also participated in counter-injection experiments by providing current profiles from the MSE data and transport analysis.

The LLNL divertor diagnostics were used to develop a comprehensive picture of detached plasmas obtained with deuterium puffing in DIII–D. The divertor plasma is cold, $T_e \sim 1$ eV, and recombination is an important process. 2–D measurements of recombination have been obtained and codes were used extensively to model the data. Based on this validation work, UEDGE predictions of the detachment behavior in the upper divertor indicate detachment will occur at lower core density and injected power than in the open lower divertor. LLNL is leading experimental efforts to check these predictions.

During the DIII–D vent at the close of FY99, the upper divertor configuration was upgraded with the installation of a baffle across the dome of the private flux (PF) region and a PF region cryopump. A series of experiments was planned to examine the effect of inner versus outer leg pumping and common flux versus PF pumping at each divertor leg with the goal of maximizing density control in the core plasma. For these experiments, LLNL acquired three new IR microbolometer focal plane array imaging cameras and a LN-cooled solid state high-speed camera. We also constructed and installed two new tangentially viewing visible TV systems to allow detailed up/down comparisons of divertor emissions. During detachment studies with gas injection, the transition from attached to detached operation evolved much more slowly in the upper divertor than is typically seen in the lower divertor. The new lower divertor tangential TV is now in a new port location so that simultaneous tangential flow and 2–D emission profile measurements can be made in future experiments. This should allow improved spatial localization of the flow measurements than has been available in the past. In some discharges, the total radiated power measured by the bolometer was greater than the injected power. LLNL modified the bolometer diagnostic to reduce internal reflections to fix this problem.

We drew from the LLNL institutional strength in that several computer models are being continually developed by the MFE Theory Group. The UEDGE code is a sophisticated (fluid) edge physics model that we use to benchmark experimental data and design future divertors. There has been significant progress with UEDGE modeling and comparisons with new experimental results. We are beginning to apply the LLNL-developed code BOUT to examine the nature of turbulence in the edge and SOL regions and to determine radial transport rates consistent with this turbulence. We have modeled the expected behavior of the plasma operated in the more tightly baffled AT divertor configuration. We have expanded the capability of both UEDGE and BOUT to enable simulations of asymmetric double-null configurations. UP/DOWN asymmetry is obtained by either the effect of drifts, or by magnetically asymmetric configurations. We have examined the effect of drifts on single-null and magnetically up/down symmetric double-null DIII–D configurations. We find the plasma asymmetries to be strongly dependent on the direction of the magnetic field.

Motivated by the FESAC checkpoint in FY04, the DIII–D team has realized the need for flexible, integrated modeling for both analysis of present results and prediction of future results. The present DIII–D analysis tools are the ONETWO and TRANSP codes, and the scenario development tools are ONETWO and CORSICA. A series of discussions resulted in a GA/LLNL work proposal to develop a code “environment” under which both ONETWO and CORSICA could operate. This would facilitate the incorporation of new, common “modules” such as ECH/ECCD (TORCH and TORAY), NCLASS (neoclassical transport), DCON (stability), MCGO (Monte Carlo neutrals transport), GLF23, and modules developed by the National Transport Computational Collaboratory. This work has started, and we expect to have the code environment running about mid-2000.

5.3. OAK RIDGE NATIONAL LABORATORY

Continuing with its theme of “Handshake Across the Separatrix,” ORNL made significant contributions to the DIII–D program in the areas of pellet injection, edge stability, advanced tokamak modeling, radiating mantle plasmas, neutral particle effects, divertor spectroscopy, impurity transport studies, magnetohydrodynamic (MHD) stability, and rf technology.

Two guide tubes for launching pellets from the inside wall of the tokamak were installed along with a pellet-injected gun capable speed below 300 m/s to allow pellets to traverse curved guide tubes without breaking. The results confirmed and extended the earlier ASDEX–U experiments showing much deeper pellet density deposition with the inside launch or high field side pellets compared with the outside or low field side. Such pellets injected during the current rise produced pellet enhanced performance mode plasmas with improved confinement with highly peaked n_e and T_e profiles and an internal transport barrier (ITB) (see Fig. 2.2–10). High field pellet injection also lowered the power threshold for H–mode transitions by about 25%.

In the area of the Edge Stability Thrust led by the ORNL staff, analysis and modeling of the current profile evolution during the edge localized mode (ELM)-free phase of a high performance discharge indicated that the current profile evolves on a much slower time scale than the pressure gradient. Analysis shows that about 70% of neoclassical bootstrap current can be present in the edge. The plasma inductive back electromagnetic field drives current negative just inside the edge peak, which impacts second stability access in the edge.

With transport coefficients derived from existing DIII–D plasmas, advanced tokamak scenarios were derived for off-axis electron cyclotron current drive (ECCD) with 3 MW of electron cyclotron heating (ECH) power discharges with an L–mode and an H–mode edge with an ITB. The ECH launching was optimized for bootstrap current alignment and ECCD efficiency. In an H–mode edge discharge, a weak negative shear with $q_{min} > 1.5$ can be sustained for 10 s with H_{89P} of 2.8 and β_N of 3.5. Stability analyses shows it is stable to the high-n ideal ballooning mode and the ideal n = 1 with a conducting wall at the DIII–D vessel.

The ORNL staff led a successful experiment to document the effects of impurity injection on turbulence and transport. Transport analyses show that reduction of transport coefficients with neon injection are observed in all transport channels, with a factor of up to 5 in the ion thermal channel, substantial reduction in toroidal momentum and particle transport, and a modest (30%) reduction in the electron thermal channel. Performance H–mode level (H ~ 2, β_N ~ 2.5) was achieved for 0.7 s with the radiative mantle.

Data from new spatially resolved neutral density measurements in the X–point used for the analysis of neutrals effects on L–H transition power thresholds. Excellent agreement was obtained with both the measured X–point neutral density profiles and the plasma diagnostic data confirming that L–H transition power thresholds are strongly correlated with neutrals in the shear layer.

Deuterium dynamics and plasma flows in the scrapeoff layer (SOL) and divertor were subjects of intensive analysis. In addition, studies to understand the production and transport of carbon the divertor have begun. The “temperature screening” effects seen in the hollow impurity profiles obtained during DIII–D VH–mode discharges may also be a feature of future larger plasmas. The quantitative model for the role of ELMs in impurity purging has been improved through an analysis of transient neon recycling.

An experiment was conducted to compare sawtoothing in an oval shape with that in a bean shape to clarify the role of the Mercier stability criterion. The bean shape appeared to maintain a pressure gradient near and inside the q = 1 surface through the sawtooth crash in contrast to the case in the oval shape.

ORNL contributed to ion cyclotron range of frequencies (ICRF) operations. Two ICRF transmitters built by Thomcast AG have been converted to Thomson TH-526 tubes for the final power amplifier stage. The conversion, with manpower assistance from ORNL and PPPL, was completed in March 1999 with acceptance tests at four discrete frequencies for each system.

5.4. PRINCETON PLASMA PHYSICS LABORATORY

PPPL physicists made substantial contributions to DIII–D results reported in journals and in papers presented at major conferences and also played leading roles in planning and execution of experiments. PPPL engineering and technical staff completed important projects and provided valuable support for the major shutdown. PPPL also continued to provide key operations engineering and applications software support.

In collaboration with Columbia University, ORNL, UKAEA-Culham, and GA, PPPL conducted the first tests of active feedback stabilization of resistive-wall-modes (RWMs) and favorable results were reported. A survey of several control methods was carried out, including a preprogrammed rotating magnetic field as well as the “smart shell” and “fake rotating shell” feedback schemes. The experiments made use of three switching power amplifiers to drive the six-segment C–coil set. Each provides ±5 kA per coil pair for feedback stabilization with full error field correction. The units were procured by PPPL and installed and commissioned by GA seven months ahead of the original schedule. In order to improve characterization of the helical structure of RWMs during CY00 experiments, PPPL installed 24 new saddle loop sensors in two toroidal arrays of 12 coils each, above and below the original 6-coil midplane array.

The first attempts at feedback stabilization of low density locked modes were not successful, but analysis suggests that application of feedback earlier in the discharge and use of improved feedback algorithms may allow control of locked modes. Soft x-ray measurements of plasmas with RWMs, using toroidally separated cameras, are in good agreement with saddle loop magnetic measurements and confirm the n = 1, kink-like mode structure. The first measurements on DIII–D of halo currents during nondisruptive MHD events were also reported.

Another area of major emphasis of the PPPL collaboration is in the formation and sustainment of ITB. Experiments in 1999 used counter-injection of neutral beams and pellet injection as tools to study ITB dynamics. The DIII–D experiments, together with results from tokamak fusion test reactor (TFTR) with co- and counter-injection, provided new insight and demonstrated the sensitivity of core barrier evolution to the relationship between pressure and rotation profiles.

Experimental evidence was reported of an internal kink instability possibly driven by barely trapped suprathermal electrons produced by off-axis ECH. A study of Alfvén instabilities during ICRF sawtooth stabilization experiments suggests that these energetic particle modes, whose frequency decreases as q_0 decreases, may cause transport of fast ions and lead to monster sawteeth. A theoretical model, based on a detailed study of fast ion orbits, showed the possibility of sustainment of core plasma rotation by ICRF.

In addition to physics results, PPPL made major hardware contributions in support of high power ECH/ECCD experiments in FY00. A remotely steerable ECH/ECCD launcher was completed, tested, and installed on DIII–D. The launcher is capable of controlling poloidal and toroidal injection angles of two 1 MW, 110 GHz gyrotrons and will play a vital role in experiments on current profile control and neoclassical tearing mode stabilization. PPPL also provided three gyrotron tanks for the 6 MW ECH Upgrade.

PPPL made several improvements to DIII–D diagnostics. In collaboration with LLNL and GA, PPPL installed the Tangential Central Thomson Scattering System, which now provides measurements of core plasma electron temperature and density. In collaboration with ORNL and GA, PPPL designed and installed modifications needed to accommodate both ASDEX and Penning gauges for gas pressure measurements in the upper divertor area.

5.5. UNIVERSITY OF CALIFORNIA, LOS ANGELES

University of California, Los Angeles (UCLA) participates in the overall DIII–D research program in two main ways: (1) by developing and applying advanced diagnostic systems for measurements of plasma parameters on DIII–D, and (2) by a focussed participation in research aimed at an improved fundamental understanding of plasma turbulence and transport, including ITB and H–mode physics. The UCLA research team at DIII–D comprises four full-time research staff on-site at DIII–D and one research staff and one engineer part time at UCLA.

UCLA brings to the DIII–D team institutional strengths in the development and implementation of advanced millimeter wave, microwave and far-infrared (FIR) plasma diagnostic systems. In FY99 UCLA operated the following diagnostic instruments on DIII–D: (1) A coherent FIR scattering system to characterize low wavenumber (~1 to 5 cm^{-1}) plasma density fluctuations. The FIR system can also monitor higher wavenumber (~12 cm^{-1}) turbulence on an as-needed basis. (2) Profile reflectometer systems for high spatial and temporal resolution density profile measurements in both the edge and core. And (3) turbulence reflectometer systems, including a system for measuring turbulence correlation lengths (correlation reflectometer) and a poloidal reflectometer system to measure plasma dispersion characteristics. These diagnostic systems provide unique measurement capabilities on DIII–D and results are made available to the wider DIII–D and U.S. fusion research communities. In particular, measurements and results from these systems directly support the turbulence and transport physics related Thrusts and Topical Science Areas in the overall DIII–D program.

Highlights of research directed towards an improved understanding of plasma turbulence and transport were as follows: (1) UCLA led a collaboration with the University of California, San Diego (UCSD) and GA to investigate evidence for self-organized criticality (SOC) in tokamak plasma turbulence. The characteristics of both edge and core turbulence on DIII–D were found to be consistent with the predictions of SOC theories. This work resulted in a paper in Physics Letters A by T. Rhodes (UCLA), and an invited talk by R. Moyer (UCSD) at the 1999 Sherwood Conference. (2) Results from the core profile reflectometer led to the identification of a plasma operating regime with simultaneous localized transport barriers (ITBs) in all four transport channels. (3) The FIR scattering system was used to look for high wavenumber/short wavelength ($k_\perp \rho_s > 1$) turbulence features which may be responsible for anomalous electron transport. Preliminary data show a correlation between this short wavelength turbulence and the electron thermal diffusivity in ITB discharges.

5.6. UNIVERSITY OF CALIFORNIA, SAN DIEGO

The UCSD team completed and published probe measurements of electric field structure in attached divertor plasmas and resulting E×B flows. A survey of parallel flows in the divertor for attached and detached plasmas was completed and published.

We completed analysis of turbulence and transport behavior in very slow L to H transitions and published results. Analysis of plasma turbulence and transport data for avalanche and SOC behavior in L and ELM-free H–modes resulted in an invited paper at the Centennial Meeting of the American

Physical Society. A newly developed digital harmonic detection technique measured SOL electron temperature fluctuations with a bandwidth of up to 200 kHz and estimate the turbulent heat flux.

Studies were carried out of radiative rates and profiles during killer pellet disruption experiments. The first measurements of the fast timescale radiated power behavior during disruption thermal quenches was made.

We found that boronized carbon in the divertor does not contribute to the core impurity level during detached divertor experiments. Results were modeled in collaboration with SNL and ANL.

5.7. INTERNATIONAL COLLABORATIONS

The DIII–D international collaboration program continues to provide a broad source of innovative ideas and opportunities which support the DIII–D research program. Collaborations were carried out with the Joint European Tokamak (JET) in England, JT–60U and JFT–2M in Japan, TEXTOR and ASDEX–Upgrade in Germany, plus many other fusion laboratories. In addition to the benefits gained from DIII–D staff assignments in these laboratories, foreign scientists visiting DIII–D have made significant contributions to DIII–D program goals. A summary of some of recent major international collaborations is given below.

Two major exchanges with JT–60U which utilized the JT–60U Data Link System were performed. These two exchanges are: “High Density Operation” and “Steady State High Performance for Advanced Operating Scenarios.” Drs. A. Mahdavi and A. Leonard from DIII–D participated in the exchange on High Density Tokamak Plasmas. Techniques for getting high confinement at high densities were discussed and compared between DIII–D and JT–60U and A. Mahdavi and A. Leonard participated in JT–60U experiments. Drs. Lang Lao, T. Osborne, and M. Murakami from DIII–D participated in the exchange on Steady State High Performance plasmas. Topics of this exchange included continuing work on equilibrium fitting (EFIT) reconstruction, techniques for long pulse operation, and participation in JT–60U “steady state” experiments. Also several scientists from JT–60U participated in long-term exchanges at DIII–D: Dr. S. Sakurai completed a long-term exchange at DIII–D studying Divertor Physics, Dr. Takeji completed a three-month exchange with DIII–D on the comparison of MHD stability physics between DIII–D and JT–60U. Dr. Takenaga has started an eight-month exchange on particle fueling, recycling, and transport.

The JET/DIII–D collaboration for the new 1999 experimental campaign began in December 1998 with C. Greenfield and D. Schissel going to JET to participate in optimized shear experiments and to establish data analysis and exchange protocols. Throughout the year, a total of more than nine DIII–D scientists from GA, ORNL and LLNL participated in a variety of JET experimental and data acquisition exchanges; including high performance long pulse optimized shear, radiative mantle, neoclassical tearing mode studies, and data analysis and acquisition discussions.

From TEXTOR, Drs. J. Ongena and A. Messiaen participated in the DIII–D RI–mode experiments. This exchange was part of an on-going collaboration between TEXTOR and DIII–D on the study of enhanced confinement caused by a radiating edge mantle of injected impurities.

Dr. M. Gryaznevich from the British START/MAST low aspect tokamaks participated in RWM experiments on DIII–D.

J. Zhang and Lei Chen of the Chinese Academy of Science completed a multimonth exchange working with Lang Lao on EFIT development and applications.

6. FY99 DIII–D RESEARCH HIGHLIGHTS

DIII–D Research Highlights report important DIII–D research progress bimonthly. The one-page reports are aimed at readers with a general interest in fusion research, rather than scientific specialists. DIII–D Research Highlights may be accessed on the DIII–D Web site http://fusion.gat.com/diii-d/highlights/.

DIII–D NATIONAL FUSION FACILITY
Research Highlights
October 1998 NO.1

Progress in Fusion Physics

DIII–D Physics Advance

Research at the DIII–D National Fusion Facility focuses on improving physics understanding of high temperature plasmas and improving the prospect of fusion energy. Increasing plasma pressure (beta) by improving plasma stability and improving energy confinement are key areas of DIII–D research.

During recent experiments, DIII–D researchers created and simultaneously sustained plasma pressure and confinement well above that of a conventional tokamak. Improving upon earlier shorter duration experiments, these high performance plasmas were sustained for five energy confinement times. Data on the right shows three key performance measures which all rise well above that of a conventional tokamak, indicated by the shaded lower band.

The new results were obtained with a special plasma shape and a magnetic field line twist that confined a high beta (pressure) plasma. In present experiments the twist slowly changes and the plasma reverts to the conventional tokamak performance level. In future experiments, current drive equipment will maintain the optimum twist to sustain the advanced tokamak performance throughout the present five second limit of the DIII–D magnet capability. Assuming success in maintaining the optimum twist, a future steady-state ignition experiment, as well as future power plants, would be reduced in both size and cost.

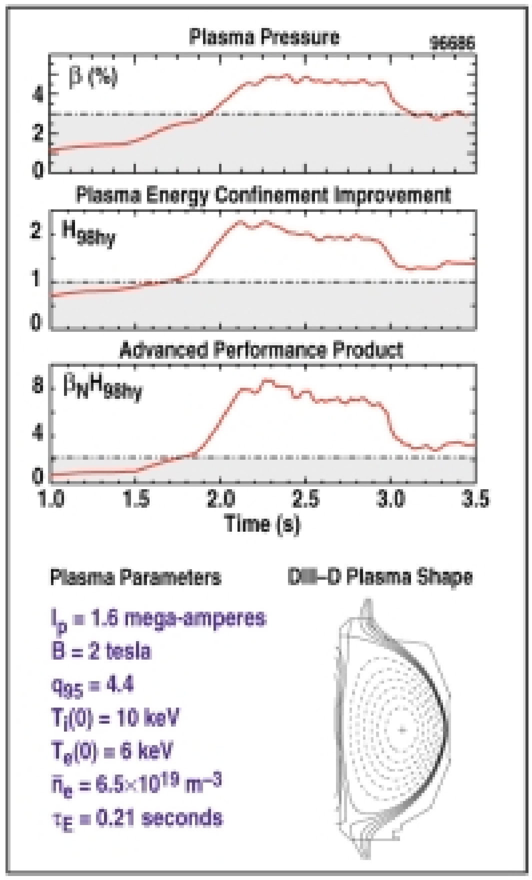

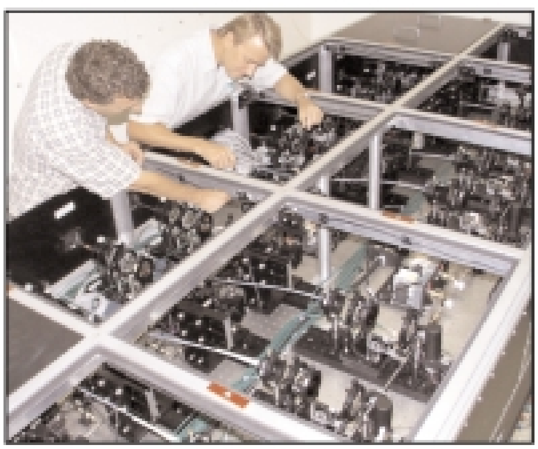

Progress in fusion research has been accelerated with improved diagnostic instruments and computational simulation codes. Shown on the left is the motional Stark effect diagnostic instrument recently upgraded to 35 channels by LLNL to measure the magnetic field twist in the high temperature (100 million degree) plasma. Although focused on improving advanced tokamak operating modes, the fundamental physics and techniques being developed on DIII–D are broadly applicable to virtually all types of magnetic fusion confinement devices.

About DIII–D

The DIII–D National Fusion Facility is the largest, best diagnosed and most versatile of all U.S. fusion experimental devices. DIII–D is the focus of over 60 active collaborations and research agreements including 8 national labs, 18 U.S. universities, and 14 other nations including Japan, Korea, Germany, France, England, China, and Russia. DIII–D is operated by General Atomics, in San Diego, CA. Please visit our website at http://fusion.gat.com

Work supported by the U.S. Department of Energy under Contract no. DE-AC03-98ER51114
For more information, contact Tom.Simonen@gat.com or (619) 455-3522

DIII–D NATIONAL FUSION FACILITY

Research Highlights

December 1998 No.2

Progress in Taming Turbulence

Experiments on DIII–D are being carried out to investigate methods of improving the confinement of the hot fusion fuel, which is a high temperature plasma. This work includes methods of reducing the effects of turbulence on energy loss out of the magnetic container. With turbulent loss, the fuel cannot be maintained at the necessary temperature unless the plasma system is very large. Our research aims to understand the physical mechanisms of turbulent energy transport so that it can be controlled in a predictive manner.

Turbulence unsettles air travelers, reduces automobile gas mileage and accompanies tropical storms. Understanding and avoiding turbulence challenges scientists in many research fields. Magnetic fusion researchers benefit from their ability to make unique diagnostic measurements and their ability to control turbulence levels with electric fields. Unlike wind shear, which upsets landing aircraft, electric-field flow shear in plasmas has a settling effect on turbulence and reduces heat loss [K.H. Burrell, "Turbulence and Sheared Flow," Science 281, 1816 (1998)].

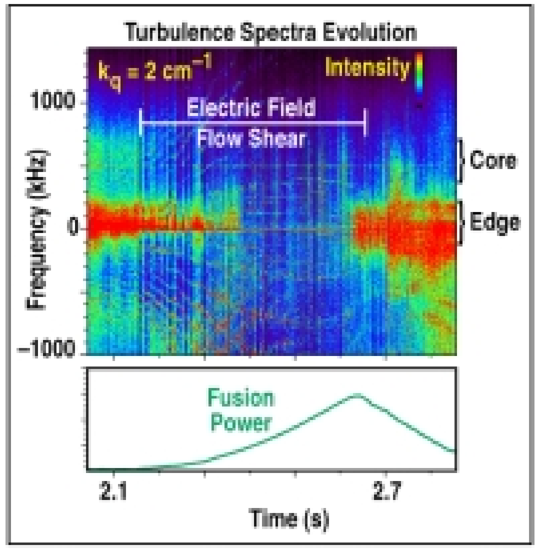

High intensity turbulence (shown as red) is quieted by electric-field flow-shear. During the quiesent period (shown in blue), the fusion power increases.

The laser diagnostic instrument developed at UCLA to characterize turbulence. This technology is also applicable for molecular spectroscopy and radiometric imaging from space.

In earlier experiments, researchers suppressed turbulence at the plasma edge and only momentarily in the plasma core. Now at recent conferences in Yokohama Japan and New Orleans, tokamak researchers from the U.S., Japan, and Europe all reported success in reducing core turbulence for the full 5 second duration of the experiments. These new results increase confidence that turbulence can be tamed indefinitely.

Laser beams are used to measure plasma turbulence. Turbulence distorts the laser beam much as heat waves often create visual distortions above a hot asphalt road. The figure above shows that laser measurements of high turbulence levels (indicated by red and green) are quieted (indicated by blue) at all frequencies in both the plasma edge and the core.

The quality and pace of this experimental research has benefited by close experiment and theory collaboration among research groups from General Atomics, Oak Ridge, Princeton University, UCLA, and UCSD. The results of this research has broad applications to other fusion concepts and to other fields of science.

About DIII–D

At the DIII–D National Fusion Facility, research is being pursued to realize fusion as a long term energy source. It is the largest, best diagnosed and most versatile of all U.S. fusion experimental devices. DIII–D is the focus of over 60 active collaborations and research agreements including 8 national labs, 18 U.S. universities, and 14 other nations including Japan, Korea, Germany, France, England, China, and Russia. DIII–D is operated by General Atomics, in San Diego, CA. Please visit our website at http://fusion.gat.com

Work supported by the U.S. Department of Energy under Contract no. DE-AC03-99ER54463

For more information, contact Tom.Simonen@gat.com or (619) 455-3522

DIII–D NATIONAL FUSION FACILITY Research Highlights
January 1999 No.3

DIII–D Begins its 1999 Research Campaign

The DIII–D tokamak has begun its 1999 research campaign. Since late summer, 1998 data was analyzed, results were published, over 30 diagnostics underwent annual calibration, facility maintenance was completed, and the vacuum vessel was reconditioned for physics experiments.

The facility now has a long pulse million watt microwave gyrotron for plasma heating and current drive, an Oak Ridge inside launch pellet injector for plasma fueling, and a GA/Livermore/Princeton laser scattering system to measure the central plasma electron temperature and density. A Princeton power supply will be installed in the spring to enable Columbia University physicists to carry out initial high beta feedback stabilization experiments. A modification will be made in the fall of 1999 to control the plasma density and purity. Three additional megawatt gyrotrons will increase the microwave power during year 2000 to 6 MW.

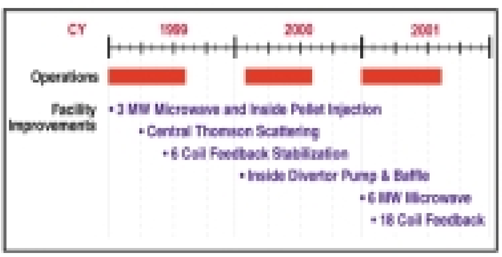

The next 3 year DIII–D research plan.

In 1999 DIII–D embarks on a new research program with the mission to establish the scientific basis for optimization of the tokamak approach to fusion energy production. DIII–D's broad program goals are to advance the science of magnetic confinement, to seek to find the ultimate potential of the tokamak as a magnetic confinement system, and to resolve key enabling issues for advancing various magnetic fusion concepts. This program stresses science understanding and has a high priority objective to establish the viability of the advanced tokamak concept.

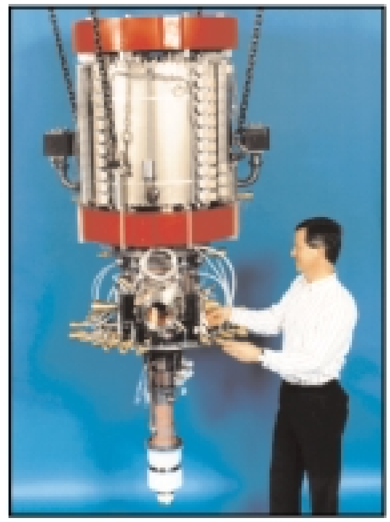

The million watt DIII–D gyrotron to heat and drive plasma current was built by CPI in Palo Alto, CA. It is the world's highest energy high-frequency microwave generator. The new gyrotron has a diamond window to enable long pulses of high power. Developed for fusion research, gyrotrons are now also being used for materials processing.

In September two hundred experiment proposals were presented in response to the 1999 research programmatic theme of 1999 Advanced Tokamak research to develop understanding to further improve the attractiveness of magnetic fusion concepts. Only 20% of the top proposals could be accommodated in the limited facility operating time. The program will be carried out with research thrusts dealing with regulating plasma currents, stabilization of high pressure plasma instabilities, varying plasma shapes, and understanding internal energy transport barriers. These experiments are preparatory for sustained advanced tokamak research beginning in 2001. Several basic fusion science experiments will also be carried out, many of which will provide desired complementary data to the MIT Alcator C–Mod and international tokamaks.

About DIII–D

At the DIII–D (Dee Three Dee) National Fusion Facility, research is being pursued to realize fusion as a long term energy source. It is the largest, best diagnosed and most versatile of all U.S. fusion experimental devices. DIII–D is the focus of over 60 active collaborations and research agreements including 8 national labs, 18 U.S. universities, and 14 other nations including Japan, Korea, Germany, France, England, China, and Russia. DIII–D is operated by General Atomics, in San Diego, CA. Please visit our website at http://fusion.gat.com

Work supported by the U.S. Department of Energy under contract DE-AC03-99ER54463
For more information, contact Tom.Simonen@gat.com or (619) 455-3522

DIII–D NATIONAL FUSION FACILITY

Research Highlights

March 1999 No. 4

Avalanches in 50 Million Degree Plasmas

Plasma turbulence is responsible for particle and heat transport in magnetic fusion experiments. However, the exact nature of the turbulence is not yet completely understood. This is due to the complex nature of turbulence and to the experimental challenges involved in making measurements in a 50 million degree temperature plasma.

A team of UCLA, UCSD and General Atomics scientists has recently made progress in understanding by considering the similarities of plasma turbulence to a sand pile that is being created by pouring sand onto it. The sand pile exhibits avalanches ranging in size from a single sand grain up to large parts of the whole sand pile. Such avalanche analogies are being applied to a wide range of physical phenomena including earthquake occurrences, forest fire distributions, traffic flows, and stellar fluctuation cycles. Data from the DIII–D plasma is also consistent with such theory models as shown in the figures below. Large transport events occur much less frequently than small transport events, consistent with predictions for the frequency of occurrence of large and small avalanches. Previously researchers knew that heat and particles were transported by both large and small scale processes (avalanches). This new research shows how their frequency changes with avalanche size.

The ideas contained in the avalanche model called self-organized criticality by physicists are powerful. Improved understanding and control of plasma turbulence will increase general understanding of turbulence in widespread applications in other fields of science as well as should lead to the improvement and optimization of magnetic fusion concepts.

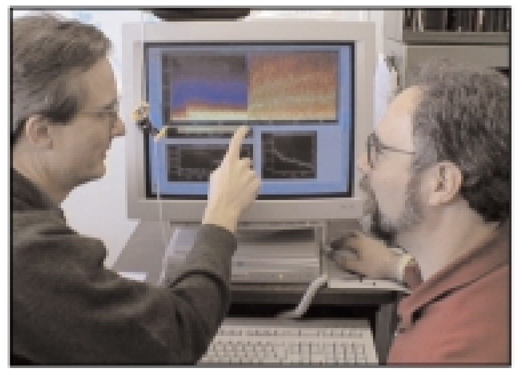

UCLA and UCSD Physicists analyzing turbulence data

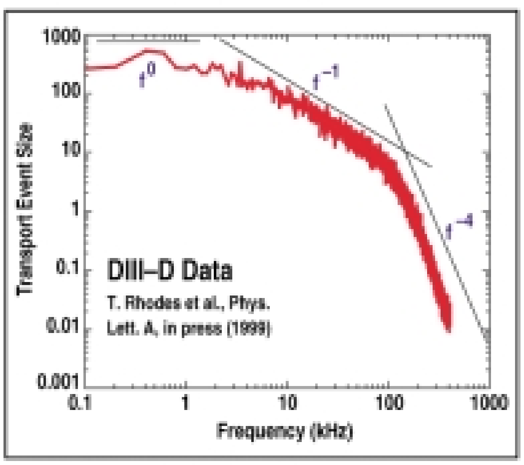

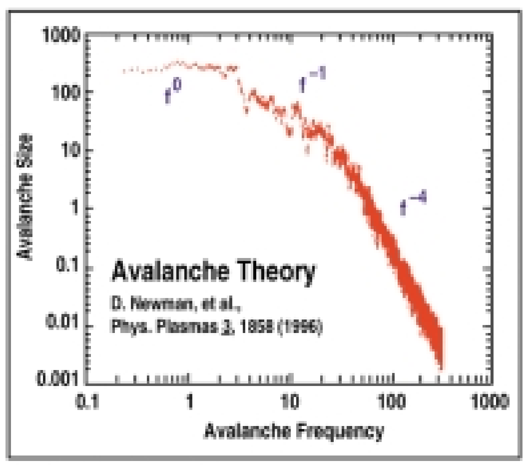

Example of data from the DIII–D fusion plasma compares well with avalanche model predictions

About DIII–D

DIII–D (Dee Three Dee) is a National Fusion Facility, where researchers work towards developing fusion as a long term energy source. DIII–D is the largest, best diagnosed, and most versatile of all U.S. fusion experimental devices. It is the focus of over 60 active collaborations and research agreements including 8 national labs, 18 U.S. universities, and 14 other nations including Japan, Korea, Germany, France, England, China, and Russia. DIII–D is operated by General Atomics, in San Diego, CA. Please visit our website at http://fusion.gat.com

Work supported by the U.S. Department of Energy under contract DE-AC03-99ER54463

For more information, contact Tom.Simonen@gat.com or (619) 455-3522

DIII–D NATIONAL FUSION FACILITY

Research Highlights

MAY 1999 No.5

Encounters Between the Extreme Cold and Hot

Fusion, the process that powers the sun and stars, is fueled by forms of hydrogen. Energy is released when hot hydrogen nuclei fuse according to Einstein's famous equation $E = mc^2$.

Oak Ridge National Laboratory researchers are investigating better ways to inject new hydrogen fuel into the center of the hot fusion plasma. Pea-size hydrogen ice pellets frozen to 450 degrees below zero Fahrenheit are hurled at a thousand miles an hour into the DIII–D plasma which is hotter than the sun. Not surprising, the small frozen ice pellets quickly melt and vaporize in a thousandth of a second before penetrating a few inches into the hot plasma. Fusion researchers must find ways to fuel deeper since future fusion power plant plasma would be several feet in size to the center.

Sparked by German experiments, the Oak Ridge pellet injector was configured to inject pellets from the outside, top, and inside of the plasma ring. DIII–D experiments showed that inside launched pellets penetrated three times deeper even though they were injected five times slower. These encouraging results suggest that the stronger magnetic field on the inside of the plasma ring propels the fuel deeper toward the plasma center. This new capability provides DIII–D fusion researchers a new tool to optimize and develop deeper understanding of high temperature plasmas and to develop better ways to fuel larger fusion plasmas including power plants.

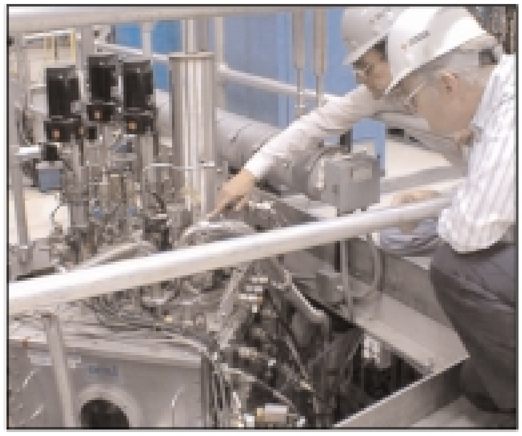

The Oak Ridge pellet injector on the DIII–D tokamak injects pea-size hydrogen ice pellets.

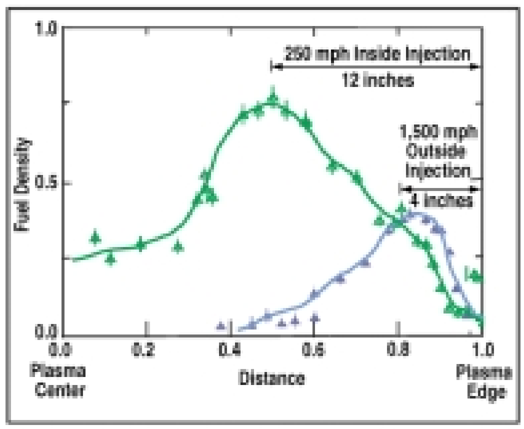

Ice pellets injected at 250 mph from the inside penetrate 12 inches into the hot plasma. Pellets injected from the outside penetrate only 4 inches even though their speed is 1500 mph.

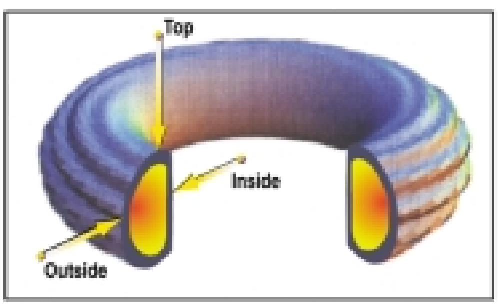

DIII–D researchers can now inject frozen hydrogen pellets in a variety of locations to determine the optimum location to fuel the hot plasma and validate theoretical models.

About DIII–D

DIII–D (Dee Three Dee) is a National Fusion Facility, where researchers work toward developing fusion as a long term energy source. DIII–D is the largest, best diagnosed, and most versatile of all U.S. fusion experimental devices. It is the focus of over 60 active collaborations and research agreements including 8 national labs, 18 U.S. universities, and 14 other nations including Japan, Korea, Germany, France, England, China, and Russia. DIII–D is operated by General Atomics in San Diego, CA. Please visit our website at http://fusion.gat.com

Work supported by the U.S. Department of Energy under contract DE-AC03-99ER54463

For more information, contact Tom.Simonen@gat.com or (619) 455-3522

DIII–D NATIONAL FUSION FACILITY
Research Highlights
JULY 1999 No.6

DIII–D Experiments are Shaping the Future

Just as shape determines the performance of cars and planes, so does shape determine the performance of high temperature plasmas. Thus magnetic fusion researchers are investigating a variety of shapes to optimize plasma performance and economics. The plasma shape is varied by electrical currents flowing in a variety of magnet coils. The DIII–D National facility has exceptional capabilities to investigate the question of plasma shape because of its combination of 18 independent poloidal magnets and its methods to control currents flowing in the plasma.

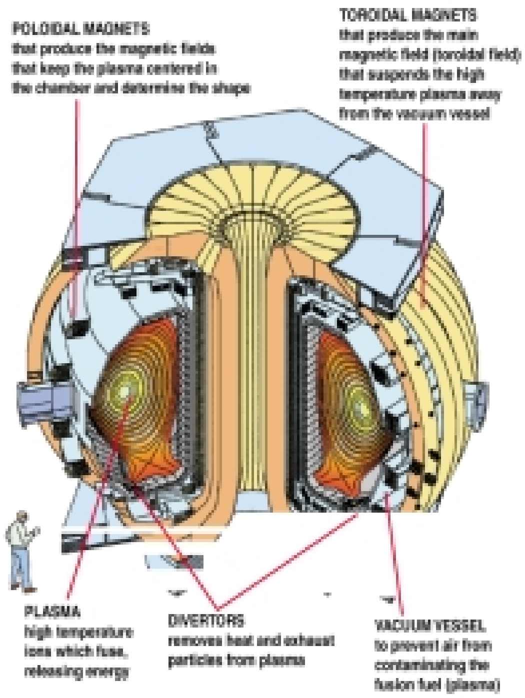

The DIII–D tokamak has the magnet flexibility to study a variety of plasma shapes

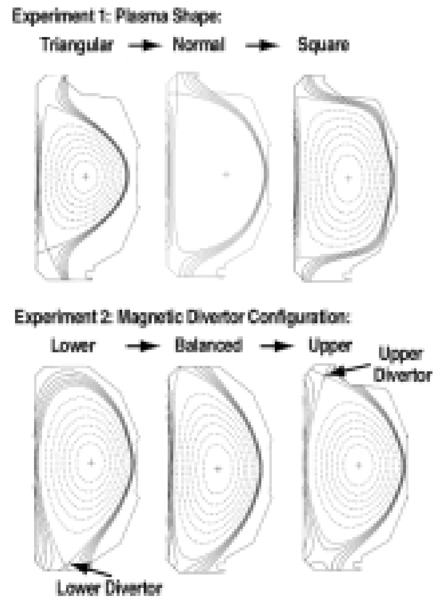

A few of the plasma shapes that DIII–D researchers studied in recent experiments.

Recently DIII–D conducted two series of experiments to investigate how certain plasma shape changes would optimize various aspects of plasma performance. In the first series of experiments, the plasma shape was varied from triangular to square shape. The more triangular shape enabled the plasma pressure at the edge to be higher but with the disadvantage that plasma energy flow across the boundary was in larger bursts. These experiments thus indicate there are trade-offs between high performance and wear and tear on the vacuum vessel.

In a second series of experiments the plasma shape was varied from lower to upper magnetic divertor shapes including a balanced magnetic double divertor. The magnetic divertor shape determines where the heat and particles are exhausted from the hot plasma. These experiments indicated that the double divertor had better energy confinement and more efficient fueling. The experiments also provided data on the degree of balance needed to realize these advantages. Experiments such as these increase the knowledge base to make fusion a viable future energy option.

About DIII–D

DIII–D (Dee Three Dee) is a National Fusion Facility where researchers work toward developing fusion as a long-term energy source. DIII–D is the largest, best diagnosed, and most versatile of all U.S. fusion experimental devices. It is the focus of over 60 active collaborations and research agreements including 8 national labs, 18 U.S. universities, and 14 other nations including Japan, Korea, Germany, France, England, China, and Russia. DIII–D is operated by General Atomics in San Diego, California. Please visit our website at http://fusion.gat.com

Work supported by the U.S. Department of Energy under contract DE-AC03-99ER54463
For more information, contact Tom.Simonen@gat.com or (619) 455-3522

7. FY99 DIII–D TECHNICAL BULLETINS

The DIII–D Technical Bulletins periodically report recent scientific advances. These one-page bulletins are aimed at plasma physics colleagues at other institutions and are primarily disseminated electronically and posted on the DIII–D Web site http://fusion.gat.com/diii-d/techbulletins/.

DIII–D TECHNICAL BULLETIN

Number 1 March 16, 1999 GA-A23064

Extended Advanced Tokamak Operation with Infrequent ELMs

B.W. Rice, LLNL

Advanced Tokamak (AT) operation strives for high β, improved confinement, and a large, well-aligned bootstrap current in order to achieve a compact steady-state tokamak configuration. While many AT characteristics have been demonstrated, the duration of sustained performance has been limited to a few energy confinement times, generally because of evolving pressure or current profiles and eventual MHD instability. Recent DIII-D experiments have explored methods for extending AT duration. Of particular interest are discharges with an ELMy edge, which are inherently steady-state and provides good edge confinement.

In a recent set of experiments, a new regime was observed when performance equal to ELM-free regimes such as VH-mode is sustained through many low-frequency ELMs. As shown in Fig. 1, β_N~3.8 and H_{98y}~2 ($\beta_N H_{98y}$>6) are sustained for 1 s.

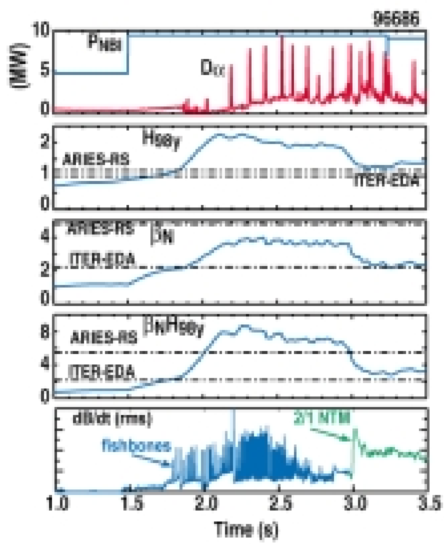

Fig. 1. Time evolution of high performance discharge with infrequent ELMs.

Note that this discharge exceeds the ARIES-RS requirement for the β_NH product. The q profile is monotonic with q_0~1, and 1/1 fishbones (but no sawteeth) are present throughout the high performance phase. Some parameters of interest during the high performance phase are: β_T~4.5%, n_e/n_{Gr}~0.5, q_{95}~4.4, t_{th}~0.21 s, and f_{bs}~50%.

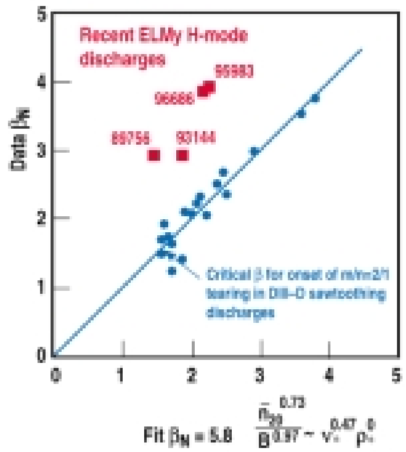

Fig. 2. The beta limit for improved performance ELMy H-mode (squares) exceeds the NTM limit established for sawtoothing discharges (circles and line) by a factor of 2.

The key elements required for access this regime are still under investigation, but the operational characteristics include a unique shape (δ=0.77, κ=1.85, single null, with the X-point at the top and the ∇B drift down), a fast current ramp that provides early magnetic shear reversal, and higher recycling near the X-point. We are investigating the possibility that this combination of features modifies the edge stability.

The high performance phase is terminated by the appearance of an m/n=2/1 mode that is believed to be a neoclassical tearing mode (NTM). Figure 2 shows that the β limit at which NTMs are excited in these discharges is significantly higher than the previous limit established in sawtoothing, lower triangularity ITER-shaped discharges. The higher β limit is most likely due to the absence of sawteeth, which provide the seed island trigger. In discharges like that shown in Fig. 1, the NTM appears to be triggered by fishbone bursts or, in some cases, ELMs. Despite the success in increasing the NTM β limit, these MHD modes continue to limit β, limit the pulse length, and adversely affect discharge reproducibility.

Future work will focus on improving our understanding of the edge stability properties of this regime and on developing techniques to suppress or stabilize the NTM. To improve AT characteristics further, somewhat higher β_N (~4.5) with higher q_{min} (>1.5) is needed to increase the bootstrap fraction.

Work supported by U.S. DOE under contract DE-AC03-99ER54463.

For more on this topic, mail rice@gav.gat.com.
Send communications about the DIII–D Technical Bulletin to politzer@gav.gat.com.
DIII–D is a national collaboration, at General Atomics, San Diego. Visit DIII–D at http://fusion.gat.com/DIII–D/ on the web.

DIII–D TECHNICAL BULLETIN

Number 2 March 25, 1999 GA-A23064

Ideal MHD Kink-Peeling Modes and Their Relation to ELMs

A.D. Turnbull, GA

The H-mode regime of improved energy confinement in tokamaks has always been accompanied in steady-state by a relaxation oscillation that regulates the pressure gradient at the plasma edge. Because of reduced thermal conductivity at the edge, the pressure gradient grows until an Edge Localized Mode (ELM) instability occurs. Since their discovery in ASDEX, the cause of ELMs has remained something of a mystery. In 1985 we conjectured that these could be ideal MHD edge-peeling modes driven by the finite edge pressure gradient and the associated Pfirsch-Schluter current. Only with recent improvements in the accuracy of equilibrium reconstruction has it been possible to make a comparison between MHD stability theory of intermediate n ideal kink mode stability and the observed onset of ELMS.

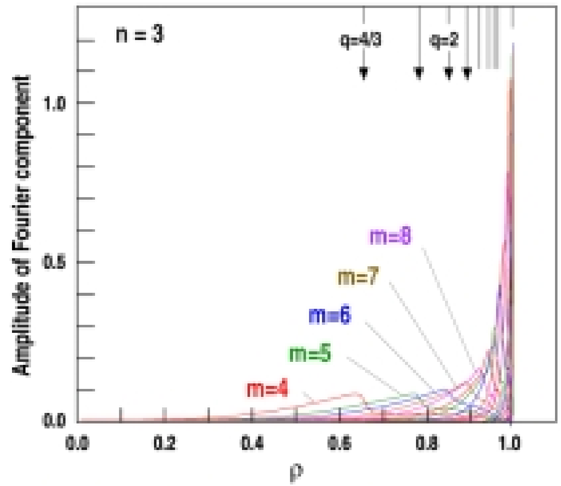

Fig. 1. Radial structure of poloidal Fourier components of the unstable ideal n=3 mode, just before an ELM. Plotted is $\xi\cdot\nabla\Psi$, where ξ is the plasma displacement and ψ is the equilibrium poloidal flux.

Equilibrium reconstruction of plasmas in DIII-D now uses the Motional Stark Effect (MSE) diagnostic with correction for the radial electric field to measure field line pitch, and improved fitting of the edge pressure gradient and current density. Large local changes in the edge pressure gradient near the edge are now accurately calculated in the EFIT equilibrium reconstruction code, with the edge current density constrained to match the bootstrap current. Without this constraint, the stability calculations predict gross violations of ballooning stability. The stability calculations also require accurate reproduction of the plasma shape, including up-down asymmetry and the presence of a divertor and of a nearby conducting wall.

Using these new procedures, calculations for an ELMing discharge immediately before an ELM show instability for n‡3 modes with the strong edge localization one expects for an ELM. The n=2 mode is marginally stable and the n=1 mode is stable. During the prior ELM-free period no instability is found for any n< 6. The calculated unstable n=3 mode is shown in Fig. 1. The mode is very strongly localized near the edge as expected for a peeling mode. This discharge is in the transition regime near the edge and so is not limited by ballooning mode instability.

While the peeling mode conjecture is substantially correct, as usual the real situation is more complex. The computed unstable modes appear to be driven by a combination of the pressure gradient and associated bootstrap current near the edge, in addition to the Pfirsch-Schluter current. Stability to ballooning modes can also play an important role: the discharges are found to have open access to the transition regime near the edge which allows the buildup of the edge pressure gradient to the point where the intermediate n modes can be destabilized. In turn, the edge bootstrap current facilitates access to the transition regime. The analysis shows a strong similarity to calculations for the so-called X-event, which terminates the high performance VH-mode and H-mode NCS plasmas. The major difference is that for the present case, the lowest unstable mode has higher n and is more strongly localized at the edge, consistent with the more localized steep edge pressure gradient in H Mode compared to the VH-mode. This is also consistent with the observation that, while the X-event irreversibly terminates the high performance, the ELM in standard H-mode causes only a temporary reduction in confinement. Our increased understanding of ELMs should lead to better control of both ELM characteristics and of high performance termination by, for example, controlling access to the transition regime through cross section shaping or edge collisionality.

Work supported by U.S. DOE under contract DE-AC03-99ER54463.

For more on this topic, mail **turnbull@gav.gat.com.**
Send communications about the DIII–D Technical Bulletin to **politzer@gav.gat.com.**
DIII–D is a national collaboration, at General Atomics, San Diego. Visit DIII–D at **http://fusion.gat.com/DIII–D/** on the web.

DIII–D TECHNICAL BULLETIN

Number 3 April 8, 1999 GA-A23064

Comprehensive Energy Confinement Scalings Derived from Similarity Experiments

C.C. Petty, GA

Significant progress has been made recently towards predicting and understanding energy confinement in plasmas on the DIII–D tokamak using the related methods of dimensional analysis, similarity, and scale invariance. Up to now, predictions of the energy confinement time were derived from empirical fits to multi-machine confinement databases. Typical of these empirical scaling relations is the one derived for the ITER project for high confinement (H-mode) plasmas,

$$\tau_{98H} = 0.036\, I^{0.97}\, B^{0.08}\, n^{0.41}\, P^{-0.63}\, R^{1.70}\, a^{0.23}\, A^{0.20}\, \kappa^{0.67}$$

where I is the plasma current, B is the magnetic field strength, n is the plasma density, P is the heating power, R is the major radius, a is the minor radius, A is the hydrogen isotope mass, and κ is the plasma elongation. A major drawback of these empirical scaling relations is that they are not constrained by the underlying plasma physics principles that govern the energy transport and loss processes; this is especially a concern when extrapolating the confinement time to future, larger machines that lie outside the parameter range of existing databases.

Recent experiments on DIII–D have applied dimensional analysis to this problem by measuring the dependence of energy confinement on the dimensionless plasma physics parameters such as the gyroradius normalized to the plasma radius ρ_*, the ratio of plasma pressure to magnetic pressure β, the detrapping collision frequency normalized to the average bounce frequency in the magnetic well ν_*, and the safety factor q. Since the principle of similarity requires that confinement in a non-rotating plasma depends only upon these dimensionless parameters, the validity of this approach can be tested by comparing the normalized energy confinement time ($\Omega\tau$ or more simply $B\tau$, where Ω is the cyclotron frequency) for two plasmas with widely different physical parameters but identical values for the dimensionless parameters. In a comparison with tokamaks both 1.8 times larger (JET) and 2.6 times smaller (Alcator C–Mod) than DIII–D, the normalized energy confinement times agreed to within the experimental uncertainties, as shown in Table I.

These experiments provide a strong constraint on theoretical models of turbulent transport. For example, ρ_* scaling experiments in H-mode plasmas have shown gyroBohm-like scaling of the energy confinement time (thermal diffusivity $\chi \propto \rho_* T/B$), which agrees with the majority of transport theories that assume that the radial wavelength (or radial correlation length) of turbulence that is responsible for transport scales with the gyroradius. Other experiments found that the energy confinement time has no β dependence, which favors theories for which E×B transport (electrostatic turbulence) is dominant over magnetic flutter transport (electromagnetic turbulence). The energy confinement time is also found to increase with decreasing safety factor, in accordance with theoretical expectations, which can explain the strong current dependence and weak magnetic field dependence of confinement since $q \propto B/I$. Finally, the energy confinement time increases with decreasing ν_*, which is a surprise since these H–mode plasmas are relatively collisionless. Recent ideas in turbulent transport theory suggest that the ν_* dependence can arise from collisional damping of radial modes in the plasma.

Combining these measured dimensionless parameter scalings for H-mode confinement results in a scaling relation that is founded in the principles of plasma physics,

$$\tau \propto B^{-1}\, \rho_*^{-3.15\pm0.2}\, \beta^{0.03\pm0.11}\, \nu_*^{-0.35\pm0.04}\, q_{95}^{-1.08\pm0.23}$$

$$\propto I^{0.78\pm0.14}\, B^{0.36\pm0.18}\, n^{0.28\pm0.07}\, P^{-0.46\pm0.05}\, L^{2.12\pm0.22},$$

where L represents the physical size scaling (a combination of major and minor radius, a and R) needed to make the relation dimensionally correct. A comparison with the ITER98H scaling finds that the I, B, n, and size dependences agree to within 2σ. The main discrepancy is in the scaling with power, where the DIII–D similarity experiments have found a weaker power degradation (resulting from the weak β scaling). This leads to a more optimistic projection for H-mode confinement on larger machines.

Table I: Test of similarity between three different tokamaks

Parameter	C–Mod	DIII–D	DIII–D	JET
ρ_*	0.34	0.35	0.35	0.34
ν_*	0.52	0.40	0.41	0.43
β	0.51	0.52	1.6	1.6
q_{95}	3.6	3.7	3.5	3.5
$B\tau$	0.14	0.13	0.22	0.21

Work supported by U.S. DOE under contract DE-AC03-99ER54463.

For more on this topic, mail petty@gav.gat.com.
Send communications about the DIII–D Technical Bulletin to politzer@gav.gat.com.
DIII–D is a national collaboration, at General Atomics, San Diego. Visit DIII–D at http://fusion.gat.com/DIII–D/ on the web.

DIII–D TECHNICAL BULLETIN

Number 4 April 28, 1999 A23064

DIII–D NATIONAL FUSION FACILITY

Plasma Convection and Electric Fields in Tokamak Divertors

J.A. Boedo, UCSD

In diverted tokamaks, where the plasma is bounded by a separatrix, an imbalance in the power and particle flows to the wall along the inboard and outboard legs of the separatrix has long been observed. This asymmetry is known to be sensitive to the direction of the toroidal magnetic field, B_T (Fig. 1). The hypothesis has been that the B_T dependence arises from the $B\times\nabla B/B^2$ and $E\times B/B^2$ single particle drift motions. Support for this idea now comes from recent numerical simulations and from the measurements described here. The computations indicate that the E×B drift is most important.

Direct measurements of plasma potential, density and temperature in two dimensions in the DIII–D tokamak divertor region quantitatively support the strong role of the E×B drift in the divertor flux asymmetry. These measurements permit the calculation of the electric field and the resulting particle flux due to the E×B drift. The measurements were obtained with a reciprocating probe and Thomson scattering in plasmas with a variety of edge conditions (H–mode and L–mode), and for both directions of toroidal magnetic field. Two-dimensional information was obtained by moving the plasma radially across the fixed divertor diagnostic views. The observations are mapped onto flux coordinates fixed in the frame of the moving plasma. Several plasma discharges are needed to develop a complete map.

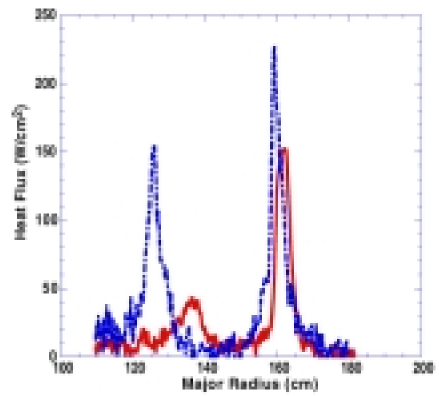

Fig. 1. Heat flux to the floor of the DIII-D vacuum vessel. The solid red line is the flux for the standard direction of B_T, and the broken blue line is for reversed B_T. The peaks at small and large major radius correspond to the inner and outer legs of the separatrix, respectively.

Perpendicular electric field strengths of ~5 kV/m are observed at the separatrix between the divertor private region and the scrape-off layer (SOL) in H–mode discharges as shown in Fig. 2 and of ~1 kV/m in L–mode discharges. The E×B drift creates a poloidal circulation pattern along the separatrix from the outer divertor target to the X–point and to the inner divertor target as indicated in Fig. 3. The drift convects about 10^{22} ion/s in the H–mode, which is about 50% of the total ion flow to a divertor target. Reversal of the toroidal magnetic field does not change the sign of the electric field, and so the direction of the E×B convection is reversed.

This convection pattern provides a mechanism for coupling the inner and outer legs of the divertor across the private flux region, and may account for the observed imbalance in inner and outer leg heat and particle fluxes.

Work was supported by the U.S. DOE under contract DE-AC03-99ER54463.

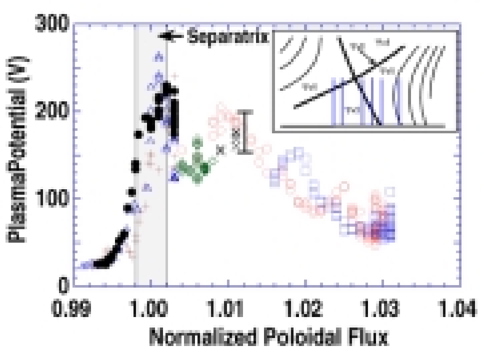

Fig. 2. Plasma potential in the divertor region as a function of normalized poloidal flux. The profile is constructed by moving the plasma between successive plunges of the reciprocating probe (indicated by different symbols). The inset shows the locations of probe plunges relative to the magnetic field.

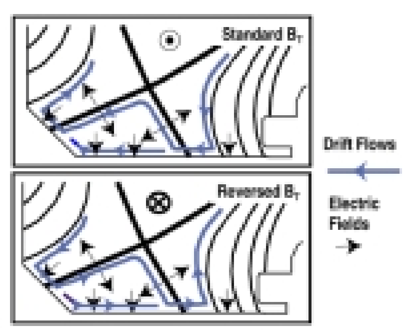

Fig. 3. Perpendicular electric field direction from plasma potential and inferred direction of E×B flow, carrying plasma across the private flux region below the x-point. When B_T is reversed, the electric field does not change sign, and so the flow reverses directions.

For more on this topic, mail boedo@gav.gat.com.
Send communications about the DIII–D Technical Bulletin to politzer@gav.gat.com.
DIII–D is a national collaboration, at General Atomics, San Diego. Visit DIII–D at http://fusion.gat.com/DIII–D/ on the web.

DIII–D TECHNICAL BULLETIN

Number 5 May 25, 1999 A23064

Turbulence Suppression and Reduced Transport Induced by Impurities

G.R. McKee, U. Wisconsin

Recent experiments on DIII–D have demonstrated improved energy and particle confinement following injection of a neon gas puff. These results suggest plasma operational modes that simultaneously achieve high core confinement and a cool, radiative mantle. In order to better understand this behavior, we compare the density fluctuations in two discharges with nearly identical operational parameters (plasma current, beam power, toroidal field), but with neon puffed into only one of them. The discharge with neon injection exhibits a 50% increase in stored energy as well as higher and broader ion and electron temperature profiles. Both plasmas had an L–mode edge (no pedestal or large pressure gradient at the edge) and a negative central shear safety factor profile. The neon was puffed in during the current ramp-up. Impurity-induced improved confinement modes have previously been seen on other tokamaks, for example in ISX-B (the "Z–mode") and in TEXTOR-94 (the "RI–mode"), though core turbulence measurements were not available in these experiments.

Density fluctuation measurements obtained with the beam emission spectroscopy (BES) diagnostic instrument on DIII–D at a normalized minor radius r/a = 0.7 show that turbulence is dramatically reduced after neon injection, suggesting that the consequent reduction in transport associated with this turbulence is at least partially responsible for the observed confinement improvement. The broadband fluctuation spectra, shown in Fig. 1, show that fully saturated turbulence in the range $0.1 \le k_\perp \rho_s \le 0.6$ exhibits a factor of five reduction in total power after neon injection, with almost complete suppression of turbulence for $k_\perp \rho_s > 0.35$. These spectra were integrated from 200 to 300 ms following the neon injection. Ion heat diffusivity, shown in Fig. 2, exhibits a corresponding four-fold reduction in ion heat transport across much of the minor radius in the neon discharge. Simulations of turbulence growth rates in these plasmas using a gyrokinetic plasma model indicate that there is a reduction in the growth rate of ion temperature gradient driven modes for $k_\perp \rho_s > 0.5$ ($k_\perp > 2$ cm^{-1}) as a result of impurity density gradient effects on main fuel ion turbulent modes. These calculations are qualitatively consistent with the measurements, though we cannot directly compare calculated linear growth rates with measurements of the amplitude of fully saturated nonlinear turbulence. Nonlinear energy cascades provide a mechanism whereby growth rates in one region of the spectrum can affect fully saturated turbulence at nearby spectral regions.

Recent experiments have assessed the relationship between measured turbulence and the density and atomic number of the impurity and should allow quantitative comparisons between measurements and nonlinear simulations.

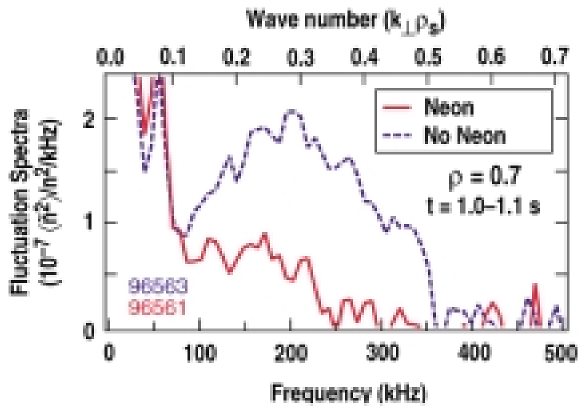

Fig. 1. Broadband density fluctuation spectra in the neon and reference discharge, obtained at r/a = 0.7 at the same time interval (1.0–1.1 s). Note the wavenumber scale on top of graph.

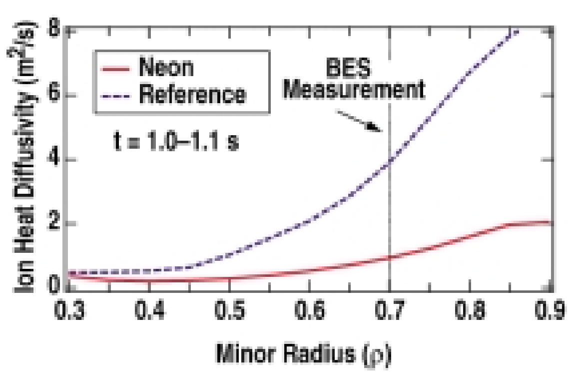

Fig. 2. Radial profile of the ion heat diffusivity obtained in the neon-puff and reference discharges during the same time interval as the fluctuation spectra in Fig. 1. Location of BES fluctuation measurements is marked with vertical dashed line.

Work supported by U.S. DOE under contract DE-AC03-99ER54463.

For more on this topic, mail **mckee@gav.gat.com**.

Send communications about the DIII–D Technical Bulletin to **politzer@gav.gat.com**.
DIII–D is a national collaboration, at General Atomics, San Diego. Visit DIII–D at **http://fusion.gat.com/DIII–D/** on the web.

DIII–D TECHNICAL BULLETIN

Number 6 June 10, 1999 A23064

Fast Wave Current Drive in H–Mode Plasmas

C.C. Petty, GA

Fast wave current drive (FWCD) is considered an attractive means of sustaining the plasma current in future tokamak reactors due to the potentially high current drive efficiency achievable. The fast Alfvén wave is absorbed directly by electrons through the coherent combination of electron Landau damping and transit time magnetic pumping. However, this damping mechanism is relatively weak in present day experiments and requires multiple passes of the fast waves through the plasma. Unfortunately, the bouncing of the fast waves near the plasma periphery can result in edge losses that dissipate the fast wave power and reduce the achievable FWCD efficiency. Such an effect has been observed recently in high confinement (H–mode) plasmas on DIII–D and points to the need to control edge localized mode (ELM) events to maintain a high FWCD efficiency in this reactor relevant regime.

The FWCD radial profile, shown in Fig. 1, is determined by changing the fast wave direction around the torus from clockwise to counter clockwise and measuring the change in the plasma non-inductive current profile. The plasma current profile is separated into its inductive and non-inductive components using time sequences of magnetic equilibria that have been reconstructed using external magnetic measurements and internal magnetic field measurements from motional Stark effect polarimetry. For the ELM-free VH–mode plasma in Fig. 1, the magnitude and profile of the measured FWCD is in agreement with theoretical calculations from both a ray tracing code with multiple pass absorption (CURRAY) and a model based on the ergodic limit of weakly damped rays (FASTCD). However, the measured FWCD for the rapidly ELMing high β_p H–mode plasma in Fig. 1 is an order of magnitude below the theoretical expectation (not shown).

The reduction in current drive with increasing ELM frequency is due to incomplete central absorption of the fast waves. The experimental FWCD, normalized to the theoretical value, is shown in Fig. 2(a) to decrease for plasmas with high ELM frequencies. The absorption of fast waves by electrons, determined by modulating the fast wave power and measuring the corresponding response in the electron temperature profile, is also observed to decrease with increasing ELM frequency as shown in Fig. 2(b). The missing fast wave power is likely deposited in the plasma periphery by an edge loss mechanism that grows stronger with increasing ELM frequency. Although the diagnostic set on DIII–D does not allow for the experimental verification of the edge loss mechanism, measurements of the edge density profile show that ELM events eject particles outside the plasma separatrix, raising the peripheral density above the fast wave cutoff density. Since the cutoff density determines the location where the fast waves are reflected back towards the plasma center during multiple pass damping, fast waves in rapidly ELMing H–mode plasmas are able to propagate to the vessel walls where dissipation in far field rectified rf sheaths is possible.

Work was supported by the U.S. DOE under contract DE-AC03-99ER54463.

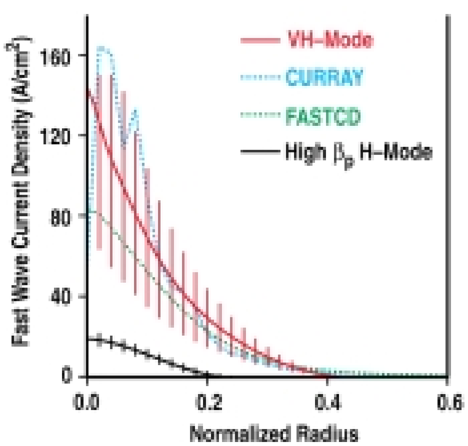

Fig. 1. Radial profile of experimental and theoretical FWCD.

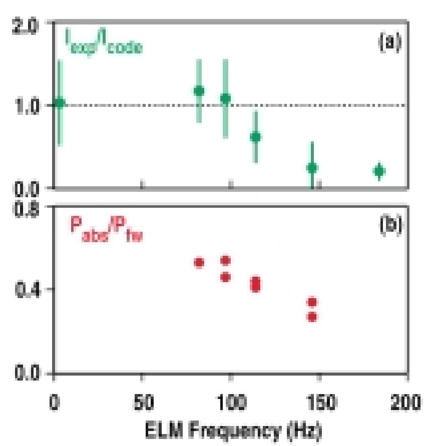

Fig. 2. Dependence on ELM frequency of (a) experimental FWCD, normalized to the theoretical value, and (b) fraction of FWCD power absorbed by electrons.

For more on this topic, mail petty@gav.gat.com.
Send communications about the DIII–D Technical Bulletin to politzer@gav.gat.com.
DIII–D is a national collaboration, at General Atomics, San Diego. Visit DIII–D at http://fusion.gat.com/DIII–D/ on the web.

DIII–D TECHNICAL BULLETIN

Number 7 July 22, 1999 A23064

Transport Across the Separatrix Near the X-Point

M.J. Schaffer, GA

Recent measurements on DIII–D reveal convective transport associated with E×B flow across the separatrix in the region near the X-point (X-region). This transport is comparable to conventionally deduced fluxes. The measurements included profiles of plasma potential Φ measured by fast–stroke insertable Langmuir probes, T_e and n_e measured by Thomson scattering, and T_i measured by charge exchange recombination spectroscopy. All data include both the X-region and the region of the scrape-off layer near the outer midplane ('upstream'), except T_i, which could be measured only near the midplane. The 2-D data set in the X-region was obtained by scanning the plasma across the diagnostic views.

Figure 1 shows the distribution in the X-region of electron pressure $p_e = n_e k T_e$ in an L–mode plasma with

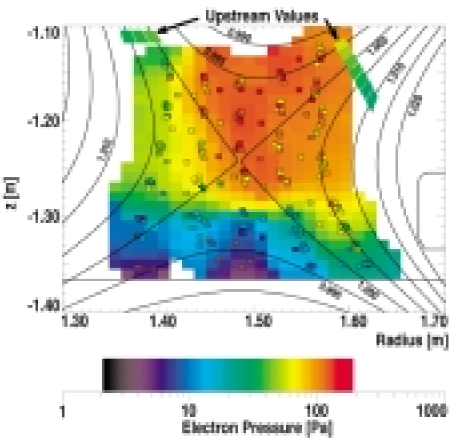

Fig. 1. X-region p_e distribution. Divertor target is at bottom. Magnetic surfaces are labeled by normalized poloidal flux. The color swatches specially labelled at the top show the upstream (midplane) electron pressure.

"attached" outer and "detached" inner divertor plasmas, as is typical of DIII–D. Clearly, the X-region electron pressure, $p_{e,x}$ is 2–3 times greater than upstream on the same magnetic surface. The high X-region pressure corresponds to locally high plasma density. The data are consistent with a classical model: the total pressure, $p_{tot} = p_e + p_i$, is constant along a magnetic line, and the locally high $p_{e,x}$ is sustained by high upstream T_i, $T_{i,ups} \approx 3\ T_{e,ups}$, if the electron and ion temperatures decouple upstream but equilibrate in the X-region.

Figure 2 shows divertor and upstream potentials from one set of probe strokes plotted versus poloidal flux as a radial coordinate. The X-region potential is ~100 V more positive than upstream, consistent with the high $p_{e,x}$

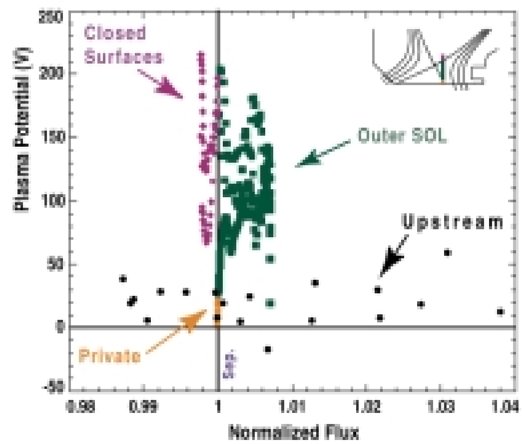

Fig. 2. Plasma potential along one divertor stroke (see inset) and upstream (black dots).

and the plasma parallel Ohm's law. Additional probe strokes yield a coarse two dimensional potential distribution featuring a potential hill in the X-region. Figure 3 gives a qualitative picture of the E×B flow. The potential does not change much with B_T direction, but the poloidal flow direction does. The E×B transport of particles, enthalpy and toroidal momentum across the separatrix is comparable to that deduced from conventional transport modeling. Therefore, X-region E×B transport is important and cannot be neglected in cross–separatrix transport.

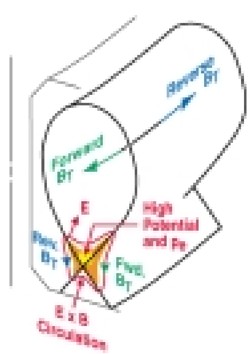

Fig. 3. Qualitative sketch of X-region E×B flow.

R.A. Moyer (UCSD) measured the potentials. This work was supported by the U.S. DOE under contract DE-AC03-99ER54463.

For more on this topic, mail schaffer@gav.gat.com.
Send communications about the DIII–D Technical Bulletin to politzer@gav.gat.com.
DIII–D is a national collaboration, at General Atomics, San Diego. Visit DIII–D at http://fusion.gat.com/DIII–D/ on the web.

DIII–D TECHNICAL BULLETIN

Number 8 May 14, 1999 A23064

Tests of Transport Models Using Modulated ECH

J.C. DeBoo, GA

Past tests of theoretical models of heat transport in tokamaks have generally relied on comparison between predicted and measured profiles, or between predicted thermal diffusivity and the experimental value inferred from a power balance analysis. Simulations have shown that perturbative transport experiments, where the dynamic plasma response is probed, can provide a more sensitive test of theory. Experiments were performed on the DIII–D tokamak using modulated, localized electron cyclotron heating (ECH) as the perturbative heat source with the resonance layer off axis in an MHD quiescent discharge. The electron and ion temperature response to the perturbation was measured and the amplitude and phase of the response was compared to predictions from several transport models.

Several theoretical and empirical models for describing electron and ion thermal transport have been examined. Two models which represent extremes in stiffness, i.e., in the strength of their dependence on temperature gradients, are the IFS/PPPL model [M. Kotchenreuther, et al., Phys. Plasmas 2, 2381 (1995)] based on ion temperature gradient (ITG) mode turbulence which depends sensitively on a critical temperature gradient and the Itoh-Itoh-Fukayama (IIF) model [S.I. Itoh, et al., Phys. Rev Lett. 72, 1200 (1994)] based on current diffusive ballooning mode theory which has no critical temperature gradient dependence. Simulations of the temperature response to the ECH perturbation indicate that these different physics models predict very different behavior after propagation closer to the plasma core, away from the ECH absorption region, as shown in Fig. 1. The figure indicates that a comparison of predicted phase of δT_e with experimental results offers a sensitive test for differentiating between models. The amplitude predictions offer considerably less discrimination between models.

For the initial experiments on DIIID a 1 MW ECH heat pulse produced perturbations $\delta T_e \sim 200$ eV at the resonant layer. The electron perturbation rapidly propagated to the plasma core with little phase shift while the amplitude was reduced to ~40 eV (Fig. 1). T_i dropped in response to the electron heat pulse at the resonant layer. The ion response also propagated rapidly to the plasma core, maintaining its out-of-phase relation to δT_e. For ITG-based models, the T_i response is largely determined by the effect of the T_i/T_e ratio on the ITG mode threshold. As the electrons are heated at the ECH resonant layer, T_i/T_e decreases which in turn destabilizes the ITG modes, thereby increasing the ion transport at that location. This behavior is consistent with the observed ion response to the electron heat pulse. However, the IFS/PPPL model incorrectly predicts a ~180° phase shift in δT_e between $\rho = 0.3$ and $\rho = 0.1$.

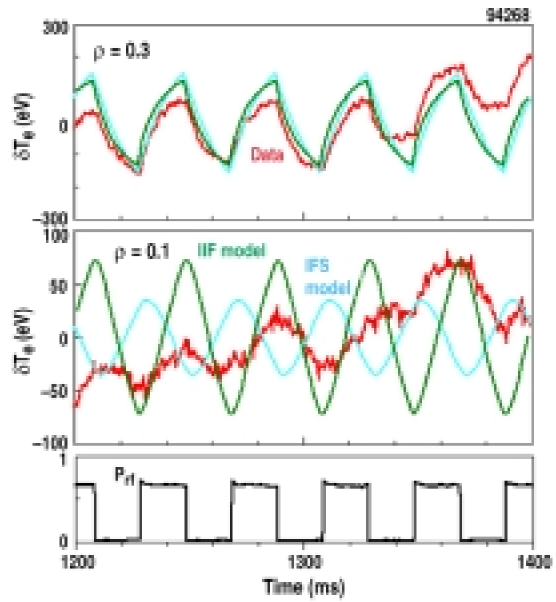

Fig. 1. δT_e (eV) at $\rho = 0.3$ and $\rho = 0.1$ for measured data (red), and simulated data from the IFS/PPPL model (blue) and IIF model (green).

Work was supported by the U.S. DOE under contract DE-AC03-99ER54463.

For more on this topic, mail **deboo@gav.gat.com**.

Send communications about the DIII–D Technical Bulletin to **politzer@gav.gat.com**.
DIII–D is a national collaboration, at General Atomics, San Diego. Visit DIII–D at **http://fusion.gat.com/DIII–D/** on the web.

DIII–D TECHNICAL BULLETIN

Number 9 August 11, 1999 A23064

Observation of the Resistive Wall Mode

A.M. Garofalo, Columbia U.

One class of MHD instabilities in a tokamak involves displacement of the plasma surface. In an ideal plasma (zero resistivity), this is the external or global kink mode. Stability can be restored if a perfectly conducting wall is placed close enough to the plasma. However, real walls have finite conductivity. In the presence of a real wall, the instability can persist, but is strongly modified, acquiring the label "resistive wall mode" or RWM. The effects of the wall on the plasma mode are due to phase differences and dissipation of the inductively coupled currents in the wall. In practice, a resistive wall of conductivity σ limits the real and imaginary parts of the mode frequency ω according to: $\mathrm{Re}(\omega) = 2\pi f \le 1/\tau_w$ and $\mathrm{Im}(\omega) = \gamma \le 1/\tau_w$, where $\tau_w \propto \sigma$.

Recent theoretical work has predicted that the presence of both dissipation in the plasma and sufficiently fast plasma rotation (toroidal) can stabilize the resistive wall mode. For beta between the n = 1 ideal external kink mode limit with no wall and the higher limit found with a perfectly conducting wall, it is expected that the fast growing ideal external kink will be converted into a slowly growing resistive wall mode that could be stabilized by sufficiently high plasma rotation, or controlled by an active feedback system.

Recent experiments have been directed toward an unambiguous identification and characterization of the RWM. Using a double-current-ramp technique, stable rotating plasmas are reliably produced with beta which exceeded the calculated no-wall limit by up to 40%. These conditions last for up to 30 characteristic resistive wall decay times (Fig. 1). Note that the rotation of the plasma gradually slows, and the high beta state is terminated by an n = 1 mode which grows when the rotation is slow enough.

Improved diagnostics have made possible a direct identification of the terminating RWM. Analysis of the perturbation in the electron temperature, as measured by electron cyclotron emission spectroscopy, shows that the radial mode structure agrees with the numerical prediction for a global n = 1 ideal plasma kink-ballooning mode (Fig. 2). Newly installed saddle flux loops show that the mode rotates at $f \sim 1/2\pi\tau_w$, as predicted for a RWM, while the plasma rotates ~100 times more rapidly as measured by charge exchange recombination spectroscopy. Accurate plasma rotation measurements also confirm the existence of a critical minimum plasma rotation required for stabilization of the mode.

Current work focuses on improving our understanding of the rotational stabilization of the RWM and on the feasibility of active feedback control of the RWM using external magnetic coils.

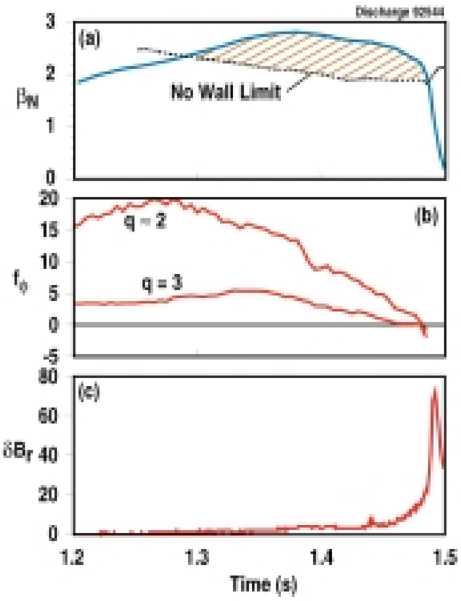

Fig. 1. Time history of a wall-stabilized discharge showing (a) normalized beta; (b) toroidal plasma rotation frequency at two radial locations; (c) and radial magnetic field at the wall due to the RWM.

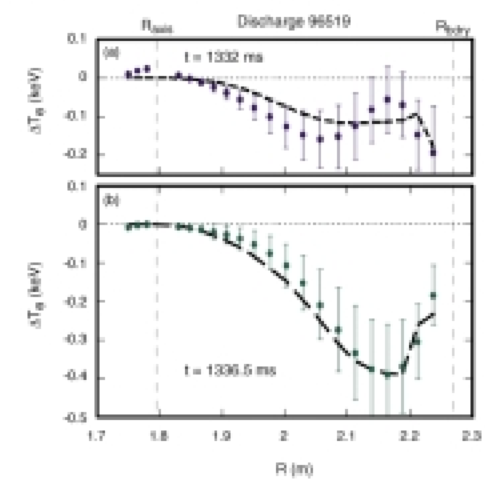

Fig. 2. Comparison of the radial profiles of the measured (data points) and predicted (dashed lines) electron temperature perturbation caused by the n=1 RWM in discharge 96519 The predicted change ΔT_e is determined from the displacement ξ by $\Delta T_e \propto \xi \cdot \nabla T_e$.

For more on this topic, mail garofalo@gav.gat.com.
Send communications about the DIII–D Technical Bulletin to politzer@gav.gat.com.
DIII–D is a national collaboration at General Atomics, San Diego. Visit DIII–D at http://fusion.gat.com/DIII–D/ on the web.

DIII–D TECHNICAL BULLETIN
Number 10 June, 1999 A23064

Reduced Transport Near Rational q Surfaces in DIII–D

M.E. Austin, U. Texas

A class of L–mode discharges has been observed on DIII–D that exhibits a transition to improved core confinement as the minimum value of q approaches 1. An example is shown in Fig. 1 where the central electron T_e and ion temperatures are seen to increase dramatically just before the onset of sawteeth. The confinement enhancement factor H89P increases from 1 to 1.2 during this transition. These discharges are typically low density and have a moderate level of early neutral beam heating which results in negative central magnetic shear (NCS). The behavior has also been seen with flat to nearly monotonic shear and the improved confinement persists into the sawtoothing phase.

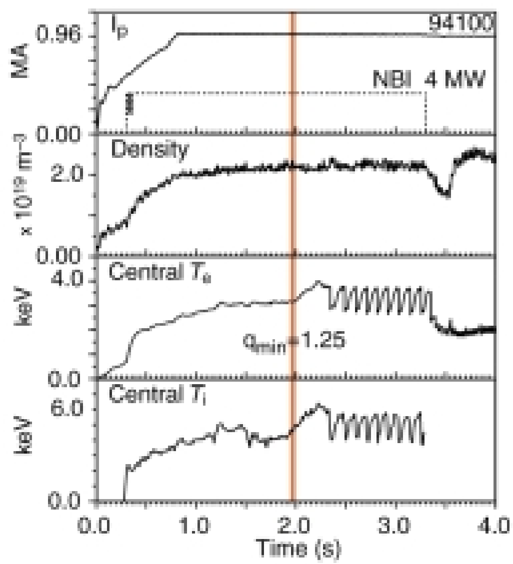

Fig. 1. Discharge with spontaneous transition to improved confinement at 2 s when q_{min} = 1.25.

Earlier in these same discharges transient improvements in energy transport are often seen near low-order rational q surfaces. Upward jumps in the electron temperature are observed as the minimum value of q passes through an integer or half-integer value as illustrated in Fig. 2. Similar effects are seen in the ion temperature and toroidal rotation. These transient jumps are only seen in DIII–D NCS plasmas. The observation in these cases is of a dipole change in temperature, with an increase inside a radius near the location of minimum q and a drop outside this radius, as shown in Fig. 3. Transient reductions in turbulent fluctuations are correlated with these jumps as well as dips in the edge D_α emission.

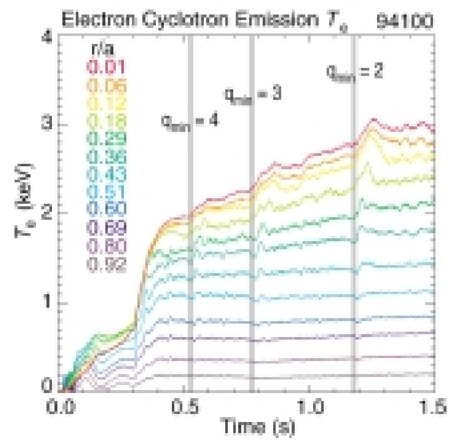

Fig. 2. Discharge with jumps in the electron temperature T_e when q_{min} is near integer values.

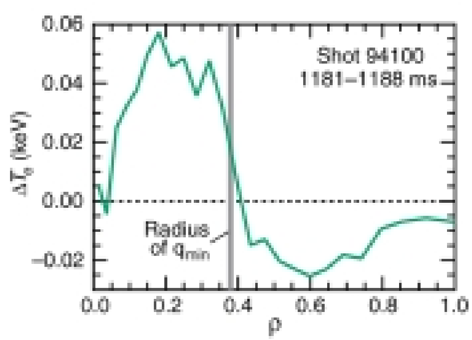

Fig. 3. Changes in the electron temperature profile ΔT_e during temperature increase at 1185 ms.

Regions of low thermal diffusivity near rational q surfaces have been reported in the RTP tokamak and others. On DIII–D however, there are some cases in NCS discharges where the temperature jumps occur at q_{min} values other than integer or half-integer. Generally these discharges have higher neutral beam injected power and/or plasma current. We are currently investigating these plasmas to try and understand the mechanism for the improved core transport and its relation to the q profile.

For more on this topic, mail **austin@gav.gat.com**.
Send communications about the DIII–D Technical Bulletin to **politzer@gav.gat.com**.
DIII–D is a national collaboration at General Atomics, San Diego. Visit DIII–D at **http://fusion.gat.com/DIII–D/** on the web.

8. PUBLICATIONS FY99

Allen, S.L., N.H. Brooks, R. Bastasz, J.A. Boedo, J.N. Brooks, J.W. Cuthbertson, T.E. Evans, M.E. Fenstermacher, D.N. Hill, D.L. Hillis, J. Hogan, R.C. Isler, G.L. Jackson, J.C. Jernigan, A.W. Hyatt, C.J. Lasnier, R.D. Lehmer, A.W. Leonard, M.A. Mahdavi, R. Maingi, W.H. Meyer, P.K. Mioduszewski, R.A. Moyer, D.G. Nilson, L.W. Owen, T.W. Petrie, G.D. Porter, M.E. Rensink, M.J. Schaffer, J.P. Smith, G.M. Staebler, R.D. Stambaugh, D.M. Thomas, M.R. Wade, W.R. Wampler, J.G. Watkins, W.P. West, D.G. Whyte, N.S. Wolf, C.P.C. Wong, R.D. Wood, DIII–D Physics and Operations Teams, "Radiative Divertor and SOL Experiments in Open and Baffled Divertors on DIII–D," presented at 17th IAEA Fusion Energy Conference, October 19–24, 1998, Yokohama, Japan, Special Issue of Nucl. Fusion **39**, 2015 (1999); General Atomics Report GA–A23004 (1998).

Allen, S.L., The DIII–D Team, "Overview of Physics Results from the 1999 DIII–D Campaign," Bull. Am. Phys. Soc. **44**, 126 (1999).

Allen, S.L., M.E. Fenstermacher, C.M. Greenfield, A.W. Hyatt, R. Maingi, G.D. Porter, M.R. Wade, A.S. Bozek, R. Ellis, D.N. Hill, M.A. Hollerbach, C.J. Lasnier, A.W. Leonard, M.A. Mahdavi, D.G. Nilson, T.W. Petrie, M.J. Schaffer, J.P. Smith, R.D. Stambaugh, D.M. Thomas, J.G. Watkins, W.P. West, D.G. Whyte, R.D. Wood, "Studies of High- (Baffled) and Low- (Open) Pumped Divertor Operation on DIII–D," presented at 13th Int. Conf. on Plasma Surface Interactions in Controlled Fusion Devices, May 18–23, 1998, San Diego, California, J. Nucl. Mater. **266–269**, 168 (1999); General Atomics Report GA–A22878 (1998).

Austin, M.E., "Reduced Transport Near Rational q Surfaces in DIII–D," General Atomics DIII–D Technical Bulletin; General Atomics Report GA–A23064, No. 10 (1999).

Austin, M.E., K.W. Gentle K.H. Burrell, C.C. Petty C.L. Rettig, "Transitions to Improved Core Transport in DIII–D L–mode NCS Discharges," Bull. Am. Phys. Soc. **44**, 73 (1999).

Baker, D.R., "Particle Transport in DIII–D Internal Transport Barriers," Bull. Am. Phys. Soc. **44**, 74 (1999).

Baker, D.R., M.R. Wade, L.Y. Sun, C.C. Petty, T.C. Luce, "Dimensionless ρ_* Scaling of Particle Transport in DIII–D L–Mode Discharges," submitted to Nucl. Fusion; General Atomics Report GA–A23088 (1999).

Bernabei, S., E.D. Fredrickson, J.S. deGrassie, C.C. Petty, R.I. Pinsker, N. Gorelenkov, W.W. Heidbrink, E.A. Lazarus, "High Harmonic Ion Cyclotron Heating in DIII–D: III. Excitation of Alfvén Instabilities," Bull. Am. Phys. Soc. **44**, 173 (1999).

Bialek, J., A.H. Boozer, A.M. Garofalo, M.E. Mauel, G.A. Navratil, A.D. Turnbull, "Optimization of Feedback Control Coils for Resistive Wall Mode Stabilization in DIII–D," Bull. Am. Phys. Soc. **44**, 76 (1999).

Boedo, J.A., “Plasma Convection and Electric Fields in Tokamak Divertors,” General Atomics DIII–D Technical Bulletin; General Atomics Report GA–A23064, No. 4 (1999).

Boedo, J.A., R. Lehmer, R.A. Moyer, J.G. Watkins, G.D. Porter, T.E. Evans, A.W. Leonard, M.J. Schaffer, “Measurements of Flows in the DIII–D Divertor by Mach Probes,” presented at 13th Int. Conf. on Plasma Surface Interactions in Controlled Fusion Devices, May 18–23, 1998, San Diego, California, J. Nucl. Mater. **266–269**, 783 (1999); General Atomics Report GA–A22859 (1998).

Boedo, J.A., R.A. Moyer, M.J. Schaffer, N.H. Brooks, M.A. Mahdavi, R.C. Isler, C.J. Lasnier, G.D. Porter, J.G. Watkins, “Plasma Flows in the DIII–D Divertor,” Bull. Am. Phys. Soc. **44**, 128 (1999).

Boedo, J., G.D. Porter, M.J. Schaffer, R. Lehmer, R.A. Moyer, J.G. Watkins, T.E. Evans, C.J. Lasnier, A.W. Leonard, S.L. Allen, “Flow Reversal, Convection, and Modeling in the DIII–D Divertor,” Phys. Plasmas **5**, 4305 (1998); General Atomics Report GA–A22910 (1998).

Boedo, J.A., M.J. Schaffer, R. Maingi, C.J. Lasnier, R.A. Moyer, J.G. Watkins, “Electric Field Induced Plasma Convection in Tokamak Divertors,” Proc. 26th European Conf. on Controlled Fusion and Plasma Physics, June 14–18, 1999, Maastricht, Netherlands, Vol. 23J, p. 1185 (European Physical Society, Nieuwegein, 1999); General Atomics Report GA–A23159 (1999).

Boedo, J.A., M.J. Schaffer, R. Maingi, C.J. Lasnier, J.G. Watkins, “Electric Field-Induced Plasma Convection in Tokamak Divertors,” submitted to Phys. Plasmas; General Atomics Report GA–A23041 (1999).

Bray, B.D., C.L. Hsieh, T.N. Carlstrom, “Calibration of a Three Path Thomson System at DIII–D,” Bull. Am. Phys. Soc. **44**, 175 (1999).

Broesch, J.D., J.C. Phillips, P.I. Petersen, M.J. Hansink, “A Handheld, Free Roaming, Data Display for DIII–D Diagnostic Data,” to be published in Proc. 11th IEEE/NPSS Real-Time Conf., June 14–18, 1999, Santa Fe, New Mexico; General Atomics Report GA–A23175 (1999).

Brooks, N.H., R.J. Colchin, D.F. Finkenthal, T.H. Jensen, R. Maingi, N. Naumenko, S. Tugarinov, M.R. Wade, “Partial Pressure Measurements with an Active Spectrometer,” presented at 12th Top. Conf. on High-Temperature Plasma Diagnostics, June 7–11, 1998, Princeton, New Jersey, Rev. Sci. Instrum. **70**, 423 (1999); General Atomics Report GA–A22855 (1998).

Brooks, N.H., D.F. Finkenthal, T.H. Jensen, N.N. Naumenko, S.N. Tugarinov, “An Active Spectrometer,” Rev. Sci. Instrum. **70**, 1258 (1999); General Atomics Report GA–A22700 (1997).

Brooks, N.H., W.P. West, M.R. Wade, D.G. White, A. Ramsey, R. Jakumar, “Impurity Behavior in DIII–D Discharges with Counter Beam Injection,” Bull. Am. Phys. Soc. **44**, 73 (1999).

Burrell, K.H., “Tests of Causality — Experimental Evidence that Sheared E×B Flow Alters Turbulence and Transport in Tokamaks,” Phys. Plasmas **6**, 4418 (1999); General Atomics Report GA–A23145 (1999).

Burrell, K.H., C.M. Greenfield, C. Rost, M.R. Wade, W.P. West, “Sawtooth-free H–mode Discharges on DIII–D with Density and Impurity Control,” Bull. Am. Phys. Soc. **44**, 127 (1999).

Busath, J.L., H.K. Chiu, “Simple Catalytic Cell for Restoring He Leak Detector Sensitivity on Vacuum Systems With High D_2 Backgrounds,” Proc. 45th Annual American Vacuum Soc. Symp. and Top. Conf., Baltimore, November 2–6, 1998, Baltimore, Maryland, J. Vac. Sci. Technol. A **17**, 2015 (1999); General Atomics Report GA–A22965 (1998).

Callen, J.D., C.C. Hegna, B.W. Rice, E.J. Strait, A.D. Turnbull, “Growth of Ideal MHD Modes Driven Slowly through their Instability Threshold — Application to Disruption Precursors,” Phys. Plasmas **6**, 2963 (1999); General Atomics Report GA–A22845 (1999).

Callis, R.W., J. Lohr, D. Ponce, R.C. O'Neill, R. Prater, T.C. Luce, “The DIII–D 3 MW, 110 GHz ECH System,” Proc. 13th Top. Conf. on Applications of Radio Frequency Power to Plasmas, April 12–14, 1999, Annapolis, Maryland, p. 433 (American Institute of Physics, Melville, 1999); General Atomics Report GA–A23082 (1999).

Carlstrom, T.N., K.H. Burrell, R.J. Groebner, A.W. Leonard, T.H. Osborne, D.M. Thomas, “Comparison of L–H Transition Measurements with Physics Models,” presented at 17th IAEA Fusion Energy Conference, October 19–24, 1998, Yokohama, Japan, Special Issue of Nucl. Fusion **39**, 1941 (1999); General Atomics Report GA–A22989 (1998).

Carlstrom, T.N., K.H. Burrell, R.J. Groebner, A.W. Leonard, T.H. Osborne, M.J. Schaffer, “Importance of X–point Physics on the H–mode Power Threshold in DIII–D,” Bull. Am. Phys. Soc. **44**, 128 (1999).

Carolipio, E.M., W.W. Heidbrink, R. White, “Physical Mechanisms of Fast-Ion Loss,” Bull. Am. Phys. Soc. **44**, 173 (1999).

Casper, T.A., L.L. LoDestro, L.D. Pearlstein, M. Murakami, L.L. Lao, H.E. St. John, “Time-dependent Modeling of Sustained Advanced Tokamak Scenarios,” Bull. Am. Phys. Soc. **44**, 174 (1999).

Colchin, R.J., T.N. Carlstrom, M.E. Fenstermacher, R.J. Groebner, R.C. Isler, R. Maingi, L.W. Owen, “Measurement of Neutral Density Near the X–Point in the DIII–D Tokamak,” to be published in Nucl. Fusion Lett.; General Atomics Report GA–A23077 (1999).

Colchin, R.J., R. Maingi, S.L. Allen, C.M. Greenfield, M.R. Wade, “Effects of Particle Exhaust on Neutral Compression RAtios in DIII–D,” presented at 13th Int. Conf. on Plasma Surface Interactions in Controlled Fusion Devices, May 18–23, 1998, San Diego, California, J. Nucl. Mater. **266–269**, 472 (1999); General Atomics Report GA–A22865 (1998).

Colchin, R.J., R. Maingi, R.C. Isler, R.W. Owen, M.E. Fenstermacher, T.N. Carlstrom, R.J. Groebner, “Measurement of DIII–D X–Point Neutral Densities at the L–H Transition,” Bull. Am. Phys. Soc. **44**, 171 (1999).

DeBoo, J.C., “Tests of Transport Models Using Modulated ECH,” General Atomics DIII–D Technical Bulletin; General Atomics Report GA–A23064, No. 8 (1999).

DeBoo, J.C., C.M. Greenfield, K.H. Burrell, E. Synakowski, B.W. Stallard, E.J. Doyle, C.L. Rettig, L. Zeng, “Plasma Profile Behavior in DIII–D Discharges with Counter NBI,” Bull. Am. Phys. Soc. **44**, 72 (1999).

DeBoo, J.C., J.E. Kinsey, R. Bravenec, E. Fredrickson, C.M. Greenfield, Y.R. Lin-Liu, J. Lohr, T.C. Luce, G.R. McKee, Jr, R. Prater, C.L. Rettig, D.P. Schissel, G.M. Staebler, R.E. Waltz, "Experimental Tests of Transport Models Using Modulated ECH," presented at 17th IAEA Fusion Energy Conference, October 19–24, 1998, Yokohama, Japan, Special Issue of Nucl. Fusion **39**, 1935 (1999); General Atomics Report GA–A22982 (1998).

deGrassie, J.S., D.R. Baker, K.H. Burrell, C.M. Greenfield, Y.R. Lin-Liu, J. Lohr, T.C. Luce, C.C. Petty, R. Prater, G.M. Staebler, W.W. Heidbrink, B.W. Rice, T.K. Mau, M. Porkolab, "Toroidal Rotation and Core Ion Confinement with RF Heating in DIII–D," Proc. 26th European Conf. on Controlled Fusion and Plasma Physics, June 14–18, 1999, Maastricht, Netherlands, Vol. 23J, p. 1189 (European Physical Society, Nieuwegein, 1999); General Atomics Report GA–A23141 (1999).

deGrassie, J.S., D.R. Baker, K.H. Burrell, C.M. Greenfield, Y.R. Lin-Liu, T.C. Luce, C.C. Petty, R. Prater, W.W. Heidbrink, B.W. Rice, "Plasma Rotation and RF Heating in DIII–D," Proc. 13th Top. Conf. on Applications of Radio Frequency Power to Plasmas, April 12–14, 1999, Annapolis, Maryland, p. 140 (American Institute of Physics, Melville, 1999); General Atomics Report GA–A23080 (1999).

deGrassie, J.S., K.H. Burrell, C.M. Greenfield, C.C. Petty, G.M. Staebler, Y.R. Lin-Liu, W.W. Heidbrink, M.R. Wade, "Plasma Rotation and Direct Electron Heating in DIII–D," Bull. Am. Phys. Soc. **44**, 174 (1999).

Deranian, R.D., R.J. Groebner, D.T. Pham, "Inductive Classification of L–Mode and H–Mode Edge Parameters," to be published in Phys. Plasmas; General Atomics Report GA–A23149 (1999).

Doyle, E.J., C.L. Rettig, T.L. Rhodes, W.A. Peebles, L. Zeng, K.H. Burrell, C.M. Greenfield, G.M. Staebler, G.R. McKee, B.W. Rice, B.W. Stallard, "Turbulence Behavior During Internal Transport Barrier (ITB) Development on DIII–D," Bull. Am. Phys. Soc. **44**, 128 (1999).

Ernst, D.R., E.J. Synakowski, G.L. Schmidt, L.R. Baylor, M. Murakami, T.C. Jernigan, C.M. Greenfield, K.H. Burrell, G.L. Jackson, "Tests of H–Mode Marginal Stability Using Pellet Perturbations on DIII–D and Transport Physics of PEP Mode Initiation and Sustainment," Bull. Am. Phys. Soc. **44**, 73 (1999).

Evans, T.E., D.F. Finkenthal, M.E. Fenstermacher, A.W. Leonard, G.D. Porter, W.P. West, "Quantitative Comparisons between Experimentally Measured 2–D Carbon Radiation and Monte Carlo Impurity (MCI) Code Simulations," presented at 13th Int. Conf. on Plasma Surface Interactions in Controlled Fusion Devices, May 18–23, 1998, San Diego, California, J. Nucl. Mater. **266–269**, 1034 (1999); General Atomics Report GA–A22876 (1998).

Evans, T.E., W.P. West, D.F. Finkenthal, K.S. Leuenroth, R.C. Isler, "Monte Carlo Impurity Studies of Carbon Dynamics in the DIII–D Divertor and Scrape-off Layer," Bull. Am. Phys. Soc. **44**, 172 (1999).

Evans, T.E., D.G. Whyte, P.L. Taylor, A.G. Kellman, P.B. Parks, D.A. Humphreys, R.W. Harvey, S.C. Luckhardt, T.C. Jernigan, M.J. Schaffer, L.R. Baylor, A.W. Hyatt, R.L. Lee, J.A. Leuer, D.S. Gray, J. Zhang, "The Production and Confinement of Runaway Electrons with Impurity," presented at 17th IAEA Fusion Energy Conference, October 19–24, 1998, Yokohama, Japan; General Atomics Report GA–A22976 (1998).

Fenstermacher, M.E., S.L. Allen, D.N. Hill, R.C. Isler, C.J. Lasnier, A.W. Leonard, T.W. Petrie, G.D. Porter, W.P. West, D.G. Whyte, R.D. Wood, "Evolution of 2D Deuterium and Impurity Radiation Profiles During Transitions from Attached to Detached Divertor Operation in DIII–D," presented at 13th Int. Conf. on Plasma Surface Interactions in Controlled Fusion Devices, May 18–23, 1998, San Diego, California, J. Nucl. Mater. **266–269**, 348 (1999); General Atomics Report GA–A22861 (1998).

Fenstermacher, M.E., J. Boedo, R.C. Isler, A.W. Leonard, G.D. Porter, D.G. Whyte, R.D. Wood, S.L. Allen, N.H. Brooks, R. Colchin, T.E. Evans, D.N. Hill, C.J. Lasnier, R.D. Lehmer, M.A. Mahdavi, R. Maingi, R.A. Moyer, T.W. Petrie, T.D. Rognlien, M.J. Schaffer, R.D. Stambaugh, M.R. Wade, J.G. Watkins, W.P. West, and N. Wolf, "Physics of the Detached Radiative Divertor Regime in DIII–D," Proc. 25th European Physical Society Conf. on Controlled Fusion and Plasma Physics, June 29–July 3, 1998, Zofin, Praha, Czech Republic, Plasma Phys. Control. Fusion **41** A345 [Institute of Physics, United Kingdom (1999)]; General Atomics Report GA–A22909 (to be printed).

Fenstermacher, M.E., N.W. Jalufka, W.H. Meyer, D.G. Nilson, J. Gafert, J.T. Hogan, C.J. Lasnier, A.W. Leonard, R.A. Pitts, G.D. Porter, "Evolution of 2D Visible and VUV Divertor Emission Profiles During DIII–D H–Mode Detachment Transitions," Proc. 26th European Conf. on Controlled Fusion and Plasma Physics, June 14–18, 1999, Maastricht, Netherlands, Vol. 23J, p. 1197 (European Physical Society, Nieuwegein, 1999); General Atomics Report GA–A23165 (1999).

Fenstermacher, M.E., C.J. Lasnier, G.D. Porter, R.J. Groebner, A.W. Leonard, T.H. Osborne, T.W. Petrie, J.G. Watkins, "Effect of Variation in Secondary Divertor Volume on Performance of Unbalanced DN Plasmas in DIII–D," Bull. Am. Phys. Soc. **44**, 170 (1999).

Ferron, J.R., "Modification of H–mode Pedestal Instabilities in the DIII–D Tokamak," Bull. Am. Phys. Soc. **44**, 286 (1999) Invited Abstract.

Ferron, J.R., M.S. Chu, G.L. Jackson, L.L. Lao, R.L. Miller, T.H. Osborne, P.B. Snyder, E.J. Strait, T.S. Taylor, A.D. Turnbull, A.M. Garofalo, M.A. Makowski, B.W. Rice, M.S. Chance, L.R. Baylor, M. Murakami, M.R. Wade, "Modification of H–Mode Pedestal Instabilities in the DIII–D Tokamak," presented at 41st Am. Phys. Soc. Annual Meeting of the Division of Plasma Physics, November 15–19, 1999, Seattle, Washington, to be published in Phys. Plasmas; General Atomics Report GA–A23303 (1999).

Ferron, J.R., L.L. Lao, R.L. Miller, T.H. Osborne, B.W. Rice, E.J. Strait, T.S. Taylor, "Modification of Tokamak Edge Instability Character through Control of Ballooning Mode Second Stability Regime Accessibility," submitted to Nucl. Fusion Lett.; General Atomics Report GA–A22974 (1999).

Ferron, J.R., L.L. Lao, T.H. Osborne, E.J. Strait, R.L. Miller, T.S. Taylor, E.J. Doyle, B.W. Rice, C. Zhang, L. Chen, M.R. Wade, M. Murakami, "Characterization and Modification of Edge-Driven Instabilities in the DIII–D Tokamak," Proc. 26th European Conf. on Controlled Fusion and Plasma Physics, June 14–18, 1999, Maastricht, Netherlands, Vol. 23J, p. 1201 (European Physical Society, Nieuwegein, 1999); General Atomics Report GA–A23156 (1999).

Fredrickson, E.D., L.C. Johnson, M. Okabayshi, R.J. LaHaye, E.J. Strait, R.T. Snider, J.T. Scoville, G.A. Navratil, A.M. Garofalo, E.A Lazarus, M. Gryaznevich, "Active Feedback on Locked Modes in DIII–D," Bull. Am. Phys. Soc. **44**, 76 (1999).

Garofalo, A.M., “Observation of the Resistive Wall Mode,” General Atomics DIII–D Technical Bulletin; General Atomics Report GA–A23064, No. 9 (1999).

Garofalo, A.M., G.A. Navratil, E.D. Fredrickson, M. Okabayashi, L.C. Johnson, E.A. Lazarus, M. Gryaznevich, R.J. La Haye, J.T. Scoville, E.J. Strait, A.D. Turnbull, “Stability of the Resistive Wall Mode in Advanced Tokamak Plasmas,” Bull. Am. Phys. Soc. **44**, 129 (1999).

Garofalo, A.M., A.D. Turnbull, M.E. Austin, J. Bialek, M.S. Chu, K.J. Comer, E. Fredrickson, R.J. Groebner, R.J. La Haye, L.L. Lao, E.A. Lazarus, G.A. Navratil, T.H. Osborne, B.W. Rice, S.A. Sabbagh, J.T. Scoville, E.J. Strait, T.S. Taylor, “Direct Observation of the Resistive Wall Mode in a Tokamak and Its Interaction with Plasma Rotation,” Phys. Rev. Lett. **82**, 3811 (1999); General Atomics Report GA–A22985 (1999).

Garofalo, A.M., A.D. Turnbull, E.J. Strait, M.E. Austin, J. Bialek, M.S. Chu, E. Fredrickson, R.J. La Haye, G.A. Navratil, L.L. Lao, E.A. Lazarus, M. Okabayashi, B.W. Rice, S.A. Sabbagh, J.T. Scoville, T.S. Taylor, M.L. Walker, DIII–D Team, “Stabilization of the External Kink and Control of the Resistive Wall Mode in Tokamaks,” presented at 40th Amer. Phys. Soc. Annual Meeting of Division of Plasma Physics, November 16–20, 1998, New Orleans, Louisiana, Phys. Plasmas **6**, 1893 (1999); General Atomics Report GA–A23023 (1999).

Garstka, G.D., R.F. Ellis, M.E. Austin, “Implementation of a Fast Broadband ECE Measurement on DIII–D,” Bull. Am. Phys. Soc. **44**, 175 (1999).

Gohil, P., K.H. Burrell, L.R. Baylor, T.C. Jernigan, “Plasma Edge Conditions During Pellet Induced H–mode Transitions in DIII–D,” Bull. Am. Phys. Soc. **44**, 73 (1999).

Gohil, P., K.H. Burrell, R.J. Groebner, K. Holtrop, K.H. Kaplan, P. Monier-Garbet, “Wavelength Calibration of the Charge Exchange Recombination Spectroscopy System on the DIII–D Tokamak,” presented at 12th Top. Conf. on High-Temperature Plasma Diagnostics, June 7–11, 1998, Princeton, New Jersey, Rev. Sci. Instrum. **70**, 878 (1999); General Atomics Report GA–A22887 (1998).

Gorelov, I., J. Lohr, D. Ponce, R.W. Callis, H. Ikezi, R.A. Legg, S.E. Tsimring, “Gyrotron Performance on the 110 GHz Installation at the DIII–D Tokamak,” to be published in Proc. 24th Int. Conf. on Infrared and Millimeter Waves, September 5–10, 1999, Monterey, California; General Atomics Report GA–A23182 (1999).

Greenfield, C.M., “Understanding and Control of Transport in Advanced Tokamak Regimes in DIII–D,” Bull. Am. Phys. Soc. **44**, 20 (1999) Invited Abstract.

Greenfield, C.M., J.C. DeBoo, T.C. Luce, B.W. Stallard, E.J. Synakowski, L.R. Baylor, K.H. Burrell, T.A. Casper, E.J. Doyle, D.R. Ernst, J.R. Ferron, P. Gohil, R.J. Groebner, L.L. Lao, M. Makowski, G.R. McKee, M. Murakami, C.C. Petty, R.I. Pinsker, P.A. Politzer, R. Prater, C.L. Rettig, T.L. Rhodes, B.W. Rice, G.L. Schmidt, G.M. Staebler, E.J. Strait, D.M. Thomas, M.R. Wade, DIII–D Team, “Understanding and Control of Transport in Advanced Tokamak Regimes in DIII–D,” presented at 41st Am. Phys. Soc. Annual Meeting of the Division of Plasma Physics, November 15–19, 1999, Seattle, Washington, to be published in Phys. Plasmas; General Atomics Report GA–A23305 (1999).

Greenfield, C.M., C.L. Rettig, G.M. Staebler, B.W. Stallard, M.E. Austin, K.H. Burrell, J.C. DeBoo, J.S. deGrassie, E.J. Doyle, P. Gohil, R.J. Groebner, J. Lohr, G.R. McKee, Jr, W.A. Peebles, C.C. Petty, R.I. Pinsker, B.W. Rice, T.L. Rhodes, E.J. Synakowski, R.E. Waltz, Z. Zheng, "Behavior of Electron and Ion Transport in Discharges with an Internal Transport Barrier in the DIII–D Tokamak," presented at 17th IAEA Fusion Energy Conference, October 19–24, 1998, Yokohama, Japan, Special Issue Nucl. Fusion **39**, 1723 (International Atomic Energy Agency, Vienna, 1999); General Atomics Report GA–A22990 (1998).

Groebner, R.J., D.M. Thomas, R.D. Deranian, "Edge Gradients as Components of the H–mode Trigger," Bull. Am. Phys. Soc. **44**, 72 (1999).

Gryaznevich, M., E.J. Strait, K.H. Burrell, R.J. La Haye, J.T. Scoville, A.D. Turnbull, E.D. Fredrickson, M. Okabayashi, A.M. Garofalo, G.A. Navratil, E.A. Lazarus, "Beta-Collapse Events in AT Regime on DIII–D," Bull. Am. Phys. Soc. **44**, 75 (1999).

Harvey, R.W., Y.R. Lin-Liu, C.C. Petty, T.C. Luce, R. Prater, "Sensitivity of Calculated Electron Cyclotron Current Drive to Variations of Parameters Around DIII–D Tokamak Conditions," Bull. Am. Phys. Soc. **44**, 174 (1999).

Harvey, R.W., Y.R. Lin-Liu, O. Sauter, A.P. Smirnov, T.C. Luce, R. Prater, "Current Drive Due to Localized Electron Cyclotron Power Deposition in DIII–D," Proc. 13th Top. Conf. on Applications of Radio Frequency Power to Plasmas, April 12–14, 1999, Annapolis, Maryland, p. 253 (American Institute of Physics, Melville, 1999); General Atomics Report GA–A23137 (1999).

Heidbrink, W.W., T. Dang, F.W. Baity, E.A. Lazarus, S. Bernabei, E.D. Fredrickson, J.S. deGrassier, C.C. Petty, R.I. Pinsker, B.W. Rice, "High Harmonic Ion Cyclotron Heating in DIII–D: II. Sawtooth Stabilization," Bull. Am. Phys. Soc. **44**, 73 (1999).

Heidbrink, W.W., E. Fredrickson, T.K. Mau, C.C. Petty, R.I. Pinsker, M. Porkolab, B.W. Rice, "High-Harmonic Ion Cyclotron Heating in DIII–D — Beam-Ion Absorption and Sawtooth Stabilization," Nucl. Fusion **39**, 1369 (1999); General Atomics Report GA–A23106 (1999).

Hinton, F.L., M.N. Rosenbluth, "Dynamics of Axisymmetric E×B and Poloidal Flows in Tokamaks," Proc. 25th European Physical Society Conf. on Controlled Fusion and Plasma Physics, June 29–July 3, 1998, Zofin, Praha, Czech Republic, Vol. 41, A653 (Institute of Physics Publishing, Bristol, 1999); General Atomics Report GA–A22904 (1998).

Holtrop, K.L., M.J. Hansink, A.G. Kellman, "Outgassing Tests on Materials Used in the DIII–D Magnetic Fusion Tokamak," Proc. 45th Annual American Vacuum Soc. Symp. and Top. Conf., Baltimore, November 2–6, 1998, Baltimore, Maryland, J. Vac. Sci. Technol. **17**, 2064 (1999); General Atomics Report GA–A22968 (1998).

Hsieh, C.L., B.D. Bray, J.C. DeBoo, T.H. Osborne, "A Model for the Energy Confinement Scaling of H–mode Plasmas in Tokamaks," Bull. Am. Phys. Soc. **44**, 75 (1999).

Humphreys, D.A., A.G. Kellman, "Analytic Modeling of Axisymmetric Disruption Halo Currents," Phys. Plasmas **6**, 2742 (1999); General Atomics Report GA–A22802 (1998).

Humphreys, D.A., M.L. Walker, J.A. Leuer, "Minimal Plasma Response Models for Design of Tokamak Equilibrium Controllers with High Dynamic Accuracy," Bull. Am. Phys. Soc. **44**, 175 (1999).

Hyatt, A.W., P.L. Taylor, A.G. Kellman, “Database Analsyis of Disruption Frequency in DIII–D,” Bull. Am. Phys. Soc. **44**, 77 (1999).

Isler, R.C., N.H. Brooks, W.P. West, A.W. Leonard, G.R. McKee, G.D. Porter, “Spectroscopic Analysis of Normal and Reversed Ion Flows in the DIII–D Divertor,” Phys. Rev. Lett. **6**, 541 (1999); General Atomics Report GA–A22815 (1998).

Isler, R.C., N.H. Brooks, W.P. West, A.W. Leonard, G.R. McKee, G.D. Porter, “Spectroscopic Measurements of Impurity Temperatures and Parallel Ion Flows in the DIII–D Divertor,” presented at 13th Int. Conf. on Plasma Surface Interactions in Controlled Fusion Devices, May 18–23, 1998, San Diego, California, J. Nucl. Mater. **266–269**, 376 (1999); General Atomics Report GA–A22852 (1998).

Isler, R.C., N.H. Brooks, W.P. West, D.G. Whyte, “Carbon Sources and Fluxes in the DIII–D Divertor,” Bull. Am. Phys. Soc. **44**, 171 (1999).

Jackson, G.L., M. Murakami, M.R. Wade, G.R. McKee, B.W. Rice, DIII–D Team, “Impurity Seeding in L–, H–, and VH–mode DIII–D Discharges,” Bull. Am. Phys. Soc. **44**, 127 (1999).

Jackson, G.L., G.M. Staebler, T.E. Evans, A.W. Hyatt, R.J. La Haye, A.W. Leonard, T.W. Petrie, W.P. West, M. Murakami, M.R. Wade, A.M. Messiaen, “Enhanced Confinement Discharges in DIII–D with Neon and Argon Induced Radiation,” presented at 13th Int. Conf. on Plasma Surface Interactions in Controlled Fusion Devices, May 18–23, 1998, San Diego, California, J. Nucl. Mater. **266–269**, 380 (1999); General Atomics Report GA–A22875 (1998).

Jakubowski, M., R.J. Fonck, G.R. McKee, K.H. Burrell, “Two-Dimensional Turbulence Dynamics During an L–H Transition on DIII–D,” Bull. Am. Phys. Soc. **44**, 138 (1999).

Jalufka. N., Q. Boney, M.E. Fenstermacher, A.W. Leonard, R.J. Colchin, “Poloidal Profile of CIV Emission in the DIII–D Divertor During PDD Operation,” Bull. Am. Phys. Soc. **44**, 170 (1999).

Jernigan, T.C., L.R. Baylor, S.K. Combs, C.R. Foust, M.R. Wade, P. Gohil, “Comparison of Deuterium Pellet Injection from Different Locations on DIII–D,” Bull. Am. Phys. Soc. **44**, 73 (1999).

Johnson, L.C., E.D. Fredrickson, M. Okabayashi, R.J. La Haye, J.T. Scoville, E.J. Strait, A.M. Garofalo, G.A. Navratil, E.A. Lazarus, M. Gryzanevich, “Internal Structure of Resistive Wall Modes in DIII–D,” Bull. Am. Phys. Soc. **44**, 74 (1999).

La Haye, R.J., R.J. Buttery, S. Guenter, G.T.A. Huysmans, H.R. Wilson, “Multi-Device Scaling of Neoclassical Tearing Mode Onset with Beta,” Proc. 26th European Conf. on Controlled Fusion and Plasma Physics, June 14–18, 1999, Maastricht, Netherlands, Vol. 23J, p. 1209 (European Physical Society, Nieuwegein, 1999); General Atomics Report GA–A23138 (1999).

La Haye, R.J., R.J. Buttery, H.R. Wilson, S. Guenter, G.T.A Huysmans, “Multi-Device Dimensionless Scaling of Neoclassical Tearing Mode Beta Limit,” Bull. Am. Phys. Soc. **44**, 129 (1999).

La Haye, R.J., B.W. Rice, E.J. Strait, “Increasing the Beta Limit Due to Neoclassical Tearing Modes by Raising the Axial Safety Factor $q(0) > 1$,” to be published in Nucl. Fusion; General Atomics Report GA–A23068 (1999).

Lao, L.L., “MHD Instabilities Occurring Near/At the Transport Barrier, Including Loss of Confinement in H–Modes,” to be published in Plasma Phys. Control. Fus.; General Atomics Report GA–A23255 (1999).

Lao, L.L., J.R. Ferron, Y.R. Lin-Liu, E.J. Strait, A.D. Turnbull, T.S. Taylor, M. Murakami, “Stability Modeling of DIII–D Discharges with Transport Barriers,” Bull. Am. Phys. Soc. **44**, 77 (1999).

Lao, L.L., J.R. Ferron, R.L. Miller, T.H. Osborne, V.S. Chan, R.J. Groebner, G.L. Jackson, R.J. La Haye, E.J. Strait, T.S. Taylor, A.D. Turnbull, E.J. Doyle, E.A. Lazarus, M. Murkamai, G.R. McKee, Jr, B.W. Rice, C. Zhang, L. Chen, “Effects of Plasma Shape and Profiles on Edge Stability in DIII–D,” presented at 17th IAEA Fusion Energy Conference, October 19–24, 1998, Yokohama, Japan, Special Issue of Nucl. Fusion **39**, 1785 (1999); General Atomics Report GA–A22993 (1998).

Lasnier, C.J., D.N. Hill, S.L. Allen, M.E. Fenstermacher, A.W. Leonard, T.W. Petrie, G.D. Porter, J.G. Watkins, “Scalings and Profiles of Heat Flux During Partial Detachment in DIII–D,” presented at 13th Int. Conf. on Plasma Surface Interactions in Controlled Fusion Devices, May 18–23, 1998, San Diego, California, J. Nucl. Mater. **266–269**, 577 (1999); General Atomics Report GA–A22872 (1998).

Lasnier, C.L., A.W. Leonard, T.W. Petrie, J.G. Watkins, “Dependence of ELM Energy Distribution in Double-null Discharges on Up/Down Magnetic Balance in DIII–D,” Bull. Am. Phys. Soc. **44**, 170 (1999).

Lazarus, E.A., M.S. Chu, T.H. Osborne, R.J. La Haye, B.W. Rice, “The Relationship of Locked Modes to Edge Current in DIII–D,” Bull. Am. Phys. Soc. **44**, 76 (1999).

Leonard, A.W., A. Hermann, K. Itami, J. Lingertat, A. Loarte, T.H. Osborne, W. Suttrop, the ITER Divertor Modeling and Database Expert Group and the ITER Divertor Physics Expert Group, “The Impact of ELMs on the ITER Divertor,” presented at 13th Int. Conf. on Plasma Surface Interactions in Controlled Fusion Devices, May 18–23, 1998, San Diego, California, J. Nucl. Mater. **266–269**, 109 (1999); General Atomics Report GA–A22860 (1998).

Leonard, A.W., M.A. Mahdavi, T.H. Osborne, T.W. Petrie, M.E. Fenstermacher, C.L. Lasnier, J.G. Watkins, “ELM Energy Scaling in DIII–D H–mode Plasmas,” Bull. Am. Phys. Soc. **44**, 169 (1999).

Leuer, J.A., J.R. Ferron, D.A. Humphreys, A.W. Hyatt, B.G. Penaflor, M.L. Walker, R.R. Khayrutdinov, V.E. Lukash, “Implementation of a Multivariable Shape Controller on DIII–D,” Bull. Am. Phys. Soc. **44**, 175 (1999).

Lin-Liu, Y.R., V.S. Chan, T.C. Luce, R. Prater, O. Sauter, R.W. Harvey, “Modeling of Electron Cyclotron Current Drive Experiments on DIII–D,” Proc. 13th Top. Conf. on Applications of Radio Frequency Power to Plasmas, April 12–14, 1999, Annapolis, Maryland, p. 249 (American Institute of Physics, Melville, 1999); General Atomics Report GA–A23132 (1999).

Lin-Liu, Y.R., V.S. Chan, O. Sauter, R.W. Harvey, “The Non-Bounce-Averaged Calculation of Electron Cyclotron Current Drive Efficiency for Recent DIII–D Experiments,” Bull. Am. Phys. Soc. **44**, 273 (1999).

Lin-Liu, Y.R., O. Sauter, R.W. Harvey, V.S. Chan, T.C. Luce, R. Prater, “Modeling of Trapped Electron Effects on Electron Cyclotron Current Drive for Recent DIII–D Experiments,” Proc. 26th European Conf. on Controlled Fusion and Plasma Physics, June 14–18, 1999, Maastricht, Netherlands, Vol. 23J, p. 1245 (European Physical Society, Nieuwegein, 1999); General Atomics Report GA–A23161 (1999).

John Lohr, D. Ponce, I. Gorelov, R.W. Callis, S.E. Tsimring, P. Cahalan, “Tests and Performance of the 110 GHz ECH System on DIII–D,” Bull. Am. Phys. Soc. **44**, 173 (1999).

Luce, T.C., Y.R. Lin-Liu, R.W. Harvey, G. Giruzzi, J. Lohr, C.C. Petty, P.A. Politzer, R. Prater, B.W. Rice, “Electron Cyclotron Current Drive in DIII–D,” Proc. 13th Top. Conf. on Applications of Radio Frequency Power to Plasmas, April 12–14, 1999, Annapolis, Maryland, p. 213 (American Institute of Physics, Melville, 1999); General Atomics Report GA–A23130 (1999).

Luce, T.C., Y.R. Lin-Liu, R.W. Harvey, G. Giruzzi, J. Lohr, C.C. Petty, P.A. Politzer, R. Prater, B.W. Rice, “Modification of the Current Profile in DIII–D by Off-Axis Electron Cyclotron Current Drive,” Plasma Phys. Control. Fus. **41**, B119 (1999); General Atomics Report GA–A23167 (1999).

Luce, T.C., Y.R. Lin-Liu, J.M. Lohr, C.C. Petty, R. Prater, R.W. Callis, J.S. deGrassie, R.I. Pinsker, D. Ponce, M.E. Austin, F.W. Baity, Jr., M. Murakami, S. Bernabei, K.-L. Wong, G. Grizzi, R.W. Harvey, B.W. Rice, M. Zerbini, “Current Profile Modification with Electron Cyclotron Current Drive in the DIII–D Tokamak,” presented at 17th IAEA Fusion Energy Conference, October 19–24, 1998, Yokohama, Japan; General Atomics Report GA–A23002 (1998).

Luce, T.C., Y.R. Lin-Liu, J. Lohr, C.C. Petty, R. Prater, G. Giruzzi, R.W. Harvey, B.W. Rice, “Generation of Localized Non-Inductive Current by Electron Cyclotron Waves on the DIII–D Tokamak,” Phys. Rev. Lett. **83**, 4550 (1999); General Atomics Report GA–A23018 (1999).

Luce, T.C., P.A. Politzer, J.R. Ferron, C.M. Greenfield, E.J. Strait, R.I. Pinsker, L.L. Lao, M.R. Wade, M. Murakami, B.W. Rice, A.M. Garofalo, M.E. Austin, “Progress Toward Long-Pulse High Performance Discharges in the DIII–D Tokamak,” Bull. Am. Phys. Soc. **44**, 126 (1999).

Mahdavi, M.A., T.H. Osborne, G.L. Jackson, R.J. La Haye, A.W. Leonard, T.W. Petrie, D.M. Thomas, W.P. West, M.E. Fenstermacher, R. Jayakumar, C.L. Lasnier, R. Maingi, M.R. Wade, J.G. Watkins, “Access to Densities Above the Greenwald Limit in High Confinement H–mode Plasmas,” Bull. Am. Phys. Soc. **44**, 169 (1999).

Maingi, R., M.A. Mahdavi, T.W. Petrie, L.R. Baylor, J.W. Cuthbertson, D.N. Hill, A.W. Hyatt, T.C. Jernigan, R.J. La Haye, C.J. Lasnier, A.W. Leonard, M. Murakami, R.T. Snider, R.D. Stambaugh, D.M. Thomas, M.R. Wade, J.G. Watkins, W.P. West, D.G. Whyte, “Investigation of Density Limit Processes in DIII–D,” presented at 17th IAEA Fusion Energy Conference, October 19–24, 1998, Yokohama, Japan; General Atomics Report GA–A23000 (1999).

Maingi, R., M.A. Mahdavi, T.W. Petrie, L.R. Baylor, T.C. Jernigan, R.J. La Haye, A.W. Hyatt, M.R. Wade, J.G. Watkins, D.G. Whyte, “Density Limit Studies on DIII–D,” presented at 13th Int. Conf. on Plasma Surface Interactions in Controlled Fusion Devices, May 18–23, 1998, San Diego, California, J. Nucl. Mater. **266–269**, 598 (1999); General Atomics Report GA–A22873 (1998).

Maingi, R., J.G. Watkins, M.A. Mahdavi, L.W. Owen, “Pump Plenum Pressure Dependence on Divertor Plasma Parameters and Magnetic Geometry in the DIII–D Tokamak,” Nucl. Fusion **39**, 1187 (1999); General Atomics Report GA–A23057 (1999).

Makowski, M., T.A. Casper, J. Jayakumar, B.W. Rice, C.M. Greenfield, T.S. Taylor, A.D. Turnbull, “L–Mode NCS Discharges with Expanded Radius,” Bull. Am. Phys. Soc. **44**, 77 (1999).

Mandrekas, J., W.M. Stacey, M. Murakami, M.R. Wade, G.L. Jackson, “Impurity Analysis and Modeling of DIII–D Radiating Mantle Discharges,” Bull. Am. Phys. Soc. **44**, 74 (1999).

McHarg, Jr., B.B., “The DIII–D Computing Environment — Characteristics and Recent Changes,” Proc. 2nd IAEA Tech. Comm. Mtg on Control, Data Acquisition, and Remote Participation on Fusion Research, July 19–21, 1999, Lisbon, Portugal, to be published in Fusion Engineering and Design; General Atomics Report GA–A23192 (1999).

McKee, G.R., “Impurity-Induced Core Turbulence Suppression and Reduced Transport in the DIII–D Tokamak,” Bull. Am. Phys. Soc. **44**, 22 (1999) Invited Abstract.

McKee, G.R., “Impurity-Induced Core Turbulence Suppression and Reduced Transport in the DIII–D Tokamak,” presented at 41st Am. Phys. Soc. Annual Meeting of the Division of Plasma Physics, November 15–19, 1999, Seattle, Washington, to be published in Phys. Plasmas; General Atomics Report GA–A23300 (to be printed).

McKee, G.R., “Turbulence Suppression and Reduced Transport Induced by Impurities,” General Atomics DIII–D Technical Bulletin; General Atomics Report GA–A23064, No. 5 (1999).

McKee, G.R., K.H. Burrell, R.J. Fonck, G.L. Jackson, M. Jakubowski, M. Murakami, G.M. Staebler, D.M. Thomas, W.P. West, “Impurity-Induced Suppression of Core Turbulence and Transport in the DIII–D Tokamak,” to be published in Phys. Rev. Lett.; General Atomics Report GA–A23079 (1999).

Middaugh, K.R., B.D. Bray, C.-L. Hsieh, B.B. McHarg, Jr., B.G. Penaflor, “DIII–D Thomson Scattering Diagnostic Data Acquisition, Processing, and Analysis Software,” Proc. 11th IEEE/NPSS Real-Time Conf., June 14–18, 1999, Santa Fe, New Mexico, p. 342 (IEEE/Nuclear and Plasma Sciences Society, Santa Fe, 1999); General Atomics Report GA–A23147 (1999).

Moyer, R.A., D. Rudakov, T.L. Rhodes, E.J. Doyle, W.A. Peebles, C.L. Rettig, T.E. Evans, R.J. Groebner, P.A. Politzer, D. Turney, “Complex Dynamics of Turbulent Edge Transport in DIII–D,” Bull. Am. Phys. Soc. **44**, 74 (1999).

Murakami, M., T.A. Casper, J.C. DeBoo, C.M. Greenfield, J.E. Kinsey, L.L. Lao, Y.R. Lin-Liu, L.L. Lodestro, T.C. Luce, L.D. Pearlstein, P.A. Politzer, R. Prater, B.W. Rice, H.E. St John, G.M. Staebler, R.D. Stambaugh, E.J. Strait, T.S. Taylor, A.D. Turnbull, “Advanced Tokamak Scenario Modeling with Off-Axis ECH in DIII–D,” Proc. 26th European Conf. on Controlled Fusion and Plasma Physics, June 14–18, 1999, Maastricht, Netherlands, Vol. 23J, p. 1213 (European Physical Society, Nieuwegein, 1999); General Atomics Report GA–A23166 (1999).

Murakami, M., M.R. Wade, T.E. Evans, G.L. Jackson, H.E. St. John, G.M. Staebler, J.E. Kinsey, G.R. McKee, DIII–D Team, “Transport Studies of L–mode Edge Radiating Mantle Discharges with Confinement Improvement in DIII–D,” Bull. Am. Phys. Soc. **44**, 127 (1999).

Navratil, G.A., J. Bialek, A.M. Garofalo, R.J. La Haye, E.J. Strait, J.T. Scoville, E.A. Lazarus, E.D. Fredrickson, L.C. Johnson, M. Okabayashi, M. Gryaznetich, "Feedback Stabilization of the Resistive Wall Mode (RWM) in DIII–D," Bull. Am. Phys. Soc. **44**, 76 (1999).

Nilson, D.G., G. Brewis, R. Ellis, M.E. Fenstermacher, N. Jalufka, R.T. Snider, "A Tangentially Viewing VUV TV System for the DIII–D Divertor," presented at 12th Top. Conf. on High-Temperature Plasma Diagnostics, June 7–11, 1998, Princeton, New Jersey, Rev. Sci. Instrum. **70**, 738 (1998); General Atomics Report GA–A22885 (1998).

Nilson, D.G., D.N. Hill, R.D. Wood, H.S. Mclean, J.M. Moller, G. Labik, T.N. Carlstrom, B. Bray, C.-L. Hsieh, "Horizontal Thomson Scattering Systems for DIII–D and SSPX," presented at 9th Int. Symp. on Laser-Aided Plasma Diagnostics, September 26 through October 1, 1999, Lake Tahoe, California; General Atomics Report GA–A23198 (1999).

Okabayashi, M., J. Bialek, M.S. Chance, M.S. Chu, E. Fredrickson, A.M. Garofalo, M. Gryaznevich, R. Hatcher, T.H. Jensen, L.C. Johnson, R.J. La Haye, E.A. Lazarus, J. Manickam, G.A. Navratil, N. Pomphrey, J.T. Scoville, E.J. Strait, T.S. Taylor, A.D. Turnbull, M.L. Walker, "The Resistive Wall Mode Feedback Stabilization Experiment on DIII–D," Proc. 26th European Conf. on Controlled Fusion and Plasma Physics, June 14–18, 1999, Maastricht, Netherlands, Vol. 23J, p. 1661 (European Physical Society, Nieuwegein, 1999); General Atomics Report GA–A23169 (1999).

Okabayashi, M., M.S. Chance, E.D. Fredrickson, R. Hatcher, L.C. Johnson, J. Manickam, N. Pomphrey, J. Bialek, A.M. Garofalo, G.A. Navratil, M.S. Chu, T.H. Jensen, R.J. La Haye, J.T. Scoville, E.J. Strait, T.S. Taylor, A.D. Turnbull, M.L. Walker, M. Gryaznevich, E.A. Lazarus, "Initial Results of the Resistive Wall Mode Feedback Stabilization Experiment on DIII–D," Bull. Am. Phys. Soc. **44**, 129 (1999).

Osborne, T.H., K.H. Burrell, R.J. Groebner, L.L. Lao, A.W. Leonard, R. Maingi, R.L. Miller, G.D. Porter, G.M. Staebler, A.D. Turnbull, "H–mode Pedestal Characteristics in ITER Shape Discharges in DIII–D," presented at 13th Int. Conf. on Plasma Surface Interactions in Controlled Fusion Devices, May 18–23, 1998, San Diego, California, J. Nucl. Mater. **266–269**, 131 (1999); General Atomics Report GA–A22882 (1998).

Osborne, T.H., J.R. Ferron, R.J. Groebner, L.L. Lao, A.W. Leonard, R. Maingi, R.L. Miller, A.D. Turnbull, M.R. Wade, J.G. Watkins, "The Effect of Plasma Shape on H–Mode Pedestal Characteristics on DIII–D," Proc. 4th IAEA Tech. Comm. Mtg on H–Mode and Transport Barrier, September 27–29, 1999, Oxford, United Kingdom, to be published in Plasma Phys. Control. Fus.; General Atomics Report GA–A23273 (1999).

Osborne, T.H., M.A. Mahdavi, A.W. Leonard, T.W Petrie, E.J. Doyle, C.L. Rettig, M.E. Fenstermacher, G.R. McKee, M.R. Wade, "H–Mode Discharges with High Energy Confinement Above the Greenwald Density on DIII–D," Bull. Am. Phys. Soc. **44**, 128 (1999).

Parks, P.B., M.N. Rosenbluth, S.V. Putvinskij, T.E. Evans, "High-Velocity Liquid Jet Injection into Tokamak Plasmas for Disruption Mitigation," Fusion Technology **35**, 267 (1999); General Atomics Report GA–A22908 (1998).

Penaflor, B.G., D.A. Piglowski, J.R. Ferron, M.L. Walker, "Current Status of DIII–D Real-Time Digital Plasma Control," to be published in Proc. 11th IEEE/NPSS Real-Time Conf., June 14–18, 1999, Santa Fe, New Mexico; General Atomics Report GA–A23146 (1999).

Peng, Q., J.M. Schachter, D.P. Schissel, L.L. Lao, "IEFIT — An Interactive Approach to High Temperature Fusion Plasma Magnetic Equilibrium Fitting," presented at 11th IEEE/NPSS Real-Time Conf., June 14–18, 1999, Santa Fe, New Mexico; General Atomics Report GA–A23153 (1999).

Petersen, P.I., "Systematic Characterization of Component Failures for the DIII–D Tokamak," to be published in Proc. 5th Int. Symp. on Fusion Nuclear Technology, September 19–24, 1999, Rome, Italy; General Atomics Report GA–A23178 (1999).

Petrie, T.W., M.E. Fenstermacher, S.L. Allen, T.N. Carlstrom, R.J. Groebner, C.J. Lasnier, A.W. Leonard, M.A. Mahdavi, R. Maingi, R.A. Moyer, T.L. Rhodes, D.M. Thomas, J.G. Watkins, W.P. West, DIII–D Team, "A Comparison of Plasma Performance Between Single-Null and Double-Null Configuration During ELMing H–Mode," Proc. 26th European Conf. on Controlled Fusion and Plasma Physics, June 14–18, 1999, Maastricht, Netherlands, Vol. 23J, p. 1237 (European Physical Society, Nieuwegein, 1999); General Atomics Report GA–A23155 (1999).

Petrie, T.W., C.M. Greenfield, R.J. Groebner, A.W. Hyatt, R.J. La Haye, A.W. Leonard, A.M. Mahdavi, T.H. Osborne, D.M. Thomas, West, S.L. Allen, M.E. Fenstermacher, C.J. Lasnier, G.D. Porter, N.S. Wolf, J.G. Watkins, DIII–D Team, "The Effect of Divertor Magnetic Balance on H–mode Performance in DIII–D," Bull. Am. Phys. Soc. **44**, 128 (1999).

Petrie, T.W., R. Maingi, G.D. Porter, S.L. Allen, M.E. Fenstermacher, R.J. Groebner, D.N. Hill, A.W. Leonard, C.J. Lasnier, M.A. Mahdavi, R.A. Moyer, M.E. Rensink, D.M. Thomas, W.P. West, and the DIII–D Team, "The Role of Neutrals in the H–L Back Transition of High Density Single-Null and Double-Null Gas-Fueled Discharges in DIII–D," presented at 13th Int. Conf. on Plasma Surface Interactions in Controlled Fusion Devices, May 18–23, 1998, San Diego, California, J. Nucl. Mater. **266–269**, 642 (1999); General Atomics Report GA–A22864 (1998).

Petty, C.C., "Comprehensive Energy Confinement Scalings Derived from Similarity Experiments," General Atomics DIII–D Technical Bulletin; General Atomics Report GA–A23064, No. 3 (1999).

Petty, C.C., "Fast Wave Current Drive in H–Mode Plasmas," General Atomics DIII–D Technical Bulletin; General Atomics Report GA–A23064, No. 6 (1999).

Petty, C.C., F.W. Baity, J.S. deGrassie, C.B. Forest, T.C. Luce, T.K. Mau, M. Murakami, R.I. Pinsker, P.A. Politzer, M. Porkolab, R. Prater, "Fast Wave Current Drive in H–Mode Plasmas," Nucl. Fusion **39**, 1421 (1999); General Atomics Report GA–A23071 (1999).

Petty, C.C., T.C. Luce, "Scaling of Heat Transport with Collisionality," Phys. Plasmas **6**, 909 (1999); General Atomics Report GA–A22853 (1998).

Petty, C.C., T.C. Luce, M.E. Austin, H. Ikezi, J. Lohr, R. Prater, "Polarization Measurements During Electron Cyclotron Heating Experiments on the DIII–D Tokamak," to be published in Proc. 4th Int. Workshop on Strong Microwaves in Plasmas, August 2–9, 1999, Nizhny Novgorod, Russia; General Atomics Report GA–A23208 (1999).

Petty, C.C., T.C. Luce, M.E. Austin, H. Ikezi, Y.R. Lin-Liu, J. Lohr, R. Prater, "Polarization, Propagation, and Deposition Measurements During ECCD Experiments on the DIII–D Tokamak," Proc. 13th Top. Conf. on Applications of Radio Frequency Power to Plasmas, April 12–14, 1999, Annapolis, Maryland, p. 245 (American Institute of Physics, Melville, 1999); General Atomics Report GA–A23087 (1999).

Petty, C.C., T.C. Luce, F.W. Baity, D.R. Baker, J.C. DeBoo, J.S. deGrassie, P. Gohil, R.J. Groebner, R.I. Pinsker, R. Prater, B.W. Rice, D.M. Thomas, M.R. Wade, R.E. Waltz, "Comprehensive Energy Transport Scalings Derived From DIII–D Similarity Experiments," presented at 17th IAEA Fusion Energy Conference, October 19–24, 1998, Yokohama, Japan; General Atomics Report GA–A22992 (1998).

Petty, C.C., T.C. Luce, Y.R. Lin-Liu, J. Lohr, R. Prater, B.W. Rice, "Counter Current Drive with ECH and NBI," Bull. Am. Phys. Soc. **44**, 127 (1999).

Petty, C.C., M.R. Wade, J.E. Kinsey, R.J. Groebner, T.C. Luce, G.M. Staebler, "Dependence of Heat and Particle Transport on the Ratio of the Ion and Electron Temperatures," Phys. Rev. Lett. **83**, 3661 (1999); General Atomics Report GA–A23114 (1999).

Phillips, J.C., K.L. Greene, A.W. Hyatt, B.B. McHarg, Jr., B.G. Penaflor, "An Algorithm to Provide Real Time Neutral Beam Substitution in the DIII–D Tokamak," to be published in Proc. 11th IEEE/NPSS Real-Time Conf., June 14–18, 1999, Santa Fe, New Mexico; General Atomics Report GA–A23152 (1999).

Piglowski, D.A., B.G. Penaflor, J.R. Ferron, "Interprocess Communication Within the DIII–D Plasma Control System," presented at 11th IEEE/NPSS Real-Time Conf., June 14–18, 1999, Santa Fe, New Mexico; General Atomics Report GA–A23150 (1999).

Pinsker, R.I., F.W. Baity, S. Bernabei, N.L. Greenough, W.W. Heidbrink, T.K. Mau, C.C. Petty, M. Porkolab, DIII–D Team, "Experiments on Ion Cyclotron Damping at the Deuterium Fourth Harmonic in DIII–D," Proc. 13th Top. Conf. on Applications of Radio Frequency Power to Plasmas, April 12–14, 1999, Annapolis, Maryland, p. 144 (American Institute of Physics, Melville, 1999); General Atomics Report GA–A23092 (1999).

Pinsker, R.I., J.S. deGrassie, C.C. Petty, F.W. Baity, S. Bernabei, W.W. Heidbrink, T.K. Mau, M. Porkolab, "High Harmonic Ion Cyclotron Heating in DIII–D: I. Beam-Ion Absorption," Bull. Am. Phys. Soc. **44**, 172 (1999).

Politzer, P.A., "Observation of Avalanche-Like Phenomena in a Magnetically Confined Plasma," submitted to Phys. Rev. Lett.; General Atomics Report GA–A23129 (1999).

Politzer, P.A., M.E. Austin, E.J. Doyle, C.L. Rettig, T.L. Rhodes, G.R. McKee, R.A. Moyer, J.G. Watkins, "Large Spatial Scale Avalanche Processes in DIII–D," Bull. Am. Phys. Soc. **44**, 74 (1999).

Prater, R., S. Bernabei, R.W. Harvey, R.J. La Haye, Y.R. Lin-Liu, J. Lohr, F.W. Perkins, K.-L. Wong, "Neoclassical Tearing Modes in DIII–D and Calculations of the Stabilizing Effects of Localized Electron Cyclotron Current Drive," Proc. 13th Top. Conf. on Applications of Radio Frequency Power to Plasmas, April 12–14, 1999, Annapolis, Maryland, p. 261 (American Institute of Physics, Melville, 1999); General Atomics Report GA–A23098 (1999).

Prater, R., C.M. Greenfield, J. Lohr, T.C. Luce, C.C. Petty, R.I. Pinsker, B.W. Rice, "RF Assisted Startup for Generation of Discharges with Reversed Magnetic Shear," Bull. Am. Phys. Soc. **44**, 173 (1999).

Project Staff, "A Decade of DIII–D Research, Final Report to the U.S. Department of Energy for the Period of Work October 1, 1989 through September 30, 1998," General Atomics Report GA–A23028 (1999).

Project Staff, "DIII–D Research Operations Annual Report, October 1, 1996 through September 30, 1997," General Atomics Report GA–A22827 (1998).

Rettig, C.L., T.L. Rhodes, W.A. Peebles, E.J. Doyle, K.H. Burrell, C.M. Greenfield, G.M. Staebler, J.E. Kinsey, G.R. McKee, C. Rost, "Comparison of Microturbulence Characteristics in Ohmic and ITB Discharges with Predictions of ITG Models," Bull. Am. Phys. Soc. **44**, 74 (1999).

Rhodes, T.L., J.-N. Leboeuf, E.J. Doyle, C.L. Rettig, R. Sydora, R.A. Moyer, K.H. Burrell, D.M. Thomas, "Turbulent Radial Correlation Lengths in the DIII–D Tokamak," Bull. Am. Phys. Soc. **44**, 74 (1999).

Rice, B.W., "Extended Advanced Tokamak Operation with Infrequent ELMs," General Atomics DIII–D Technical Bulletin; General Atomics Report GA–A23064, No. 1 (1999).

Rice, B.W., K.H. Burrell, J.R. Ferron, C.M. Greenfield, G.L. Jackson, L.L. Lao, R.J. La Haye, T.C. Luce, B.W. Stallard, E.J. Strait, E.J. Synakowski, T.S. Taylor, A.D. Turnbull, M.R. Wade, "Progress Towards Sustainment of Advanced Tokamak Modes in DIII–D," presented at 17th IAEA Fusion Energy Conference, October 19–24, 1998, Yokohama, Japan, Special Issue of Nucl. Fusion **39**, 1855 (1999); General Atomics Report GA–A22999 (1998).

Rice, B.W., K.H. Burrell, L.L. Lao, D.G. Nilson, "Simultaneous Measurement of q and Er Profiles Using the Motional Stark Effect in High-Performance DIII–D Plasmas," presented at 12th Top. Conf. on High-Temperature Plasma Diagnostics, June 7–11, 1998, Princeton, New Jersey, Rev. Sci. Instrum. **70**, 815 (1999); General Atomics Report GA–A22888 (1998).

Rudakov, D.L., J.A. Boedo, R.D. Lehmer, R.A. Moyer, G. Gunner, J.G. Watkins, "Fast Electron Temperature Measurements Based on Langmuir Probe Current Harmonic Detection on DIII–D," Bull. Am. Phys. Soc. **44**, 175 (1999).

Schachter, J.M., Q. Peng, D.P. Schissel, "Data Analysis Software Tools for Enhanced Collaboration at the DIII–D National Fusion Facility," Proc. 2nd IAEA Tech. Comm. Mtg on Control, Data Acquisition, and Remote Participation on Fusion Research, July 19–21, 1999, Lisbon, Portugal, to be published in Fusion Engineering and Design; General Atomics Report GA–A23187 (1999).

Schaffer, M.J., "Transport Across the Separatrix Near the X–Point," General Atomics DIII–D Technical Bulletin; General Atomics Report GA–A23064, No. 7 (1999).

Schaffer, M.J., J.A. Boedo, N.H. Brooks, R.C. Isler, R.A. Moyer, "Plasma Pressure and Flows During Divertor Detachment," presented at 13th Int. Conf. on Plasma Surface Interactions in Controlled Fusion Devices, May 18–23, 1998, San Diego, California, J. Nucl. Mater. **266–269**, 264 (1999); General Atomics Report GA–A22863 (1998).

Schissel, D.P., Q. Peng, J. Schachter, J. Freeman, K.M. Keith, Jr. Mc Harg, C.T. Parker, T.B. Terpstra, T.A. Casper, R. Jong, W.H. Meyer, "Enhanced Computational Infrastructure for Data Analysis at the DIII–D National Fusion Facility," Bull. Am. Phys. Soc. **44**, 176 (1999).

Schissel, D.P., Q. Peng, J.M. Schachter, T.B. Terpstra, T.A. Casper, J. Freeman, R.A. Jong, K.M. Keith, B.B. McHarg, Jr., W.H. Meyer, C.T. Parker, A.M. Warner, "Enhanced Computational Infrastructure for Data Analysis at the DIII–D National Fusion Facility," Proc. 2nd IAEA Tech. Comm. Mtg on Control, Data Acquisition, and Remote Participation on Fusion Research, July 19–21, 1999, Lisbon, Portugal, to be published in Fusion Engineering and Design; General Atomics Report GA–A23206 (1999).

Schissel, D.P., Q. Peng, J.M. Schachter, T.B. Terpstra, W.H. Meyer, T.A. Casper, R. Jong, "Enhanced Computational Infrastructure for Data Analysis at the DIII–D National Fusion Facility," Proc. 26th European Conf. on Controlled Fusion and Plasma Physics, June 14–18, 1999, Maastricht, Netherlands, Vol. 23J, p.1225 (European Physical Society, Nieuwegein, 1999); General Atomics Report GA–A23162 (1999).

Schmidt, G.L., E.D. Fredrickson, S. Jardin, L.R. Baylor, T.C. Jernigan, M.E. Austin, R.T. Snider, "Interpretation of Fast ECE and Soft X–ray Measurements During High Field Launch Pellet Fueling on DIII–D," Bull. Am. Phys. Soc. **44**, 73 (1999).

Scoville, J.T., E.J. Strait, R.J. La Haye, A.M. Garofalo, "The Effect of Error Fields on Resistive Wall Modes," Bull. Am. Phys. Soc. **44**, 76 (1999).

Stacey, W.M., M.A. Mahdavi, T.W. Petrie, "Effects of Neutrals in Determining Maximum Density in DIII–D," Bull. Am. Phys. Soc. **44**, 129 (1999).

Staebler, G.M., "Theory of Jets in Tokamaks," submitted to Phys. Rev. Lett.; General Atomics Report GA–A23120 (1999).

Staebler, G.M., G.L. Jackson, W.P. West, S.L. Allen, R.J. Groebner, M.J. Schaffer, D.G. Whyte, "Improved High-Mode with Neon Injection in the DIII–D Tokamak," Phys. Rev. Lett. **82,** 1692 (1999); General Atomics Report GA–A22674 (1997).

Stallard, B.W., "Electron Heat Transport in Improved Confinement Discharges in DIII–D," presented at 40th Amer. Phys. Soc. Annual Meeting of Division of Plasma Physics, November 16–20, 1998, New Orleans, Louisiana, Phys. Plasmas **6**, 1978 (1999); General Atomics Report GA–A23020 (1999).

Stallard, B.W., T.A. Casper, C.M. Greenfield, K.H. Burrell, P. Gohil, J. Lohr, C.C. Petty, E. Synakowski, M.E. Austin, G.R. McKee, C.L. Rettig, T.L. Rhodes, L. Zeng, "Thermal Transport in NCS Plasmas with Counter Neutral Beam Injection," Bull. Am. Phys. Soc. **44**, 72 (1999).

Stambaugh, R.D., DIII–D Team, "DIII–D Three-Year Program Plan 1999–2001," General Atomics Report GA–A23056 (1999).

Strait, E.J., A.M. Garofalo, M.E. Austin, J. Bialek, M.S. Chu, E. Fredrickson, L.L. Lao, R.J. La Haye, E.A. Lazarus, G.R. McKee, Jr, G.A. Navratil, M. Okabayashi, B.W. Rice, S.A. Sabbagh, J.T. Scoville, T.S. Taylor, A.D. Turnbull, M.L. Walker, DIII–D Team, "Observation and Control of Resistive Wall Modes," presented at 17th IAEA Fusion Energy Conference, October 19–24, 1998, Yokohama, Japan, Special Issue of Nucl. Fusion **39**, 1977 (1999); General Atomics Report GA–A22994 (1998).

Strait, E.J., R.J. La Haye, J.T. Scoville, A.D. Turnbull, A.M. Garofalo, G.A. Navratil, E.D. Fredrickson, L.C. Johnson, M. Okabayashi, M. Gryaznevich, E.A. Lazarus, "Stabilization of Resistive Wall Modes by Plasma Rotation," Bull. Am. Phys. Soc. **44**, 75 (1999).

Synakowski, E.J., D. Ernst, G. Schmidt, K.H. Burrell, C.M. Greenfield, DIII–D Team, D.E. Newman, "Differences in Dynamics of Enhanced Core Confinement States in Various Experimental Configurations and the Role of Driven Rotation," Bull. Am. Phys. Soc. **44**, 72 (1999).

Takahashi, H., E.D. Fredrickson, M.J. Schaffer, T.E. Evans, L.L. Lao, "Measurement of Current in Scrape-off Layer (SOL) Plasma in the DIII–D Tokamak," Bull. Am. Phys. Soc. **44**, 76 (1999).

Takenaga, H., A Sakasai, H. Kubo, N. Asakura, M.J. Schaffer, T.W. Petrie, M.A. Mahdavi, D.R. Baker, S.L. Allen, G.D. Porter, T.D. Rognlien, M.E. Rensink, D.P. Stolter, C.F.F. Karney, “Divertor Geometry Effects on Particle Pumping in JT–60U and DIII–D,” Bull. Am. Phys. Soc. **44**, 170 (1999).

Taylor, P.L., “Disruption Mitigation Studies in DIII–D,” presented at 40th Amer. Phys. Soc. Annual Meeting of Division of Plasma Physics, November 16–20, 1998, New Orleans, Louisiana, Phys. Plasmas **6**, 1872 (1999); General Atomics Report GA–A23019 (1999).

Taylor, T.S., K.H. Burrell, D.R. Baker, G.L. Jackson, R.J. La Haye, M.A. Mahdavi, R. Prater, T.C. Simonen, A.D. Turnbull, DIII–D Team, “Results From the DIII–D Scientific Research Program,” presented at 17th IAEA Fusion Energy Conference, October 19–24, 1998, Yokohama, Japan; General Atomics Report GA–A23007 (1998).

Taylor, T.S., S.L. Allen, P.M. Anderson, M.E. Austin, D.S. Baggest, F.W. Baity, D.R. Baker, D.E. Baldwin, G.C. Barber, R. Bastasz, C.B. Baxi, L.R. Baylor, S. Bernabei, J. Bialek, J.A. Boedo, A. Bondeson, A.S. Bozek, R.V. Bravenec, B.D. Bray, J.D. Broesch, N.H. Brooks, K.H. Burrell, J.D. Callen, R.W. Callis, C.S. Campo, T.N. Carlstrom, E.M. Carolipio, B.A. Carreras, W.P. Cary, T.A. Casper, V.S. Chan, M.S. Chance, L. Chen, E. Chin, H.K. Chiu, M.S. Chu, R.J. Colchin, S.K. Combs, J.W. Cuthbertson, W. Davis, J.C. DeBoo, J.S. deGrassie, R. Deranian, G. Diao, J.L. Doane, E.J. Doyle, R.L. Ellis, T.E. Evans, M.E. Fenstermacher, J.R. Ferron, D.K. Finkenthal, R.J. Fonck, E. Fredrickson, J. Freeman, R.L. Freeman, J. Gafert, S.A. Galkin, A.M. Garofalo, G.D. Garstka, G. Giruzzi, P. Gohil, A.M. Gootgeld, F. Grantham, D.S. Gray, J.M. Greene, K.L. Greene, C.M. Greenfield, N.L. Greenough, R.J. Groebner, S. Guenter, M.J. Hansink, T.E. Harris, R.W. Harvey, T. Hatae, C.C. Hegna, W.W. Heidbrink, D.N. Hill, F.L. Hinton, E.H. Hoffmann, J.T. Hogan, K.L. Holtrop, R.-M. Hong, W.A. Houlberg, C.-L. Hsieh, D.A. Humphreys, A.W. Hyatt, H. Ikezi, R.C. Isler, G.L. Jackson, N.W. Jalufka, T.H. Jensen, T.C. Jernigan, R.D. Johnson, L. Johnson, D.H. Kaplan, K.M. Keith, A.G. Kellman, D.H. Kellman, R.R. Khayrutdinov, J.E. Kinsey, R.J. La Haye, G. Labik, L.L. Lao, C.J. Lasnier, E.A. Lazarus, R.L. Lee, J.-H. Lee, R.A. Legg, R.D. Lehmer, A.W. Leonard, J.A. Leuer, Y.R. Lin-Liu, J. Lohr, T.C. Luce, S.C. Luckhardt, V.E. Lukash, J. Luo, J.L. Luxon, M.A. Mahdavi, R. Maingi, C.C. Makariou, J. Mandrekas, B.B. McHarg, Jr., G.R. McKee, W.H. Meyer, K.R. Middaugh, R.L. Miller, P.K. Mioduszewski, J.M. Moller, R.A. Moyer, M. Murakami, A. Nagy, G.A. Navratil, A. Nerem, W.M. Nevins, D.G. Nilson, L.E. Nissley, R.C. O’Neill, T.H. Osborne, L.W. Owen, P.B. Parks, R. Parsell, W.A. Peebles, B.G. Penaflor, Q. Peng, F.W. Perkins, P.I. Petersen, T.W. Petrie, C.C. Petty, J.C. Phillips, D.A. Piglowski, R.I. Pinsker, P.A. Politzer, D. Ponce, G.D. Porter, R. Prater, S.G. Pronko, A. Punjabi, A. Ramsey, E.E. Reis, D.B. Remsen, C. Ren, M.E. Rensink, C.L. Rettig, T.L. Rhodes, B.W. Rice, J.I. Robinson, D.W. Ross, C. Rost, S.A. Sabbagh, S. Sakurai, R.I. Savercool, J.M. Schachter, M.J. Schaffer, D.P. Schissel, J.T. Scoville, D.L. Sevier, T.C. Simonen, S.M. Skinner, J.P. Smith, R.T. Snider, H.E. St John, W.M. Stacey, G.M. Staebler, B.W. Stallard, R.D. Stambaugh, E.J. Strait, E.J. Synakowski, P.L. Taylor, T.B. Terpstra, D.M. Thomas, S.N. Tugarinov, A.D. Turnbull, R. Vernon, M.R. Wade, M.L. Walker, R.E. Waltz, W.R. Wampler, Z. Wang, A.M. Warner, J.G. Watkins, W.P. West, J. Whaley Jr, D.G. Whyte, H.R. Wilson, N.S. Wolf, R. Wolf, C.P.C. Wong, K.-L. Wong, F. Yin, L. Zeng, M. Zerbini, C. Zhang, “Advanced Tokamak Physics Experiments on DIII–D,” to be published in Proc. Annual Meeting of Physical Society of Japan, December 1–4, 1998, Yokohama, Japan; General Atomics Report GA–A23029 (1998).

Thomas, D.M., K.H. Burrell, P. Gohil, R. Jayakumar, D. Nilson, B.W. Rice, “Edge Current Density Determination Using Laser-Enhanced LIBEAM on DIII–D,” Bull. Am. Phys. Soc. **44**, 174 (1999).

Thomas, D.M., K.H. Burrell, M.R. Wade, R.T. Snider, “Prospects for Charge-Exchange-Recombination-Based Measurements on ITER using a Helium Diagnostic Neutral Beam,” presented at 12th Top. Conf. on High-Temperature Plasma Diagnostics, June 7–11, 1998, Princeton, New Jersey, Rev. Sci. Instrum. **70**, 886 (1999); General Atomics Report GA–A22886 (1998).

Turnbull, A.D., “Ideal MHD Kink-Peeling Modes and Their Relation to ELMs,” General Atomics DIII–D Technical Bulletin; General Atomics Report GA–A23064, No. 2 (1999).

Wade, M.R., DIII–D Divertor Physics Team, “Demonstration of the ITER Power Exhaust Solution Using the Puff and Pump Technique on DIII–D,” Proc. 26th European Conf. on Controlled Fusion and Plasma Physics, June 14–18, 1999, Maastricht, Netherlands, Vol. 23J, p. 1229 (European Physical Society, Nieuwegein, 1999); General Atomics Report GA–A23171 (1999).

Wade, M.R., J.T. Hogan, S.L. Allen, N.H. Brooks, D.N. Hill, R. Maingi, M.J. Schaffer, J.G. Watkins, D.G. Whyte, R.D. Wood, W.P. West, “Impurity Enrichment Studies With Induced Scrape-Off-Layer Flow on DIII–D,” Nucl. Fusion **38**, 1839 (1998); General Atomics Report GA–A22698 (1998).

Wade, M.R., J.T. Hogan, R.C. Isler, R. Maingi, W.P. West, N.H. Brooks, A.W. Leonard, T.W. Petrie, M.J. Schaffer, D.N. Hill, S.L. Allen, M.E. Fenstermacher, C.J. Lasnier, R.D. Wood, J.A. Boedo, R.D. Lehmer, R.A. Moyer, D.G. Whyte, J.G. Watkins, “Impurity Control Studies Using SOL Flow in DIII–D,” presented at 17th IAEA Fusion Energy Conference, October 19–24, 1998, Yokohama, Japan; General Atomics Report GA–A23001 (1998).

Wade, M.R., W.A. Houlberg, L.R. Baylor, “Experimental Confirmation of Impurity Convection Driven by the Ion Temperature Gradient in Toroidal Plasmas,” to be published in Phys. Rev. Lett.; General Atomics Report GA–A23034 (1999).

Wade, M.R., W.P. West, R.D. Wood, S.L. Allen, J.A. Boedo, N.H. Brooks, M.E. Fenstermacher, D.N. Hill, J.T. Hogan, R.C. Isler, G.L. Jackson, C.J. Lasnier, R.D. Lehmer, A.W. Leonard, M.A. Mahdavi, R. Maingi, R.A. Moyer, T.H. Osborne, T.W. Petrie, M.J. Schaffer, R.D. Stambaugh, J.G. Watkins, D.G. Whyte, “Impurity Enrichment and Radiative Enhancement Using Induced SOL Flow in DIII–D,” presented at 13th Int. Conf. on Plasma Surface Interactions in Controlled Fusion Devices, May 18–23, 1998, San Diego, California, J. Nucl. Mater. **266–269**, 44 (1999); General Atomics Report GA–A22874 (1998).

Walker, M.L., “Development of Multivariable Control Techniques for Use with the DIII–D Plasma Control System,” General Atomics Report GA–A23151 (1999).

Watkins, J.G., O. Batishchev, J.A. Boedo, D.N. Hill, C.J. Lasnier, R. Lehmer, A.W. Leonard, R.A. Moyer, “An Evaluation of Kinetic Effects in the DIII–D Divertor,” presented at 13th Int. Conf. on Plasma Surface Interactions in Controlled Fusion Devices, May 18–23, 1998, San Diego, California, J. Nucl. Mater. **266–269**, 980 (1999); General Atomics Report GA–A22879 (1998).

Watkins, J.G., C.L. Lasnier, M.E. Fenstermacher, O. Batishchev, J.A. Boedo, R.A. Moyer, T.W. Petrie, A.W. Leonard, “SOL and Divertor Langmuir Probe Measurements in Balanced and Unbalanced Double Null Plasmas,” Bull. Am. Phys. Soc. **44**, 170 (1999).

Watson, G.W., W.W. Heidbrink, H. Ikezi, R.I. Pinsker, “ICRF Loops: Emission Measurements and Diagnostic Applications,” Bull. Am. Phys. Soc. **44**, 173 (1999).

West, W.P., N.H. Brooks, M.E. Fenstermacher, R.C. Isler, G.L. Jackson, C.J. Lasnier, A. Ramsey, M.R. Wade, D.G. Whyte, R.D. Wood, “Carbon Influx in He and D Plasmas in DIII–D,” presented at 13th Int. Conf. on Plasma Surface Interactions in Controlled Fusion Devices, May 18–23, 1998, San Diego, California, J. Nucl. Mater. **266–269**, 732 (1999); General Atomics Report GA–A22880 (1998).

West, W.P., T.E. Evans, N.H. Brooks, D.G. Whyte, R.C. Isler, G.D. Porter, N. Wolf, “Modeling of the Weak Dependence of Core Plasma Carbon Content on the Wall Sputtering Rates in DIII–D using the 2D Multifluid Code UEDGE,” Bull. Am. Phys. Soc. **44**, 171 (1999).

Whyte, D.G., R. Bastasz, J.N. Brooks, W.R. Wampler, W.P. West, C.P.C. Wong, O.I. Buzhinskij, I.V. Opimach, “Divertor Erosion in DIII–D,” presented at 13th Int. Conf. on Plasma Surface Interactions in Controlled Fusion Devices, May 18–23, 1998, San Diego, California, J. Nucl. Mater. **266–269**, 67 (1999); General Atomics Report GA–A22858 (1998).

Whyte, D.G., R. Doerner, W.P. West, R.L. Lee, N.H. Brooks, R.C. Isler, M.R. Wade, G.D. Porter, “Long-term Reduction of Divertor Carbon Sources in DIII–D,” Bull. Am. Phys. Soc. **44**, 171 (1999).

Wong, C.P.C., R.E. Nygren, C.B. Baxi, P.J. Fogarty, N. Ghoniem, H. Khater, K. McCarthy, B. Merrill, B. Nelson, E.E. Reis, S. Sharafat, R. Schleicher, D.K. Sze, M. Ulrickson, R.S. Willms, M. Youssef, S. Zinkel, APEX Team, “Helium-Cooled Refractory Alloys First Wall and Blanket Evaluation,” to be published in Proc. 5th Int. Symp. on Fusion Nuclear Technology, September 19–24, 1999, Rome, Italy; General Atomics Report GA–A23177 (1999).

Wong, K.L., L.C. Johnson, T.C. Luce, M.S. Chu, C.C. Petty, P.A. Politzer, R. Prater, R.J. La Haye, R.T. Snider, L. Chen, R.W. Harvey, M.E. Austin, “Internal Kink Instability during Off-Axis Electron Cyclotron Current Drive in the DIII–D Tokamak,” Bull. Am. Phys. Soc. **44**, 127 (1999).

Zeng, L., E.J. Doyle, W.A. Peebles, T.L. Rhodes, T.C. Luce, “Implementation of Reflectometry as a Standard Density Profile Diagnostic on DIII–D,” Bull. Am. Phys. Soc. **44**, 174 (1999).

Zerbini, M., M.E. Austin, S. Bernabei, G. Giruzzi, M. Murakami, J. Lohr, T.C. Luce, C.C. Petty, D. Ponce, R. Prater, “Correlation Analysis of 110 GHz ECH Modulation Experiments on DIII–D Tokamak,” Plasma Phys. Control. Fus. **41**, 931 (1999); General Atomics Report GA–A22830 (1998).